RESULTATS

I. ESTUDI DE LES INTERACCIONS DE L' α-SINUCLEÏNA

I.I. Dalfó E, Barrachina M, Rosa JL, Ambrosio S, Ferrer I *Abnormal α-synuclein interactions with rab3a and rabphilin in diffuse lewy body disease. Neurobiol Disease 16 (2004) 92-97.*

L'α-sinucleïna és el component principal dels cossos de Lewy i de les neurites distròfiques dins del grup de patologies anomenades sinucleïnopaties. Les alteracions en la transmissió sinàptica d'aquestes malalties és evident, però es desconeix de quina manera l'α-sinucleïna participa en el procés sinàptic. Donat que experiments fets amb ratolins nuls per a rab3a concorden fenotípicament a nivell de sinapsi amb ratolins nuls per a l'α-sinucleïna, ens vam plantejar una possible relació entre ambdues proteïnes. La nostra hipòtesi venia abalada per uns arrays d'anticossos fets amb teixit cerebral procedent de pacients amb Demència amb cossos de Lewy, en els que s'observava una interacció entre rab3a i α-sinucleïna. Mitjançant experiments de *pull-down* i d'immunoprecipitació hem observat la interacció de rab3a amb l' α-sinucleïna només en condicions patològiques, mentre que en aquestes mateixes condicions, la interacció de rab3a amb una de les seves proteïnes efectores com és la rabfilina, s'ha detectat més reduïda. En canvi, en condicions no patològiques, sí que hem detectat la interacció de rab3a amb la seva proteïna efectora rabfilina, i curiosament, també s'ha detectat interacció de la rabfilina amb l'α-sinucleïna. Així doncs la rabfilina actuaria de vincle d'unió entre la rab3a i l'α-sinucleïna. Donat que la rab3a està implicada en l'acoblament de les vesícules a la terminal, podem postular que aquesta funció es veu alterada en la Demència amb cossos de Lewy.

I.II. Dalfó E, Barrachina M, Rosa JL, Ambrosio S, Ferrer I *Abnormal α-synuclein interactions with rab proteins in α-synuclein A30P transgenic mice. J Neuropathol Exp Neurol. 2004 Apr;63(4):302-13.*

Ratolins transgènics que expressen la forma mutada de l'α-sinucleïna (A30P) juntament amb la sinucleïna pròpia, presenten alteracions motores progressives juntament amb l'acumulació d'α-sinucleïna en el soma neuronal i neurites. Donat que amb altres tipus de ratolins transgènics per α-sinucleïna s'han observat alteracions a la sinapsis, hem volgut estudiar en aquesta línia de ratolins, l'efecte de la mutació humana en l'estat d'agregació de la sinucleïna de ratolí, igual com l'efecte de la mutació en el procés sinàptic. També hem volgut comprovar de quina manera hi afectaven l'MPTP i la rotenona, com a exemples d'estrès oxidatiu. Mitjançant un protocol d'aïllament d'agregats insolubles d'α-sinucleïna hem pogut comprovar que només en els ratolins transgènics que contenen la mutació A30P, es poden observar bandes d'α-sinucleïna d'elevat pes mol.lecular. L'MPTP i la rotenona augmenten l'aparició de bandes immunoreactives per a l'α-sinucleïna. D'altra banda, i per estudiar els efectes de la mutació en el procés sinàptic, s'ha utilitzat el mètode de pull-down amb rab3, rab5 i rab8. Així, només els ratolins que contenen la forma mutada de l'α-sinucleïna humana, presenten interacció de les proteïnes rab amb l'α-sinucleïna. Sembla que l'MPTP i la rotenona no tenen cap efecte en aquesta interacció. Així doncs, la mutació *per se* de l'α-sinucleïna afecta tan a la capacitat d'interaccionar amb altres proteïnes com en el seu estat d'agregació, reflectint-se després en un estat patològic concret.

I.III Dalfó E, Ferrer I (2004) *α-Synuclein binding to rab3a in multiple system atrophy: immunoprecipitation studies indicate generalized abnormal interactions.(Enviat a Journal of Neurochemistry).*

Les Inclusions glials citoplasmàtiques (GCI) són acúmuls de proteïna amb l'α-sinucleïna com component principal, característics de l'Atròfia Multisistèmica (MSA) i que es troben en subtància blanca de pacients afectats. Donat que anteriorment havíem demostrat interaccions anòmales de l'α-sinucleïna amb les proteïnes sinàptiques rab3a i rabfilina en subtància gris de pacients amb Demència amb cossos de Lewy, igualment com en un model de ratolí transgènic per a la forma humana mutada A30P, vam voler investigar les mateixes interaccions en una patologia on les inclusions d'α-sinucleïna predominessin en substància blanca, per tal d'estudiar si les interaccions de l'α-sinucleïna diferien depenent del tipus de patologia, o si, ben al contrari, existia un mecanisme comú d'alteració sinàptica per al conjunt de sinucleïnopaties. Així doncs utilitzant mètodes d'immunoprecipitació hem estudiat la interacció rab3a-rabfilina-α-sinucleïna tan en còrtex com en cerebel de pacients amb MSA. Els resultats obtinguts apunten cap a un mecanisme comú d'alteració sinàptica donat que, una vegada més, rab3a interacciona amb l' α-sinucleïna i no amb el seu efector rabfilina en condicions patològiques tan allà on no hi ha acúmuls d'α-sinucleïna en MSA, com és el còrtex, com en cerebel, que és on s'acumulen els GCIs. En canvi en condicions no patològiques, tan en còrtex com en cerebel, rab3a i α-sinucleïna interaccionen amb la rabfilina, mantenint-se la hipòtesi de cooperació entre les tres proteïnes per a una correcta transmissió sinàptica.

α-synuclein binding to rab3a in multiple system atrophy: immunoprecipitation studies indicate generalized abnormal interactions.

E. Dalfó, I. Ferrer

Institut de Neuropatologia, Servei Anatomia Patològica, Hospital Universitari de Bellvitge, carrer Feixa Llarga sn, 08907 Hospitalet de Llobregat, Spain

corresponding author:

Prof. I. Ferrer

e-mail: 8082ifa@comb.es

or

iferrer@csub.scs.es

Abstract

Glial cytoplasmic inclusions (GCIs) are characteristic protein deposits in Multiple System Atrophy (MSA), which are composed of abnormally phosphorylated, partially insoluble α-synuclein that forms aggregates of probably truncated isoforms, together with ubiquitin, αB-crystallin, tubulin and *tau*, among other components. The present study demonstrates the accumulation of rab3a, a member of the Ras super-family of small (21-25 kDa) GTP-binding proteins, which is involved in the regulation of the internal trafficking, exocytosis and neurotransmission, and vesicle endocytosis, in a small percentage of GCIs in the cerebellar white matter of MSA-C and MSA-P cases (olivopontocerebellar atrophy and striatonigral degeneration types, respectively). Combined α-synuclein and rab3a immunoprecipitation assays have shown α-synuclein/rab3a binding in MSA but not in normal cerebellar white matter, thus indicating abnormal interactions of α-synuclein and rab3a in diseased brains. Whether these interactions are restricted to oligodendroglial inclusions or they are the manifestation of a more generalized abnormality in MSA has been explored in the frontal cortex of MSA cases in which no GCIs were observed. Similarly to that found in the cerebellum, α-synuclein and rab3a immunoprecipitation assays have shown α-synuclein/rab3a binding in MSA frontal cortex but not in normal frontal cortex. These findings suggest membrane and synaptic vesicle trafficking as vulnerable targets in MSA resulting from the fatal attraction of abnormal α-synuclein with at least some members of the rab family. Abnormal α-synuclein/rab3a interactions may sustain generalized impairment of synaptic transmission in MSA.

Key words: α-synuclein, glial cytoplasmic inclusions, multiple system atrophy, rab, *tau*, tubulin

Introduction

Multiple system atrophy (MSA) is a sporadic neurodegenerative disease manifested with variable parkinsonism, cerebellar ataxia and autonomic dysfunction, and characterized by olivopontocerebellar atrophy, degeneration of the substantia nigra and striatum, and loss of neurons in the autonomic system. The combination of clinical and neuropathological phenotypes leads to MSA-C: olivopontocerebellar atrophy (OPCA), and MSA-P: striatonigral degeneration. The term Shy-Drager syndrome, formerly used to designate the predominance of autonomic symptoms in some patients, is no longer considered in the modern classification of MSA [9, 21, 26]. The singularity of MSA is further supported by the identification of typical oligodendroglial inclusions, glial cytoplasmic inclusions (GCIs), as signature lesions of MSA [9, 25]. Immunohistochemical studies have shown that GCIs are composed of ubiquitin [23, 34], α- and β-tubulins [1, 34], αB-crystallin [12, 30, 38], and non-phosphorylated *tau* [5, 35], among other constituents [26]. Crucially, several studies have demonstrated accumulation of α-synuclein as a main component and fibrillar core of GCIs [4, 12, 13, 36, 39, 41]. Moreover, α-synuclein in MSA has particular properties leading to differences in solubility and to the formation of molecular species of high molecular weight corresponding to α-synuclein aggregates, some of them of possibly truncated α-synuclein [10, 12, 39]. Recently, it has been demonstrated that α-synuclein in MSA (and in Parkinson's disease: PD) is phosphorylated at Ser129, and that phosphorylation of α-synuclein at Ser 129 promotes fibril formation *in vitro* [11].

Previous studies have shown binding of α-synuclein to proteins of the rab family in Diffuse Lewy body disease (DLBD), another α-synucleinopathy [7]. Moreover, anomalous α-synuclein/rab protein interactions occur in transgenic mice over-expressing human mutant A30P α-synuclein [8]. Binding α-synuclein/rab does not occur in normal human and mouse brains. This is an important feature as rab proteins, a subgroup of the Ras super-family of small (21-25 kDa) GTP-binding proteins, are involved in the regulation of internal trafficking, exocytosis and neurotransmission, and vesicle endocytosis [14, 15, 42]. More precisely, abnormal α-synuclein/rab3a interactions in DLBD and A30P α-synuclein transgenic mice may endanger synaptic vesicle exocytosis and impair synaptic transmission, thus accounting for crucial aberrant synaptic function in these conditions [7, 8]. Whether abnormal interactions of α-synuclein and rab come up in MSA is not known. This is an important issue as recent studies using a antibody specific for phosphorylated α-synuclein (anti-Pser129) have shown extensive accumulation of phosphorylated α-synuclein in neurites in the deeper layers of the cerebral cortex,

thalamus and diencephalons, and in neurons in the inferior pontine and olivary nuclei [32].

The present study is addressed to explore α-synuclein/rab3a binding, by using immunoprecipitation assays, in the cerebellar white matter (enriched in GCIs) and cerebral cortex (with no GCIs) in MSA cases compared with corresponding regions in age-matched controls.

Materials and Methods

General procedures and immunohistochemistry

Five cases of MSA were examined in the present study. They were four males aged 54, 57, 61 and 62 years, and one woman aged 62. Three cases (two men and the woman) had suffered from parkinsonism, urinary disturbances and postural hypotension with L-dopa therapy (two cases). Two cases had suffered from predominant gait and limb ataxia, nystagmus, tremor and dysarthria followed by rigidity. Death occurred between six and eight years after onset as a result of respiratory infections, excepting one case of sudden death of unknown origin but presumably related with autonomic failure. The clinical diagnosis was MSA in three cases and Parkinson's disease in the remaining two. Autopsy was carried out between three and eight hours after death. Brain samples were obtained from the Institute of Neuropathology and University of Barcelona Brain Banks following the guidelines of the local Ethics Committees. At autopsy, half of the brain was fixed in 10% formalin for no less than three weeks, whereas the other half was cut in coronal sections 1 mm thick, frozen on dry ice and stored at -80ºC until use. The neuropathological study was carried out in formalin-fixed, paraffin-embedded sections of the frontal, primary motor, primary somatosensory, posterior parietal, primary and association visual, temporal superior, temporal inferior, anterior insular, anterior cingulate and enthorinal cortices; subiculum, and anterior and posterior levels of the hippocampus; caudate and putamen, nucleus pallidus, amygdala, Meynert nucleus, and medial and posterior levels of the thalamus; midbrain (two levels); pons (two levels, including the locus ceruleus) and medulla oblongata (two levels); and upper vermis, lateral hemisphere and dentate nucleus of the cerebellum. The spinal cord was available for study in three cases. De-waxed sections were stained with haematoxylin and eosin, luxol fast blue-Klüver Barrera, or processed for immunohistochemistry following the streptavidin-peroxidase method (Supersensitive kit, Menarini) or with the EnVision + System Peroxidase (DAB) procedure (Dako) to βA4 amyloid (M. Sarasa, Zaragoza; Boehringer-Mannheim), *tau* (Sigma) phospho-*tau* (phospho-specific antibodies Thr^{181}, Ser^{202}, Ser^{214}, Ser^{262}, Ser^{396}, Ser^{422}: Calbiochem), αB-crystallin (Novocastra), α-synuclein (Chemicon), ubiquitin (Dako), phosphorylated neurofilament epitopes (Boehringer), and α- and β-tubulin (Sigma). Antibodies to rab3a were obtained from Santa Cruz Biotechnology and Calbiochem, and were used at dilutions of 1:700 and 1:500, respectively.

Control cases were two men and two women (mean age 67 years) with no neurological disease. The post-mortem delay in tissue processing was between four and six hours. Control and diseased cases were processed in parallel.

α-synuclein and rab3a immunoprecipitation and Western blotting

To test rab3a binding to α-synuclein, α-synuclein immunoprecipitation and immunoblot were carried out in samples (0.3 g) of the cerebellar white matter and cerebral cortex (area 8) of MSA and control cases. The samples were homogenized in a glass homogenizer in 10 volumes of ice-cold immunoprecipitation buffer (Hepes 20 mM pH 7.2, 1% Triton X-100, 1% sodium deoxycholate, 0.2% SDS, 150 mM NaCl, 1 mM sodium orthovanadate, 1 mM sodium fluoride, 10% glycerol, 10 µg/ml aprotinin, 1 mM phenylmethylsulfonyl fluoride), sonicated and centrifuged at 5,000 rpm for 10 min at 4ºC. The supernatant S1 was further centrifuged at 37,000 rpm for 1 h at 4ºC to generate the cytosolic fraction, S2. The S2 fraction was pre-cleared with protein G-sepharose (Amersham) for 30 min at 4ºC. Protein concentration was determined using the BCA method (Pierce) with bovine serum albumin as a standard. Equal aliquots of pre-cleared sample were incubated with anti-α-synuclein antibody (Neomarkers) and 30 µl of 1:1 (v:v) protein G-sepharose for 4 hours at 4ºC. The immune complexes were collected by centrifugation and washed five times with a buffer containing 20 mM Tris-HCl pH 7.5, 1 mM EDTA, 1 mM EGTA, 150 mM NaCl, 2 mM sodium orthovanadate, 10% glycerol and 1% Nonidet P-40 (Sigma). The pellet was re-suspended with 20 µl of reducing sample buffer, and the immunocomplexes were processed for 10% SDS-PAGE electrophoresis and Western blot analysis. The membranes were incubated with anti-α-synuclein (Chemicon), anti-rab3a (Santa Cruz Biotechnology), anti-tubulin (Sigma) and anti-*tau* (Sigma) used at dilutions 1:2,000, 1:1,000, 1:1,000 and 1:500, respectively. The protein bands were visualized using the ECL method (Amersham). Total homogenates and immunoprecipitated samples were processed in parallel; an additional lane contained the antibody used for immunoprecipitation bound to protein G-sepharose with no sample, and was used as a control of the immunoprecipitation.

Rab3a immunoprecipitation assay was performed following a modified protocol. Briefly, 0.2 g of cerebellar white matter from MSA and control cases was homogenized in 7 volumes of immunoprecipitation buffer (20 mM Tris-HCl pH 8.0, 1 mM EDTA, 150 mM NaCl and 1% Nonidet P-40) and sonicated. After centrifugation at 5,000 rpm for 10 min at 4ºC, the pellet was discarded and the supernatant S1 was ultracentrifuged at 37,000 rpm for 1 h at 4ºC. The pellet was discarded, and the supernatant S2 was pre-cleared with 40 µl of protein G-sepharose for 30 min at 4ºC. The protein concentration was

determined by the BCA method, and 2.5 mg of the pre-cleared sample was incubated at 4ºC overnight with the anti-rab3a antibody (Calbiochem) immobilized in protein G-sepharose beads. After washing, bound proteins were eluted by re-suspending in non-reducing SDS sample buffer and boiled. Then, the samples were processed for 10% SDS-PAGE electrophoresis followed by Western blot analysis with anti-rab3a (Santa Cruz Biotechnology) or anti-α-synuclein (Chemicon) antibodies used at dilutions of 1:1,000 and 1:2,000, respectively. The protein bands were visualized using the ECL method. Total homogenates and immunoprecipitated samples were processed in parallel, together with a lane containing the antibody used for immunoprecipitation bound to protein G-sepharose with no sample.

Results

General neuropathological findings and rab3a immunohistochemistry

The neuropathological study showed predominant neuron loss, astrocytic gliosis and microgliosis in the substantia nigra, caudate and putamen, locus ceruleus, inferior olive, pontine nuclei, Purkinje cell layer of the cerebellum and intermediodorsal columns of the spinal cord. Involvement of the globus pallidus, thalamus and cerebral cortex was less severe and variable from one case to another. Cases presenting with cerebellar symptoms showed marked cerebellar atrophy with granule cell loss, in addition to Purkinje cell loss and axonal torpedoes in the remaining Purkinje cells, loss of neurons in the dentate nucleus, and severe atrophy and demyelination of the middle and inner cerebellar peduncles and cerebellar white matter. The neuropathological findings were consistent with the clinical symptoms in individual cases as recognized in MSA-C and MSA-P phenotypes [26].

The most characteristic finding was the presence of GCIs in the majority of oligodendroglial cells in the brain stem, cerebellar peduncles, cerebellar white matter, caudate, putamen, globus pallidus, internal and external capsules, the motor cortex and the frontal cerebral white matter. GCIs were also observed in the spinal cord.
GCIs were stained with anti-α-synuclein, αB-crystallin, ubiquitin, tubulin and *tau* antibodies (Fig. 1 A-E). The inclusions were not stained with anti-phospho-*tau* antibodies and with antibodies to phosphorylated neurofilament epitopes. GCIs were also immunostained with anti-rab3a antibodies (equal results with the two anti-rab3a antibodies used in the present study) (Fig. 1 F). Yet the number of rab3a-positive GCIs was roughly 1/10 of the total GCIs, when compared with consecutive serial sections stained with anti-α-synuclein antibodies.

Immunoprecipitation and Western blotting

Since previous studies have shown α-synuclein association with certain cytoskeletal proteins [5, 12, 22], we first processed the α-synuclein-immunoprecitated samples with anti-*tau* and anti-tubulin antibodies. Specific bands at the appropriate molecular weights (60 kDa and about 55 kDa, respectively) were obtained in total homogenates and in α-synuclein-immunoprecipitated samples from control and MSA cases (Fig. 2). These results indicate that α-synuclein binds to *tau* and tubulin equally in MSA and control cerebellar white matter, even considering the higher amount of *tau* in controls when compared with MSA brains (Fig. 2).

Total homogenates and α-synuclein-immunoprecipitated samples were immunoblotted with α-synuclein to validate the immunoprecipitation. Similar density bands of α-synuclein were recovered in total homogenates of control and MSA cases. No differences in the density of α-synuclein-immunoprecipitated bands were found in the cerebellar white matter of control and MSA cases (Fig. 3, upper panel). However, different patterns were seen in α-synuclein-immunoprecipitated samples immunoblotted with anti-rab3a antibodies. No immunoreaction was found in control cases, but a slight band was obtained in the cerebellar white matter in MSA (Fig. 3, middle panel). This reaction was specific as no bands were observed in the lane containing the antibody with protein G-sepharose with no sample.

To confirm the veracity of this observation, rab3a immunoprecipitation assay was performed. Total homogenates and immunoprecipitated samples of the cerebellar white matter were immunoblotted with anti-α-synuclein antibodies. Distinct patterns were seen between control and MSA rab3a-immunoprecipitated samples. No immunoreaction was observed in control cases, but a slight α-synuclein-immunoreactive band was obtained in the cerebellar white matter in MSA. Positive controls were total homogenates and the negative control was the lane containing the antibody and protein G-sepharose with no sample (Fig. 3, inner panel).

Cerebral cortex (Fig. 4)

Discussion

GCIs are composed of protein collections with a core of fibrils of abnormal, partially insoluble and phosphorylated α-synuclein that forms aggregates of truncated isoforms [10, 11, 12, 13, 39]. Normally, α-synuclein is mainly expressed in neurons and participates in synaptic function [6, 16, 24, 29]. The reason for its accumulation in MSA oligodendrocytes is not known. Extended α-synuclein immunoreactivity has been demonstrated in MSA [9], but the expression levels of α-synuclein mRNA in MSA do not differ from those for controls, thus suggesting that the transcriptional regulation of the α-synuclein gene is not affected in MSA [33]. Whether α-synuclein is synthesized in neurons and then transferred to oligodendroglia, or is primarily produced in oligodendrocytes, is not known. Yet it is worth emphasizing that α-synuclein is over-expressed in the whole brain in MSA [9], and that α-synuclein is also present in neuronal nuclear inclusions and neurites in MSA as revealed by immunoelectronmicroscopy [28]. Moreover, α-synuclein deposition is also encountered in glial cells in Lewy body diseases, including PD [3, 37, 40]. Taken together, these findings show the wide distribution of abnormal α-synuclein in MSA, and the expression of α-synuclein in glial cells under determinate conditions.

In addition to α-synuclein, ubiquitin, αB-crystallin, *tau*, tubulin, microtubule-associated protein-5 (MAP-5), protein 14-3-3, cyclin-dependent kinase 5 (cdk5) and its activator p39, and mitogen activated protein kinase (MAPK) and its substrate transcription factor Elk-1 are components of GCIs [1, 2, 5, 12, 16, 19, 20, 26, 30, 31, 34]. Protein nitration occurs in DLBD and MSA inclusions, but nitration is not a prerequisite for α-synuclein deposition [18]. The nature of these constituents indicates an involvement of major and associated components of microtubules, including kinases (i.e. MAPK and cdk5) that regulate phosphorylation of *tau*, MAPs and neurofilaments. The relationship between α-synuclein and protein aggregates is not clear, but some insights point to possible direct and cross interactions. Combined biochemical assays have shown that *tau* binds to the C terminus of α-synuclein and only *tau* that is not bound to microtubules can interact with α-synuclein [22]. Although there is no evidence of direct binding between α-synuclein and Elk-1, recent studies have shown that α-synuclein and Elk-1 both bind to MAP/ERK-2 kinase in cells co-transfected with α-synuclein and Elk-1 [20].

Previous studies in our laboratory have shown abnormal α-synuclein/rab interactions in DLBD and in transgenic mice expressing A30P mutant human α-synuclein [7, 8]. This is a notable event, as rab family members are crucial membrane organizers that coordinate membrane transport, vesicle formation, and vesicle and organelle motility [42]. Rab3a is mainly found in exocytotic and synaptic vesicles, and facilitates, in association with

rabphilin-3, α-actinin and rabphilin-5, exocytic and synaptic vesicle motility and fusion to the cytoplasmic membrane [14, 15, 42]. It has been proposed that abnormal α-synuclein/rab interactions impair synaptic transmission, protein transport and endocytosis (including dopamine endocytosis) in human and experimental α-synucleinopathies [7, 8].

The present findings show rab3a immunoreactivity in a low percentage of GCIs in MSA-P and MSA-C; rab3a immunoreactivity is less abundant than ubiquitin, αB-crystallin, *tau* and tubulin immunostaining in GCIs. Moreover, rab3a binds to α-synuclein in cerebellar white matter of MSA cases but not in cerebellar white matter of controls. MSA but not in control white matter, as revealed by combined α-synuclein and rab3a immunoprecipitation assays.

Recent immunohistochemical studies using antibodies directed to phosphorylated α-synuclein have shown widespread α-synuclein accumulation not only in GCIs but also in neuropil threads in the diencephalon and brain stem, and in the cerebral cortex and thalamus [32]. This important observation indicates that, although abnormal α-synuclein is mainly accumulated in glial cells, there is a substantial amount of abnormal α-synuclein in neurons in MSA, and, therefore, MSA has to be considered a generalized α-synucleinopathy with glial and neuronal involvement.

In line with these observations, immunoprecipitation studies in the frontal cortex (in which no GCIs were present) have shown abnormal α-synuclein/rab3a binding in MSA cases when compared with control brains. These findings demonstrate that abnormal α-synuclein/rab3a interactions in MSA occur in regions with GCIs (some of them containing both α-synuclein and rab3a), and in regions with no GCIs.

These findings indicate that abnormal α-synuclein in MSA has the capacity to interact with rab3a, and to sustain fatal protein attractions that are common to other protein aggregates in neurodegenerative disorders [27]. Finally, these observations may also sustain generalized functional implications as impaired transport of membranes and synaptic vesicles, and abnormal synaptic transmission in MSA.

Acknowledgements

This work was supported in part by FIS grants PI02/0004, C03-006 and G03-0167, and by Brain Net II. We thank T. Yohannan for editorial assistance.

References

1. Abe H, Yagishita S, Amano N, Iwabuchi K, Hasegawa K, Kowa K (1992) Argyrophilic glial intracytoplasmic inclusions in multiple system atrophy: immunocytochemical and ultrastructural study. Acta Neuropathol 84: 273-277

2. Arai N, Nishimura M, Oda M, Morimatsu Y, Ohe R, Nagatomo H (1992) Immunohistochemical expression of microtubule-associated protein 5 (MAP5) in glial cells in multiple system atrophy. J Neurol Sci 109: 102-106

3. Arai T, Ueda K, Ikeda K, Akiyama H, Haga C, Kondo H, Kuroki N, Niizato K, Iritani S, Tsuchiya K (1999) Argyrophilic glial inclusions in the midbrain of patients with Parkinson's disease and diffuse Lewy body disease are immunopositive for NACP/-α-synuclein. Neurosci Lett 259: 83-86

4. Arima K, Ueda K, Sunohara N, Arakawa K, Hirai S, Nakamura M, Tonozuka-Uehara H, Kawai M (1998) NACP/α-synuclein immunoreactivity in fibrillary components of neuronal and oligodendroglial cytoplasmic inclusions in the pontine nuclei in multiple system atrophy. Acta Neuropathol 96: 439-444

5. Cairns NJ, Atkinson PF, Hanger DP, Anderton BH, Daniel SE, Lantos PL (1997) *Tau* protein in the glial cytoplasmic inclusions of multiple system atrophy can be distinguished from abnormal *tau* in Alzheimer's disease. Neurosci Lett 230: 49-52

6. Clayton DF, George JM (1998) The synucleins: a family of proteins involved in synaptic function, plasticity, neurodegeneration and disease. Trends Neurosci 21: 249-254

7. Dalfó E, Barrachina M, Rosa JL, Ambrosio S, Ferrer I (2004a) Abnormal α-synuclein interactions with rab3a and rabphilin in Diffuse Lewy body disease. Neurobiol Dis (in press)

8. Dalfó E, Gómez-Isla T, Rosa JL, Nieto Bodelón M, Cuadrado Tejedor M, Barrachina M, Ambrosio S, Ferrer I (2004b) Abnormal α-synuclein interactions with rab proteins in α-synuclein A30P transgenic mice. J Neuropathol Exp Neurol (in press)

9. Dickson DW, Liu W-K, Hardy J, Farrer M, Mehta N, Uitti R, Mark M, Zimmerman T, Golbe L, Sage J, Sima A, D'Amato C, Albin R, Gilman S, Yen S-H (1999) Widespread alterations of α-synuclein in multiple system atrophy. Am J Pathol 155: 1241-1251

10. Duda JE, Giasson BI, Gur TL, Montine TJ, Robertson D, Biaggioni I, Hutig HI, Stern MB, Gollomp SM, Grossman M, Lee VM, Trojanowski JQ (2000) Immunohistochemical and biochemical studies demonstrate a distinct profile of α-synuclein permutations in multiple system atrophy. J Neuropathol Exp Neurol 59: 830-841

11. Fujiwara H, Hasegawa M, Dohmae N, Kawashima A, Masliah E, Goldberg S, Shen J, Takio K, Iwatsubo T (2002) α-synuclein is phosphorylated in synocleinopathy lesions. Nature Cell Biol 4: 160-164

12. Gai WP, Power JHT, Blumbergs PC, Culvenor JG, Jensen PH (1999) α-synuclein immunoisolation of glial inclusions from multiple system atrophy brain reveals multiprotein components. J Neurochem 73: 2093-2100

13. Gai WP, Pountney DL, Power JHT, Li QX, Culvenor JG, McLean CA, Jensen PH, Blumbergs PC (2003) α-synuclein fibrils constitute the central core of oligodendroglial inclusion filaments in multiple system atrophy. Exp Neurol 181: 68-78

14. Geppert M, Bolshakov VY, Siegelbaum SA, Takei K, DeCamilli P, Hammer RE, Südhof TC (1994) The role of Rab3a in neurotransmitter release. Nature 369: 493-497

15. Geppert M, Südhof TC (1998) Rab3 and synaptotagmin: The yin and yang of synaptic membrane fusion. Annu Rev Neurosci 21: 75-95

16. Giasson BI, Mabon ME, Duda JE, Montine TJ, Robertson D, Hurtig HI, Lee VM, Trojanowski JQ (2003) Tau and 14-3-3 in glial cytoplasmic inclusions of multiple system atrophy. Acta Neuropathol 106: 243-250

17. Goedert M (2001) Alpha-synuclein and neurodegenerative diseases. Nat Rev Neurosci 2: 492-501

18. Gómez-Tortosa E, Gonzalo I, Newell K, García de Yébenes J, Vonsattel JP, Hyman BT (2002) Patterns of protein nitration in dementia with Lewy bodies and striatonigral degeneration. Acta Neuropathol 103: 495-500

19. Honjyo Y, Kawamoto Y, Nakamura S, Nakano S, Akiguchi I (2001) p39 immunoreactivity in glial cytoplasmic inclusions in brains with multiple system atrophy. Acta Neuropathol 101: 190-194

20. Iwata A, Miura S, Kanazawa I, Sawada M, Nukina N (2001) α-synuclein forms a complex with transcription factor Elk-1. J Neurochem 77: 239-252

21. Jellinger K (2003) Neuropathological spectrum of synucleinopathies. Mov Disord Suppl 6: S2-12

22. Jensen PH, Hager H, Nielsen MS, Hojrup P, Glieman J, Jakes R (1999) Alpha-synuclein binds to *tau* and stimulates the protein kinase A - catalyzed *tau* phosphorylation of serine residues 262 and 356. J Biol Chem 274: 25481-25489

23. Kato S, Nakamura H (1990) Cytoplasmic argyrophilic inclusions in neurons of pontine nuclei in patients with olivopontocerebellar atrophy: immunohistochemical and ultrastructural studies. Acta Neuropathol 79: 584-594

24. Khale PJ, Haas C, Kretzschmar HA, Neumann M (2002) Structure/function of α-synuclein in health and disease: rational development of animal models for Parkinson's and related diseases. J Neurochem 82: 449-457

25. Lantos PL (1998) The definition of multiple system atrophy: a review of recent developments. J Neuropathol Exp Neurol 57: 1099-1111

26. Lantos PL, Quinn N (2003) Multiple system atrophy. In: Dickson D (edit) Neurodegeneration: The molecular pathology of dementia and movement disorders, ISN Neuropath Press, Basel, pp 203-213

27. Lee VMY, Trojanowski JQ, Buée L, Christen Y (2000) Fatal attractions: protein aggregates in neurodegenerative disorders. Springer, Berlin, Heidelberg, New York, Barcelona, Hong Kong, London, Milan, Paris, Singapore, Tokyo

28. Lin WL, DeLucia MW, Dickson DW (2004) α-synuclein immunoreactivity in neuronal nuclear inclusions and neurites in multiple system atrophy. Acta Neuropathol 9: 99-102

29. Lykkebo S, Jensen PH (2002) Alpha-synuclein and presynaptic function. NeuroMolec Med 2: 115-129

30. Murayama S, Arima K, Nakazato Y, Satoh J, Oda M, Inose T (1992) Immunocytochemical and ultrastructural studies of neuronal and oligodendroglial cytoplasmic inclusions in multiple system atrophy. 2. Oligodendroglial cytoplasmic inclusions. Acta Neuropathol 84: 32-38

31. Nakamura S, Kawamoto Y, Nakano S, Akiguchi I, Kimura J (1998) Cyclin-dependent kinase 5 and mitogen-activated protein kinase in glial cytoplasmic inclusions in multiple system atrophy. J Neuropathol Exp Neurol 57: 690-698

32. Nishie M, Mori F, Fujiwara H, Hasegawa M, Yoshimoto M, Iwatsubo T, Takahashi H, Wakabayashi K (2004) Accumulation of phosphorylated synuclein in the brain and peripheral ganglia of patients with multiple system atrophy. Acta Neuropathol

33. Ozawa T, Okuizumi K, Ikeuchi T, Wakabayashi K, Takahashi H, Tsuji S (2001) Analysis of the expression level of α-synuclein mRNA using post-mortem brain samples from pathologically confirmed cases of multiple system atrophy. Acta Neuropathol 102: 188-190

34. Papp MI, Kahn JE, Lantos PL (1989) Glial cytoplasmic inclusions in the CNS of patients with multiple system atrophy (striatonigral degeneration, olivopontocerebellar atrophy and Shy-Drager syndrome). J Neurol Sci 94: 79-100

35. Shibuya K, Uchihara T, Nakamura A, Ishiyama M, Yamaoka K, Yagishita S, Iwabuchi K, Kosaka K (2003) Reversible conformational change of tau2 epitope on exposure to detergent in glial cytoplasmic inclusions of multiple system atrophy. Acta Neuropathol 105: 508-514

36. Spillantini MG, Crowther RA, Jakes R, Cairns NJ, Lantos PL, Goedert M (1998) Filamentous α-synuclein inclusions link multiple system atrophy with Parkinson's disease and dementia with Lewy bodies. Neurosci Lett 251: 205-208

37. Takeda A, Hashimoto M, Mallory M, Sundsumo M, Hansen L, Masliah E (2000) C-terminal α-synuclein immunoreactivity in structures other than Lewy bodies in neurodegenerative diseases. Acta Neuropathol 99: 296-304

38. Tamaoka A, Mizusawa H, Mori H, Shoji S (1995) Ubiquitinated αB-crystallin in glial cytoplasmic inclusions from the brain of a patient with multiple system atrophy. J Neurol Sci 129: 192-198

39. Tu PH, Galvin JE, Baba M, Giasson B, Tomita T, Leight S, Nakajo S, Iwatsubo T, Trojanowski JQ, Lee VM (1998) Glial cytoplasmic inclusions in white matter oligodendrocytes of multiple system atrophy: brains contain insoluble α-synuclein. Ann Neurol 44: 415-422

40. Wakabayashi K, Hayashi S, Yoshimoto M, Kudo H, Takahashi H (2000) NACP/ α-synuclein-positive filamentous inclusions in astrocytres and oligodendrocytes of Parkinson's disease brains. Acta Neuropathol 99: 14-20

41. Wakabayashi K, Yoshimoto M, Tsuji S, Takahashi H (1998) α-synuclein immunoreactivity in glial cytoplasmic inclusions in multiple system atrophy. Neurosci Lett 249: 180-182

42. Zerial M, McBride H (2001) Rab proteins as membrane organizers. Nature Rev 2: 107-119

Figure legends

Fig. 1: GCIs in the cerebellar white matter in MSA as revealed with antibodies to α-synuclein (A), αB-crystallin, ubiquitin (C), β-tubulin (D), *tau* (E) (Sigma; GCIs were not stained with anti-phospho-*tau* antibodies) and rab3a (F). Note that a small percentage of GCIs is immunostained with anti-rab3a. Paraffin sections, slight haematoxylin counterstaining, bar = 25 µm.

Fig. 2: Total homogenates and α-synuclein-immunoprecipitated samples of the cerebellar white matter of control (CB) and Multiple System Atrophy (MSA) cases immunoblotted for anti-*tau* (right panel) reveal specific bands at the appropriate molecular weights (between 45 and 70 kDa) in total homogenates. Similar and additional bands of lower molecular weights are found in CB and MSA immunoprecipitates The same membranes exposed to anti-tubulin antibody (left panel) reveal specific bands at the corresponding molecular weight (55 kDa) in total homogenates and in α-synuclein-immunoprecipitated samples from CB and MSA. No immunoreaction is seen in the lanes corresponding to the antibody and protein G-sepharose with no sample (Anti-α-syn + protG).

Fig. 3: Total homogenates and α-synuclein-immunoprecipitated samples of the cerebellar white matter of control (CB) and Multiple System Atrophy (MSA) cases immunoblotted for anti-α-synuclein reveal specific bands at the appropriate molecular weight (19 kDa) in total homogenates and in α-synuclein-immunoprecipitated samples of CB and MSA cases (upper panel). The membrane also shows several non-specific bands of higher molecular weight (36 and 66 kDa) which are also present in the lane containing the antibody and protein G-sepharose with no sample. The same membranes immunoblotted with anti-rab3a antibody (lower left panel) show a strong band at the appropriate molecular weight (24 kDa) in total homogenates from CB and MSA. A discrete rab3a-immunoreactive band is recovered in α-synuclein-immunoprecipitated samples from MSA cases, but not from control brains. Non-specific bands of about 30 kDa are also present in the immunoprecipitates. Total homogenates and rab3a-immunoprecipitated samples of CB and MSA cases immunoblotted for anti-α-synuclein (lower right panel) show a strong band at the appropriate molecular weight (19 kDa) in total homogenates from CB and MSA. A discrete α-synuclein-immunoreactive band is recovered in rab3a-immunoprecipitated samples from MSA cases, but not from control brains. No immunoreaction is seen in the lane containing the corresponding antibody and protein G-sepharose with no sample (Anti-α-syn + protG and Anti-rab3a + protG).

Fig. 4: Total homogenates and α-synuclein-immunoprecipitated (IP syn) samples of the cerebral cortex (area 8) (C) and Multiple System Atrophy (MSA) cases immunoblotted for anti-α-synuclein reveal specific bands at the appropriate molecular weight (20 kDa) in total homogenates and in α-synuclein-immunoprecipitated samples of C and MSA cases (upper panel). The same membranes blotted with anti-rab3a show a band of 24 kDa only in MSA. Non specific bands of about 29 kDa can also bee seen in the blot.

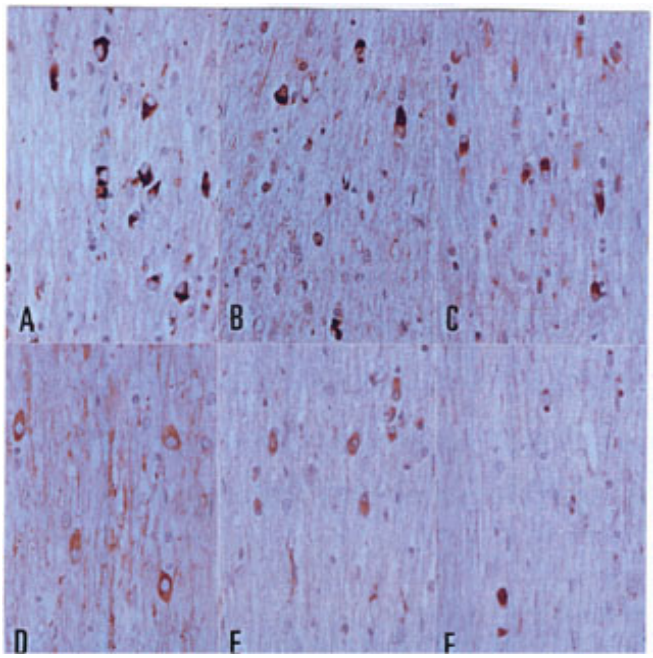

Fig.1

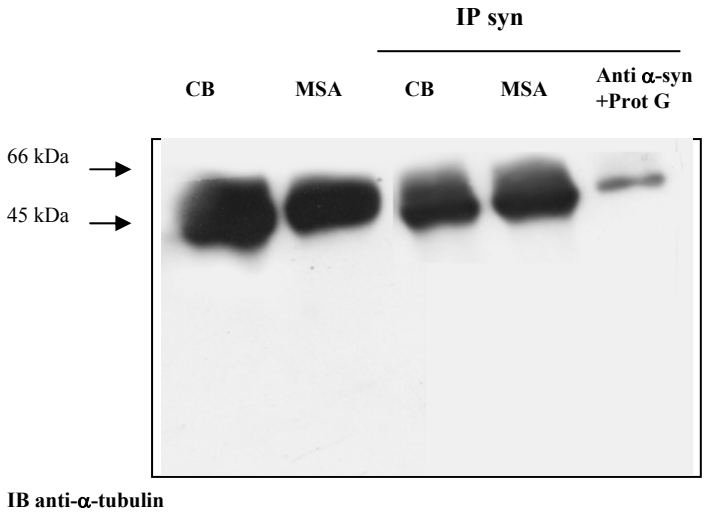
IP syn
CB
MSA
CB
MSA
Anti α-syn
+Prot G
66 kDa
45 kDa
IB anti-α-tubulin

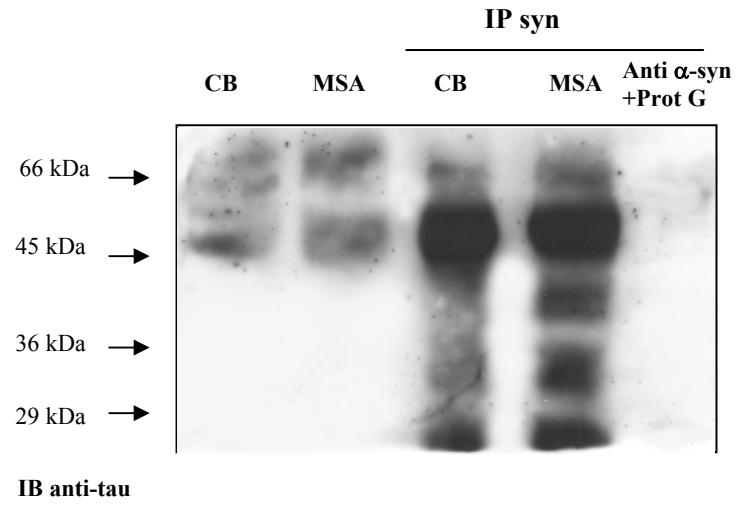
IP syn
CB
MSA
CB
MSA
Anti α-syn
+Prot G
66 kDa
45 kDa
36 kDa
29 kDa
IB anti-tau

Fig.2

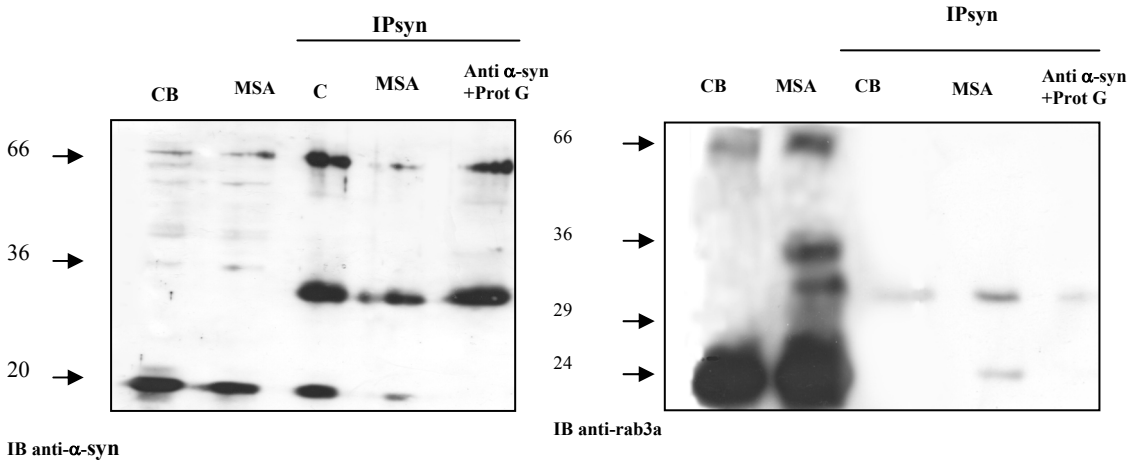
IPsyn
CB
MSA
C
MSA
Anti α-syn
+Prot G
66
36
20
IB anti-α-syn
IPsyn
CB
MSA
CB
MSA
Anti α-syn
+Prot G
66
36
29
24
IB anti-rab3a

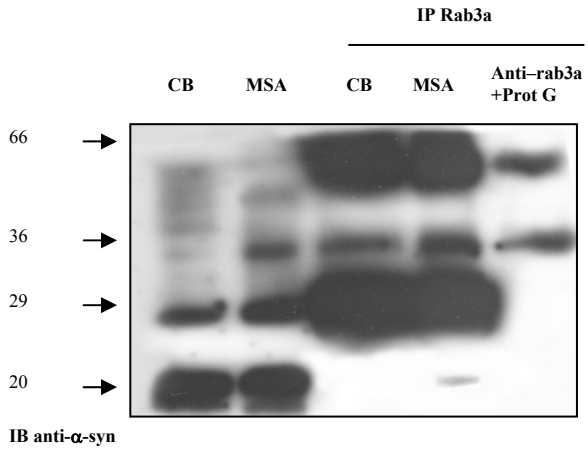
IP Rab3a
CB
MSA
CB
MSA
Anti–rab3a
+Prot G
66
36
29
20
IB anti-α-syn

Fig.3

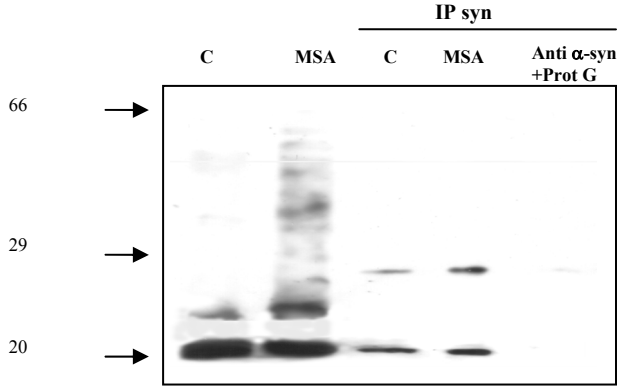

IB anti-α-syn

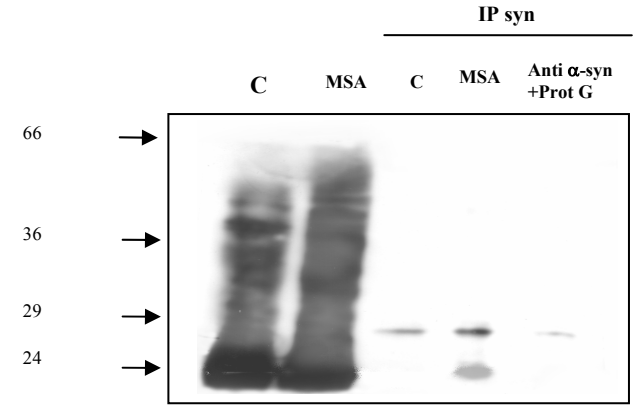

IB anti-rab3a

Fig.4

II ALTERACIONS DELS RECEPTORS METABOTRÒPICS DEL GLUTAMAT EN LA DEMÈNCIA AMB COSSOS DE LEWY

II.I. Dalfó E, Albasanz JL, Martin M, Ferrer I *Abnormal metabotropic glutamate receptor expression and signalling in the cerebral cortex in diffuse Lewy body Disease is associated with irregular α-synuclein/phospholipase C (PLCβ1) interactions. Brain Pathol 2004;14:388-398.*

La demència amb cossos de Lewy és una malaltia del sistema nerviós que es caracteritza per la presència d'inclusions proteiques anomenades cossos de Lewy, dels quals l'α-sinucleïna n'és el principal component. La demència amb cossos de Lewy es pot presentar de dues maneres diferents. O bé associada a canvis tipus Alzheimer anomenant-se forma comú (DLBDc), o bé sense aquests canvis esmentats, de manera que es parla de la forma pura (DLBDp). Ambdues formes de demència presenten anormalitats en els sistema de neurotransmissors dopaminèrgics, noradrenèrgics, serotoninèrgics i colinèrgics. El que hem volgut estudiar en el següent treball és si els receptors metabotròpics del glutamat també resultaven afectats i si l'α-sinucleïna participava d'alguna manera en aquesta alteració. Per dur a terme l'estudi dels receptors metabotròpics s'han fet experiments de captació d'aquests receptors, així com l'anàlisi de la seva expressió per western blot. Al mateix temps, i donat que un dels efectors més importants d'aquest receptors és la fosfolipasa Cβ1 (PLCβ1), s'han analitzat tan l'activitat com l'expressió d'aquesta proteïna en DLBD. Donada la capacitat d'interacció de l'α-sinucleïna amb altres proteïnes així com la seva importància en les DLBDs, hem volgut estudiar la influència de l'α-sinucleïna en tot aquest sistema mitjançant experiments d'immunoprecipitació i d'aïllament d'agregats isolubles d'α-sinucleïna. Hem trobat alteració en el sistema glutamatèrgic així com disminució tan en l'expressió com en l'activitat de la PLCβ1. Curiosament també hem demostrat que PLCβ1 interacciona amb l'α-sinucleïna en condicions control i no en condicions patològiques, mentre que en DLBDs la PLCβ1 es localitza a la fracció més insoluble de l'α-sinucleïna, corresponent a la seva forma més tòxica. Per tant en condicions no patològiques la interacció de l'α-sinucleïna seria necessària per a una correcta funció de la PLCβ1, mentre que en condicions patològiques la PLCβ1 restaria segrestada juntament amb altres proteïnes en la fracció insoluble de l'α-sinucleïna, impedint-se d'aquesta manera que realitzi la seva funció com a efectora dels receptors del glutamat.

III. L'ESTRÈS OXIDATIU

III.I. Portero-Otín M, Dalfó E, Ayala MV, Pamplona R, Ferrer I (2004) *Evidence of oxidative stress in the cerebral cortex in asymptomatic Parkinson's disease (incidental Lewy body disease with brain stem involvement). (Enviat a Journal of Neuropathology and experimental Neurology).*

Tot i que l'estrès oxidatiu està sobradament descrit a la substància negra de la malaltia de Parkinson (PD), no es coneix si el seu efecte en el córtex cerebral podria tenir algun efecte en la progressió de la malaltia. Per portar a terme l'estudi s'ha analitzat l'estrès oxidatiu en sis casos de malalts de Parkinson verificats neuropatològicament, que en vida no van presentar gairebé símptomes neurològics, i per tant no es van sotmetre a teràpia anti-parkinsoniana. Igualment tampoc no presentaven altres anomalies neuropatològiques com les deposicions amiloidees. Paral.lelament es van comparar amb pacients control, analitzant-se per cromatografia de gasos els productes següents, estudiats prèviament en substància negra: El Semialdehid Glutàmic (GSA) i el Semialdehid Aminoadípic (AASA) ambdós marcadors de l'oxidació catalitzada per metalls i indicatius de l'alteració en l'oxidació proteica; l' N^{ε} (carboximetil) lisina (CML) i l' N^{ε} (carboxietil) lisina (CEL) com a marcadors de l'alteració glicoxidativa/lipoxidativa; l' N^{ε} (malondialdehid)-lisina (MDAL) com a marcador específic de l'alteració lipoxidativa juntament amb l'anàlisi dels perfils dels àcids grassos insaturats (UFA) i dels poliinsaturats (PUFA). A més a més, també s'han analitzat els productes derivats de glicosilació avançada (AGE) i els grups carbonils de les proteïnes reactius a la 2,4 dinitrofenilhidrazina (DNP). Mitjançant western blot també s'han analitzat tan els AGE com els seus receptors (RAGE). Els resultats obtinguts demostren que, així com es conserven els nivells de GSA i d' AASA, els nivells dels marcadors d'alteracions tan glicooxidativa com lipoooxidativa (CML i MDAL), els dels carbonils proteics reactius a DNP així com el nivell d'expressió del RAGE estan augmentats, demostrant-se d'aquesta manera una alteració proteica estructural en córtex de PD. També hi ha un augment en el contingut dels PUFA (n-6 i n-3), resultant en un augment en l'índex de peroxidació en el córtex de PD. Amb aquest estudi demostrem que hi ha estrès oxidatiu en estadis primerencs de la malaltia de Parkinson, en absència al tractament amb L-dopa, de manera que suggerim la possible utilització d'una teràpia anti-oxidant per combatre l'estrès oxidatiu i fer front a la malaltia de Parkinson.

EVIDENCE OF OXIDATIVE STRESS IN THE CEREBRAL CORTEX IN ASYMPTOMATIC PARKINSON'S DISEASE (INCIDENTAL LEWY BODY DISEASE WITH BRAIN STEM INVOLVEMENT)

Manuel Portero-Otín (2), Esther Dalfó (1), Mª Victoria Ayala (2), Reinald Pamplona (2) Isidre Ferrer (1, 3)

(1) Institut de Neuropatologia, Servei Anatomia Patològica, Hospital de Bellvitge; (3) Departament de Biologia Cel.lular i Anatomia Patològica, Facultad de Medicina, Universitat de Barcelona, Hospitalet de Llobregat, Spain

(2) Fisiopatologia Metabòlica, Departament de Ciències Mèdiques Bàsiques, Facultat de Medicina, Universitat de Lleida Lleida, Spain

Corresponding author:

Prof. I. Ferrer , Institut de Neuropatologia, Servei Anatomia Patològica, Hospital de Bellvitge, carrer Feixa Llarga sn, 08907 Hospitalet de Llobregat, Spain

E-mail : 8082ifa@comb.es or iferrer@csub.scs.es

Short Title: Oxidative stress in the PD cerebral cortex

Number of words: 7248

Pages: 31

Abstract

Oxidative stress has been well documented in the substantia nigra in Parkinson's disease (PD). However, little is known on oxidative changes in the cerebral cortex that may have a role in disease progression. The present study was undertaken to analyse oxidative stress damage in the frontal cortex of a six selected cases with neuropathologically-verified PD (brain stem Lewy body disease) who presented during life with no or with minor neurological symptoms that were not the object of anti-parkinsonian therapy. Other neuropathological abnormalities, particularly amyloid deposition, were absent in the present series. Six age-matched cases with no neurological symptoms and with normal neuropathological examination were used as controls and processed in parallel. The brains were obtained following the guidelines of the local Ethic Committee with post-mortem delays between 2 and 6 hours in control and diseased brains. Gas-chromatography coupled to mass spectrometry to detect and quantify the structurally characterized products of protein oxidative damage glutamic semialdehyde (GSA) and aminoadipic semialdehyde (AASA) as markers of metal-catalysed oxidation; N^{ε} (carboxymethyl) lysine (CML) and N^{ε} (carboxyethyl)lysine (CEL) as markers of mixed glycoxidative/lipoxidative damage, and N^{ε} □(malondyaldehyde)-lysine (MDAL) as a marker of specific lipoxidative damage, in addition to UFA and PUFA lipid profiles. Advanced glycation end (AGE) products and 2,4 dinitrophenilhydrazine (DNP)-reactive protein carbonyls have been examined by Western blotting as well as the expression of AGE receptors (RAGE). Results of the present study have shown preserved GSA and AASA concentrations, but increased glycoxidative and lipoxidative damage (increased levels of CML and MDAL), increased (DNP)-reactive carbonyls in delipidized and non-delipidized samples, and increased expression of RAGE, demonstrating structurally characterized protein oxidative damage in the cerebral cortex in PD. In addition, there is an increase in the content of the highly peroxidable decosahexaenoic acid, reduced content of PUFA n-6 family and increased content in the n-3 family of PUFA, overall resulting in a significant increase in the peroxidizatibility index in PD cortex. This study demonstrates oxidative stress in the cerebral cortex at relatively early stages of PD in the absence of L-dopa or other antiparkinsonian treatment. These findings further support anti-oxidant therapy in the treatment of PD in order to reduce cortical damage associated with oxidative stress.

***Key words**: Parkinson's disease, cerebral cortex, oxidative stress*

Introduction

Parkinson's disease (PD), characterized by resting tremor, slowness of initial movement, rigidity, and general postural instability, is one of the most prevailing neurodegenerative disorders among elderly population (Forno, 1996; Burke, 1999). The disease is pathologically defined by loss of neurons in the substantia nigra pars compacta, locus ceruleus, other nuclei of the brain stem, basal nucleus of Meynert and amygdala, and by the presence of eosinophilic intraneuronal proteinaceous inclusions called Lewy bodies and aberrant neurites (Forno, 1996; Gai et al., 2000; Jellinger and Mizuno, 2003). Lewy bodies and Lewy neurites are protein aggregates mainly composed of α-synuclein (Spillantini et al., 1998; Baba et al., 1998; Iwatsubo, 2003). α-synuclein is nitrated (Duda et al., 2000; Giasson et al., 2000), and residue Ser^{129} of α-synuclein is selectively and extensively phosphorylated in PD (Giasson et al., 2000; Fujiwara et al., 2002). Moreover, phosphorylation of α-synuclein at Ser^{129} promotes fibril formation (Fujiwara et al., 2002). Finally, altered conformation of α-synuclein and direct intermolecular interaction between the N-terminus of α-synuclein and ubiquitin occurs in Lewy bodies when compared with the neuropil (Sharma et al., 2001). The pathogenic role of α-synuclein is further supported by the association of autosomal dominant PD in families bearing mutations in the *α-synuclein* gene (Polymeropoulos et al., 1997; Krüger et al., 1998; Zarranz et al., 2003), and by the observation of *α-synuclein* locus triplication in a family with autosomal dominant PD (Singleton et al., 2003). Increased levels of α-synuclein (Hashimoto and Masliah, 1999), mutations in the *α-synuclein* gene (Narhi et al., 1999) and oxidative stress (Hashimoto et al., 1999; Paik et al., 2000) lead to α-synuclein aggregation. PD is considered within the spectrum of Lewy body diseases together with Diffuse Lewy body disease (DLBD) or Dementia with Lewy bodies (DLB), which is characterized by PD changes and widespread Lewy bodies and Lewy neurites in the cerebral isocortex and diencephalic nuclei (Kosaka and Iseki, 1996; Hansen, 1997; Ince et al., 1998)

Oxidative stress is a main contributory factor in the pathogenesis of PD (Markesbery et al., 2001; Silva and Schapira, 2001; Jenner, 2003). The sources of such oxidative stress are not clear but autoxidation of dopamine, and degradation of dopamine by monoamine oxidase are putative sources of oxidative stress in the substantia nigra; α-synuclein also promotes mitochondrial dysfunction and oxidative stress (Hsu et al., 2000; Lustbader et al., 2004). Decreased levels of reduced glutathione, consistent with reduced antioxidant capacity, have been also described in the substantia nigra in PD (Perry et al., 1982; Sian et al., 1994). This is accompanied by increased superoxide dismutase I and II protein and mRNA levels, suggesting response to superoxide generation, in nigral neurons

(Martilla et al., 1988; Saggu et al., 1989; Ceballos et al., 1990). Oxidative stress in PD is also evidenced by the observation of increased lipid hydroperoxides in the substantia nigra (Dexter et al., 1989; -94), increased levels of 4-hydroxy-2-nonenal (HNE), an end-product of lipid peroxidation, in the midbrain (Dexter et al., 1994; Yoritaka et al., 1996; Shelley, 1998), increased levels of polyunsaturated fatty acids (PUFA) (Dexter et al., 1986), and malondialdehyde and hydroperoxides in the substantia nigra (Jenner, 1991; -98). Moreover, protein oxidation is high in the substantia nigra, as evidenced by increased protein carbonyls in the substantia nigra and other brain regions in PD (Alam et al., 1997a; Floor et al., 1998). Advanced glycation end products (AGE) have been found in the substantia nigra and locus ceruleus in PD (Castellani et al., 1996). Finally, oxidative RNA and DNA damage also occurs in PD (Alam et al., 1997b; Zhang et al., 1999). These works rely on the reaction of 2,4-dinitrophenylhydrazine (DNP) with carbonyl groups. However, this assay has been criticised due to the possibility of artefacts (Cao et al., 1995). The direct measure of the concentration of structurally characterized products could overcome this fact and be used as a complement for assessing the effects of oxidative stress in vivo. Glutamic semialdehyde (GSA) derives from the metal-catalysed oxidation (MCO) of polyproline and polyarginine while aminoadipic semialdehyde (AASA) results from polylysine oxidation (Requena et al., 2001). These products are among the main carbonyl products of MCO of proteins (Requena et al., 2001), thus specific products of oxidation of amino-acids in protein. However, their presence and the factors affecting their concentrations in human brains are unknown up to date.

In spite of these observations focused on the substantia nigra, little is known about the possibility of oxidative stress in telencephalic structures in PD. Yet recent immunohistochemical studies using novel antibodies raised against oxidized α-synuclein have shown widespread α-synuclein pathology in the striatum in PD (Duda et al., 2002). Interestingly, oxidative DNA damage, as revealed by increased levels of 8-hydroxyguanine, not only occur in the substantia nigra but also in the basal ganglia and cerebral cortex in PD (Sánchez-Ramos et al., 1994).

The present study is directed to gain understanding on whether oxidative stress occurs in the cerebral cortex in cases with incidental PD, and therefore not subjected to pharmacological treatment for parkinsonism. Thus, in the present study we used gas-chromatography coupled to mass spectrometry (GC/MS) to detect and quantify the structurally characterized products of protein oxidative damage GSA and AASA as markers of MCO; N^{ε} (carboxymethyl) lysine (CML) and N^{ε} (carboxyethyl)lysine (CEL) as markers of mixed glycoxidative/lipoxidative damage, and N^{ε} □(malondyaldehyde)-lysine (MDAL) as a marker of specific lipoxidative damage, in addition to UFA and PUFA lipid

profiles. AGE products and DNP-reactive protein carbonyls have been examined by Western blotting as well as the expression of AGE receptors. The receptor for advanced glycation end products (RAGE) is a member of the immunoglobulin superfamily sensitive to the generation of reactive oxygen species that is crucial for many AGE-induced changes in cellular properties including activation of protein kinase pathways (Lander et al., 1997; Schmidt et al., 2000). Results of the present study, demonstrating structurally characterized protein oxidative damage, evidence oxidative stress in the cerebral cortex in PD.

Materials and methods

Tissue samples

Brain samples were obtained from the Institute of Neuropathology Brain Bank following the guidelines of the local Ethics Committee. At autopsy, half of the brain was fixed in formalin, whereas the other half was cut in coronal sections 1 cm thick, frozen on dry ice and stored at -80ºC until use. Six patients with PD and six age-matched controls were used in the present study. The post-mortem delay was between 2 and 6 h in control and diseased cases. Cases with prolonged agonal status were not considered for study. The neuropathological examination was carried out on 5 mμ thick de-waxed paraffin sections of the frontal (area 8), primary motor, primary sensoy, parietal posterior, anterior cingulate, visual (primary and association), superior, middle and inferior temporal, and anterior insular cortices; entorhinal and perirhinal cortex, subiculum and hippocampus; amygdala, nucleus basalis of Meynert; caudate and putamen; putamen and globus pallidus; thalamus and subthalamus; midbrain (two levels) including substantia nigra; pons (two levels, including on with locus ceruleus); medulla oblongata (two levels); cerebellar vermis and dentate nucleus of the cerebellum. Sections were stained with haematoxylin and eosin, luxol fast blue-Klüver Barrera, and processed for immunohistochemistry to glial fibrillary acidic protein for astroytes, CD68 and lectin to *Licopericum esculentum* for microglia, *tau* (including phospho-specific anti-*tau* antibodies to Thr181, Ser202, Ser214, Ser262, Ser396 and Ser422), β-amyloid, ubiquitin, phosphorylated neurofilament epitopes, αB-crystallin and α-synuclein. The same protocol was used in control and diseased brains.

In the present series, Lewy body pathology including Lewy bodies and Lewy neurites was practically restricted to characteristic nuclei of the brain stem. Lewy bodies and Lewy neurites were also present in the amygdala and nucleus basalis of Meynert; and Lewy neurites in the hippocampus, but cases with more than one Lewy body per section in the entorhinal cortex or in the cingulate cortex were excluded. No other anomalies were seen in these cases in the neuropathological examination. Particularly, cases with associated amyloid plaques or *tau* deposits in the cerebral cortex, including basal regions (stage A of Braak and Braak for amyloid plaques) or entorhinal cortex (stages I and II of Braak and Braak for neurofibrillary pathology), respectively, were excluded of the present study (Braak and Braak, 1999).

In every case, no neurological symptoms, if present, were the object of pharmacological treatment. Minor symptoms characterized by slight tremor, increased salivation and unusual inexpressive face and boredom, to use the terms applied for the relatives to the

neurological symptoms, were recorded in three cases. Based on the paucity of neurological deficits and the characteristic neuropathological features, the patients in the present series were categorized as asymptomatic Parkinson's disease or incidental Lewy body disease with brain stem involvement (Ferrer, 2002).

Biochemical studies

Samples of the frontal cortex (area 8) were homogenized at 4ºC in a buffer containing KCl 180 mM, MOPS 5 mM, EDTA 2 mM, DTPAC 1 mM and BHT 1 µM, pH 7.3. After a brief centrifugation (500 x G, 5 min, 4ºC) to pellet cellular debris, protein concentrations were measured in the supernatants using the Bio-Rad protein assay (Bio-Rad Laboratories, Hercules, CA, USA).

Measurement of GSA, AASA, CML, CEL and MDAL.

GSA, AASA, CML, CEL and MDAL concentrations in total proteins from frontal cortex (area 8) homogenates were measured by GC/MS as previously described (Pamplona et al., 2002). Samples containing 0.75-1 mg of protein were delipidated using chloroform:methanol (2:1 v/v), and proteins were precipitated by adding 10% trichloroacetic acid (final concentration) and subsequent centrifugation. Protein samples were reduced overnight with 500 mM $NaBH_4$ (final concentration) in 0.2 M borate buffer, pH 9.2, containing 1 drop of hexanol as an anti-foam reagent. Proteins were then re-precipitated by adding 1 ml of 20% trichloroacetic acid and subsequent centrifugation. The following isotopically labeled internal standards were then added: [$^2H_8$]Lysine (d8-Lys; CDN Isotopes); [$^2H_4$]CML (d4-CML), [$^2H_4$]CEL (d4-CEL), and [$^2H_8$]MDAL (d8-MDAL), prepared as described elsewhere (Knecht et al., 1991; Ahmed et al., 1997; Requena et al., 1997) [$^2H_5$]glutamic semialdehyde (d5-glutamic semialdehyde) and [$^2H_4$]aminoadipic semialdehyde (d4-aminoadipic semialdehyde), prepared as described (Requena et al., 2001). The samples were hydrolysed at 155^{o}C for 30 min in 1ml of 6 N HCl, and then dried *in vacuo*. The N,O-trifluoroacetyl methyl ester derivatives of the protein hydrolysate were prepared as previously described (Knecht et al., 1991). GC/MS analyses were carried out on a Hewlett-Packard model 6890 gas chromatograph equipped with a 30 m HP-5MS capillary column (30 m x 0.25 mm x 0.25 µm) coupled to a Hewlett-Packard model 5973A mass selective detector (Hewlett-Packard Española, S.A., Barcelona, Spain). The injection port was maintained at 275^{o}C; the temperature program was 5 min at 110^{o}C, then 2^{o}C/min to 150^{o}C, then 5^{o}C/min to 240^{o}C, then 25^{o}C/min to 300^{o}C, and finally hold at 300^{o}C for 5 min. Quantification was performed by external standardisation using standard curves constructed from mixtures of deuterated and non-deuterated standards. Analytes were detected by selected ion-monitoring GC/MS (SIM-GC/MS). The ions used were: lysine and d8-lysine, *m/z* 180 and 187, respectively; glutamic semialdehyde and d5-glutamic semialdehyde, *m/z* 280 and 285, respectively;

aminoadipic semialdehyde and d4-aminoadipic semialdehyde, *m/z* 294 and 298, respectively; CML and d4-CML , *m/z* 392 and 396, respectively; CEL and d4-CEL, *m/z* 379 and 383, respectively; and MDAL and d8-MDAL, *m/z* 474 and 482, respectively. The amounts of products were expressed as the ratio µmol glutamic semialdehyde, aminoadipic semialdehyde, CML, CEL or MDAL/mol lysine.

Electrophoresis and Westen blotting

Derivatization of proteins for carbonyl detection

Prior to electrophoresis, pools of samples were derivatized with DNP as previously described (Portero-Otin et al, 1999). Briefly, to 15 µl homogenates adjusted to 3,75 µg/µl protein SDS was added to a final concentration of 6%, and, after boiling for 3 min, 20 µl 10 mM 2,4-DNPH in 10% trifluoroacetic acid (TFA) were added. After 10 min at room temperature, 20 µl of a solution containing 2M Tris base, 30% glycerol and 15% β-mercaptoethanol were added for neutralisation and sample preparation for loading onto SDS-gels. For sample delipidation, prior to derivatization, chloroform (2:1 v/v) was added to an aliquot of the homogenates. Samples were then vortexed for 1 min and centrifuged at 13000 x G for 10 min. The proteins in the resulting supernatant were measured using the Bio-Rad protein assay and equalized.

Immunodetection of protein-bound 2,4-dinitrophenylhydrazones, AGEs and the glycoxidation product CML

For immunodetection, after SDS-PAGE, proteins were transferred using a Mini Trans-Blot Transfer Cell (Bio-Rad Laboratories, Madrid, Spain) to PVDF membranes (Immobilon-P Millipore, Bedford, MA). Immunodetection was performed using as primary antibodies: a rabbit anti-DNP antiserum (1:4,000, Dako V401, Carpenteria, CA); a monoclonal anti-CML antibody (1:2,000, Transgenic Inc 6D12, , Kumamoto, Japan); and a polyclonal anti-AGE antiserum, raised against glyoxilic acid-treated keyhole limpet hemocyanin (1:2,000). Peroxidase-coupled secondary antibodies were used from the Tropix chemiluminescence kit (Bedford, MA). Signal quantification and recording was performed with a CCD camera-based system (Lumi-Imager) from Boehringer Mannheim.

Detection of Receptor for Advanded Glycation End products (RAGE)

A slightly modified protocol was used. Briefly, samples (0.2 g) were homogenized in a glass homogenizer in 10 volumes of ice-cold lysis buffer (20 mM Hepes pH 7.5, 250 mM sucrose, 10 mM KCl, 1.5 mM $MgCl_2$, 1 mM EDTA, 1 mM EGTA, 1 mM DTT ,10 µg/ml aprotinin, 1 mM phenylmethylsulfonyl fluoride), and centrifuged at 5,000 rpm for 10 min at 4 °C. Pellet fractions were discarded and protein concentrations of the supernatants were determined by the BCA method with bovine serum albumin as a standard. Samples containing 50 µg of protein were loaded onto 10% acrylamide gels. Proteins were

separated by SDS-PAGE and electrophoretically transferred to nitrocellulose filters. After transfer, the filters were blocked by incubation with 5% skim milk in TBS-T buffer (100 mM Tris-buffered saline, 140 mM NaCl and 0.1% Tween 20, pH 7.4) for 1 h at room temperature (r.t.). Then, the filters were incubated overnight with TBS-T containing 3% Bovine Serum Albumin (BSA) (Sigma, Barcelona) and goat polyclonal anti-RAGE antibody (Santa Cruz, Quimigranel, Barcelona, Spain) used at a dilution of 1:100. Next, the filters were washed three times in TBS-T and incubated with TBS-T containing 5 % skim milk and horseradish peroxidase-linked goat immunoglobulins (Dako, Barcelona) diluted 1:1,000 for 45 minutes at r.t. Filters were washed several times in TBS-T, and the immunoreactivity was detected using an enhanced chemiluminescence Western blot detection system (Amersham), followed by exposure to ECL HYPER film (Amersham, Barcelona). Control of protein loading was tested by the mouse monoclonal anti-α-tubulin antibody (Sigma, Barcelona) used at a dilution of 1:5000; the secondary anti-mouse antibodies were also from Dako.

Fatty Acid Analysis

Fatty acid analysis was performed as previously described (Pamplona et al., 2002). Total lipids from human brain homogenates were extracted with chloroform:methanol (2:1, v/v) in the presence of 0.01% butylated hydroxytoluene. The chloroform phase was evaporated under nitrogen, and the fatty acids were trans-esterified by incubation in 2.5 ml of 5% methanolic HCl for 90 min at 75^{o}C. The resulting fatty acid methyl esters were extracted by adding 2.5 ml of n-pentane and 1 ml of saturated NaCl solution. The n-pentane phase was separated, evaporated under nitrogen, redissolved in 75 µl of carbon disulphide and 1 µl was used for GC/MS analysis. Separation was performed in a SP2330 capillary column (30m x 0.25mm x 0.20µm) in a Hewlett Packard 6890 Series II gas chromatograph (Hewlett-Packard Española, S.A., Barcelona, Spain). A Hewlett Packard 5973A mass spectrometer was used as detector in the electron-impact mode. The injection port was maintained at 220^{o}C, and the detector at 250^{o}C; the temperature program was 2 min at 100^{o}C, then 10^{o}C/min to 200^{o}C, then 5^{o}C/min to 240^{o}C, and finally hold at 240^{o}C for 10 min. Identification of fatty acid methyl esters was made by comparison with authentic standards and on the basis of mass spectra. Results are expressed as mol%.

From fatty acid composition, the following FA indexes were calculated: Saturated Fatty Acids (SFA)= Σ % of saturated fatty acids; Unsaturated Fatty Acids (UFA)= Σ % unsaturated fatty acids; Monounsaturated Fatty Acids (MUFA)= Σ % of monoenoic fatty acids ; Polyunsaturated n-3 Fatty Acids (PUFAn-3)= Σ % of polyunsaturated fatty acids n-3 serie; Polyunsaturated n-6 Fatty Acids (PUFAn-6)= Σ % of polyunsaturated fatty acids n-6 serie; Average Chain Length (ACL)= [(Σ %Total$_{14}$ x 14) + …+ (Σ %Total$_{n}$ x

n)]/100 (*n*= carbon atom number);Unsaturation Index (UI)= [(Σ mol% Monoenoic x 1) + (Σ mol% Dienoic x 2) + (Σ mol% Trienoic x 3) + (Σ mol% Tetraenoic x 4) + (Σ mol% Pentaenoic x 5) + (Σ mol% Hexaenoic x 6)]; Peroxidizability Index (PI) = [(Σ mol% Monoenoic x 0.025) + (Σ mol% Dienoic x 1) + (Σ mol% Trienoic x 2) + (Σ mol% Tetraenoic x 4) + (Σ mol% Pentaenoic x 6) + (Σ mol% Hexaenoic x 8)] (Cosgrove et al., 1984).

Statistical Analysis

All statistics calculations were performed using the SPSS software (SPSS, Chicago). Differences between control and PD samples were analyzed by the Student's t tests. The 0.05 level was selected as the point of minimal statistical significance in every comparison.

Results

Western blot analyses of protein carbonyl, AGEs and CML in PD

The Western blot analyses of total homogenates showed higher background and differences in the distribution of oxidative damage in proteins from PD (Figure 1). After delipidation, several bands around 65 to 40 kDa showed increased oxidative damage in PD samples (Figure 1). No major differences in staining were detected by a polyclonal anti-AGE. However, increased CML protein modification was evident in PD samples, and the targets of these modifications showed different molecular weights, from 30 to 50 kDa (Figure 1).

Mass spectrometry evidences of protein modifications by MCO, glycoxidation and lipoxidation in PD

In order to offer a more accurate quantitative measurement of free-radical derived damage in brain neocortex proteins, these were analyzed by isotope-dilution GC/MS. The mean concentrations of GSA, AASA, and CML were not different in brain samples from PD patients when compared with control, age-matched individuals while CEL concentrations were significantly decreased (Table I). However, the concentration of MDAL, a specific lipoxidation product, was significantly increased in samples from PD patients ($p<0,0001$; Figure 2).

RAGE expression in PD neocortex

Immunoblotting for RAGE demonstrated two major bands at approximately 50 kDa and 60 kDa, corresponding to full-length RAGE, in the cerebral cortex of PD cases but not in controls (Fig. 3).

Fatty Acid Analysis

The analyses of fatty acid revealed significant differences in brain samples, both in global indexes and in individual fatty acids (Table II). The highly peroxidizable docosahexaenoic acid (DHA) also showed a significant increase in its content ($p<0,001$; Figure 2) in PD samples. With reference to fatty acid derived indexes, significant decreases in the content of PUFA of the n-6 family and increases in the n-3 family were found in PD cortex (Table II). Overall, this resulted in a significantly increased peroxidizability index (Figure 2).

Discussion

The cases studied in the present series were selected on the basis of no apparent or minimal neurological signs and symptoms, absence of treatment for parkinsonism, neuropathological criteria of PD, and absence of other abnormalities of the nervous system, particularly absence of neuropathological features of Alzheimer's disease. Regarding neuropathological findings, systematic studies on necropsy series have suggested that PD starts in certain nuclei of the medulla oblongata before any evidence of involvement of the substantia nigra is observed (Del Tredici et al., 2002). Yet Lewy bodies and Lewy neurites occurred in several nuclei of the medulla oblongata, pons and midbrain, including locus ceruleus and substantia nigra, and in the amygdala and nucleus basalis of Meynert in the present series, thus fulfilling the criteria of midbrain stage of PD (Braak et al., 2003). Pigmentation of the substantia nigra and preservation in the number of neurons in the pigmented nuclei were crucial features probably accounting for the minimal clinical deficits in these patients.

Although several studies have shown oxidative stress in the substantia nigra, the present results have shown evidence of oxidative damage in the frontal cortex of asymptomatic non-treated PD. The mean concentrations of GSA and AASA, markers of MCO-derived protein damage, are not altered; but the concentration of MDAL, a marker of lipoxidative damage, is significantly increased in the PD frontal cortex. In contrast, western-blot analyses show increased carbonyl content in some proteins from PD cortices. This may be due to cross-reactivity of DNP with lipoxidation derived products (Berlett and Stadman, 1997) . The unexpected finding of decreased CEL concentrations might be explained by an impairment of glycolysis in affected neurons, as this pathway is considered one of the major sources of CEL precursors (Ahmed et al., 2001; -03). The concentrations of CML, marker of mixed lipo/glycoxidative damage, are not elevated but increased CML-immunoreactivity, when combined with MDAL and lipid findings, suggests selective protein lipoxidative damage in PD neocortex. Increase in protein carbonyls in several brain regions has been reported in PD but not in patients with incidental Lewy Body disease (Alam et al., 1997a). This suggests that protein oxidation occurs later in the disease or that L-dopa treatment contributes to protein oxidation (Markesberry et al., 2001). Yet increased DNP-reactive carbonyls have been observed in non-delipidized and delipidized samples of PD frontal cortex in the present series, thus indicating that protein oxidation is produced in the absence of L-dopa. Discrepancies between the present results and those of Alam et al. are probably due to differences in the sampling of the cases for study. Previous studies have shown that hydroxynonenal adducts indicate a role for lipid peroxidation in neocortical and brainstem Lewy bodies (Castellani et al., 2002).

Yet the present results show that similar biochemical findings may precede the formation of Lewy bodies.

In line with these observations, increased RAGE expression, as revealed by Western blotting in frontal cortex homogenates, also occurs in PD. Interestingly, AGE immunoreactivity has been detected in the frontal and temporal cortex in DLBD (Castellani et al., 1996). Differences in the sensibility of these methods point to the opportunity to study RAGE expression by Western blot in order to test possible increments in RAGE with the progression of the α-synuclein pathology when comparing PD and DLBD. It has been shown that CML is recognized by RAGE (Kislinger et al., 1999). The hypothetical RAGE activation under these circumstances would lead to an increased pro-inflammatory status, previously implicated in PD pathogenesis (Beal, 2003)

Recent studies (Sharon et al., 2001; -03a; -03b) have evidenced interactions of neuronal α-synuclein with fatty acids, and particularly PUFA, under normal and pathological states. Thus, it has been described that: i) PUFA, particularly DHA, have a direct regulatory role on α-synuclein assembly state; and ii) α-synuclein-PUFA interactions appear to regulate neuronal PUFA levels, based on the suggestion that α-synuclein is a novel brain-specific fatty acid binding protein. α-synuclein could be directly involved in the proper maintenance of the neuronal membrane vesicle system through its interaction with PUFAs. In this scenario, our findings showing an increased content in PUFAn-3 and particularly DHA, and by extension, in the degree of membrane un-saturation, in the cerebral cortex at relatively early stages of PD reinforces a potential key role for an alteration in brain PUFA composition in the accumulation of α-synuclein oligomers, and in the progression toward a pathological state.

Our data also show that additional lipid factors can also play an early role in the nucleation of pathological aggregates. PUFA residues are extremely sensitive to oxidation. Every phospholipid in every cellular membrane contains an unsaturated fatty acid residue. Many of these are polyunsaturated and the presence of a methylene group between two double bonds renders the fatty acid sensitive to ROS-induced damage, their sensitivity to oxidation exponentially increasing as a function of the number of double bonds per fatty acid molecule (Bielski et al., 1983). Consequently, the high concentration of PUFAs in brain phospholipids not only makes them prime targets for reaction with oxidizing agents but also enables them to participate in long free radical chain reactions. Lipid peroxidation generates hydroperoxides and endoperoxides, which undergo fragmentation to produce a broad range of reactive intermediates, like alkanals, alkenals, hydroxyalkenals, glyoxal, and malondialdehyde. These carbonyl compounds could react primarily with lysine, arginine and cysteine residues, leading to the formation of both

non-enzymatic adducts and cross-links in protein, which can be useful indicators of protein oxidative stress *in vivo*. In this context, we have documented a significantly higher steady-sate levels of the lipoxidative marker MDAL in PD. Considering that lysine residues are particularly abundant in synuclein, as well as the increase in the peroxidizability index in the cerebral cortex in PD also observed in our study, it can be suggested that the non-enzymatic modification of aS, and particularly lipoxidation-derived protein damage, play a key role in the nucleation of pathological aggregates, as suggested also for AGE-mediated cross-linking in incidental Lewy body disease (Münch et al., 2000).

In summary, the present study has shown abnormal fatty acid composition, augmented lipoxidative and glycoxidative damage, and increased RAGE expression in the frontal cortex of a selected group of asymptomatic PD cases with extended Lewy bodies and Lewy neurites in the brain stem, amygdala and basal nucleus of Meynert, but with rather preservation in the number of neurons in the substantia nigra pars compacta. This study demonstrates oxidative stress in the cerebral cortex at relatively early stages of PD in the absence of L-dopa or other antiparkinsonian treatment. These findings support anti-oxidant therapy as a primary goal in the treatment of PD in order to reduce disease progression and cortical damage associated with oxidative stress.

References

Ahmed MU, Brinkmann-Frye, E., Degenhardt TP, Thorpe SR, Baynes JW. N^{ε}-(carboxyethyl)lysine, a product of the chemical modification of proteins by methylglyoxal, increases with age in human lens proteins. Biochem J 1997; 324: 565-70.

Ahmed N, Battah S, Karachalias N, Babaei-Jadidi R, Horanyi M, Baroti K, Hollan S, Thornalley PJ. Increased formation of methylglyoxal and protein glycation, oxidation and nitrosation in triosephosphate isomerase deficiency. Biochim Biophys Acta 2003; 1639:121-32.

Alam ZI, Daniel SE, Lees AJ, Marsden DC, Jenner P, Halliwell B . A generalized increase in protein carbonyls in the brain in Parkinson's disease but not in incidental Lewy Body disease. J Neurochem 1997a; 69: 1326-29.

Alam ZI, Jenner A, Daniel SE, Lees AJ, Cairns N, Marsden CD, Jenner P, Halliwell B. Oxidative DNA damage in the parkisonian brain: an apparent selective increase in 8-hydroxyguanine levels in substantia nigra. J Neurochem 1997b; 69: 1196-203.

Baba M, Nakajo S, Tu PH, Tomita T, Nakaya K, Lee VMY, Trojanowski JQ, Iwatsubo T. Aggregation of α-synuclein in Lewy bodies of sporadic Parkinson's disease and dementia with Lewy bodies. Am J Pathol 1998; 152: 879-84.

Beal MF . Mitochondria, oxidative damage, and inflammation in Parkinson's disease. Ann N Y Acad Sci 2003; 991:120-31.

Berlett BS, Stadtman ER. Protein oxidation in aging, disease, and oxidative stress. J Biol Chem 1997; 272: 20313-6.

Bielski BHJ, Arudi RL, Sutherland MW. A study of the reactivity of $HO_2/O_2^{\cdot -}$ with unsaturated fatty acids. J Biol Chem 1983; 258: 4759-61.

Braak H, Braak E . Temporal sequence of Alzheimer's disease-related pathology. In: Peters A, Morrison JH, editors, Cerebral cortex., vol 14: Neurodegenerative and related changes in structure and function of cerebral cortex. New York, Boston, Dordrecht, London, Moscow: Kluwer Academic/Plenum Publishers; 1999, p: 475-512.

Braak H, Del Tredici K, Rub U, de Vos RA, Jansen Steur EN, Braak E. Staging of brain pathology related to sporadic Parkinson's disease. Neurobiol Aging 2003; 24: 197-211.

Burke RE. Parkinson's disease. In: Koliatsos VE, Ratan RR, Choi D, editors, Cell death and diseases of the nervous system. Totowa, New Jersey: Humana Press; 1999, p. 459-76.

Cao G, Cutler RG. Protein oxidation and aging. I. Difficulties in measuring reactive protein carbonyls in tissues using 2,4-dinitrophenylhydrazine. Arch Biochem Biophys 1995; 320:106-14.

Castellani R, Smith MA, Richey PL, Perry G. Glycoxidation and oxidative stress in Parkinson's disease and Diffuse Lewy Body disease. Brain Res 1996; 737: 195-200.

Castellani RJ, Perry G, Siedlak SL, Nunomura A, Shimohama S, Zhang J, Montine T, Sayre LM, Smith MA. Hydroxynonenal adducts indicate a role for lipid peroxidation in neocortical and brainstem Lewy bodies in humans. Neurosci Lett 2002; 319:25-8.

Ceballos I, Lafon M, Javoy-Agid F, Hirsch E, Nicole A, Sinet PM, Agid Y. Superoxide dismutase and Parkinson's disease. Lancet 1990; 335: 1035-6.

Cosgrove JP, Church DF, Pryor WA. The kinetics of the autoxidation of polyunsaturated fatty acids. Lipids 1987; 22: 299-304.

Del Tredici K, Rub U, De Vos RA, Bohl JR, Braak H. Where does Parkinson disease pathology begin in the brain? J Neuropathol Exp Neurol 2002; 61: 413-26.

Dexter DT, Carter C, Agid F. Lipid peroxidation as a cause of nigral death in Parkinson's disease. Lancet 1986; 2: 639-40.

Dexter DT, Carter CJ, Wells FR, Javoy-Agid F, Agid Y, Lees A, Jenner P, Marsden CD. Basal lipid peroxidation in substantia nigra is increased in Parkinson's disease. J Neurochem 1989; 52: 381-9.

Dexter DT, Holley AE, Flitter WD, Slater TF, Wells FR, Daniel SE, Lees AJ, Jenner P, Marsden CD. Increased levels of lipid hydroxperoxides in the parkinsonian substantia nigra: an HPLC and ESR study. Mov Disord 1994; 9: 92-7.

Duda JE, Giasson BI, Chen Q, Gur TL, Hurtig HI, Stern MB, Gollomp SM, Ischiropoulos H, Lee VMY, Trojanowski JQ. Widespread nitration of pathological inclusions in neurodegenerative synucleinopathies. Am J Pathol 2000; 157: 1439-45.

Duda JE, Giasson BI, Mabon ME, Lee VMY, Trojanowski JQ. Novel antibodies to synuclein show abundant striatal pathology in Lewy body disease. Ann Neurol 2002; 52: 205-10.

Ferrer I. The neuropathological spectrum of Lewy body disorders. En: Tolosa E, Schulz JB, McKeith IG, Ferrer I, editors, Neurodegenerative disorders associated with α-synuclein pathology. Barcelona: Ars Medica; 2002,p: 83-98.

Floor E, Wetzel MG. Increased protein oxidation in human substantia nigra pars compacta in comparison with basal ganglia and prefrontal cortex measured with an improved dinitrophenylhydrazine assay. J Neurochem 1998; 70: 268-75.

Forno LS. Neuropathology of Parkinson's disease. J Neuropathol Exp Neurol 1996; 55: 259-72.

Fujiwara H, Hasegawa M, Dohmae N, Kawashima A, Masliah E, Goldberg MS, Shen J, Takio K, Iwatsubo T. α-synuclein is phosphorylated in synucleinopathy lesions. Nature Cell Biol 2002; 4: 160-4.

Gai WP, Yuan HX, Li XQ, Power JTH, Blumbergs PC, Jensen PH. *In situ* and *in vitro* study of colocalization and segregation of α-synuclein, ubiquitin and lipids in Lewy bodies. Exp Neurol 2000; 166: 324-3.

Giasson BI, Duda JE, Murray IV, Chen Q, Souza JM, Hurrig HI, Ischiropoulas H, Trojanowski IQ, Lee VM. Oxidative damage linked to neurodegeneration by selective α-synuclein nitration in synucleinopathy lesions. Science 2000; 290: 985-9.

Hansen LA. The Lewy body variant of Alzheimer disease. J Neural Transm Suppl 1997; 51: 83-93.

Hashimoto M, Hsu LJ, Xia Y, Takeda A, Sundsmo M, Mashliah E. Oxidative stress induces amyloid-like aggregates formation of NACP/α-synuclein *in vitro*. NeuroReport 1999; 10: 717-21.

Hashimoto M, Masliah E. Alpha-synuclein in Lewy body disease and Alzheimer's disease. Brain Pathol 1999; 9: 707-20.

Hsu LJ, Sagara Y, Arroyo A, Rockenstein E, Sisk A, Mallory M, Wong J, Takenouchi T, Hashimoto M, Masliah E. α-synuclein promotes mitochondrial deficit and oxidative stress. Am J Pathol 2000; 157: 401-10.

Ince PG, Pery EK, Morris CM. Dementia with Lewy bodies. A distinct non-Alzheimer dementia syndrome. Brain Pathol 1998; 8: 299-324.

Iwatsubo T. Aggregation of α-synuclein in the pathogenesis of Parkinson's disease. J Neurol 2003; 250 suppl 3: 11-4.

Jellinger K, Mizuno Y. Parkinson's disease. In: Dickson D, editor, Neurodegeneration: The molecular pathology of dementia and movement disorders, Basel: ISN Neuropath Press; 2003, p 159-87.

Jenner P. Oxidative stress as a cause of Parkinson's disease. Acta Neurol Scand 1991; 84: 6-15.

Jenner P. Oxidative mechanisms in nigral cell death in Parkinson's disease. Mov Disord 1998; 13: 24-34.

Jenner P. Oxidative stress in Parkinson's disease. Ann Neurol 2003; 53 suppl 3: S26-S38.

Kislinger T, Fu C, Huber B, Qu W, Taguchi A, Du Yan S, Hofmann M, Yan SF, Pischetsrieder M, Stern D, Schmidt AM. N(epsilon)-(carboxymethyl)lysine adducts of proteins are ligands for receptor for advanced glycation end products that activate cell signaling pathways and modulate gene expression. J Biol Chem 1999; 274: 31740-9.

Knecht KJ, Dunn JA, McFarland KF, McCance DR, Lyons TJ, Thorpe SR, Baynes JW. Effect of diabetes and aging on carboxymethyllysine levels in human urine. Diabetes 1991; 40:190-6.

Kosaka K, Iseki E. Diffuse Lewy body disease within the spectrum of Lewy body diseases. In: Perry RH, McKeith IG, Perry EK, editors, Dementia with Lewy bodies, Cambridge: Cambridge University Press; 1996, p: 238-47.

Krüger R, Kuhn W, Müller T, Woitalla D, Graeber M, Kösel S, Przuntek H, Epplen JT, Schöls, Riess O. Ala30Pro mutation in the gene encoding alpha-synuclein in Parkinson's disease. Nat Genet 1998; 18: 106-8.

Lander HM, Tauras JM, Ogiste JS, Hori O, Moss RA, Schmidt AM. Activation of the receptor for advanced glycation end products triggers a $p21^{ras}$-dependent mitogen-activated protein kinase pathway regulated by oxidant stress. J Biol Chem 1997; 272: 17810-4.

Lustbader JW, Cirilli M, Lin C, Xu HW, Takuma K, Wang N, Caspersen C, Chen X, Pollak S, Chaney M, Trinchese F, Liu S, Gunn-Moore F, Lue LF, Walker G, Kuppusamy P, Zewier ZL, Arancio O, Stern D, Yan SS, Wu H. ABAD directly links Abeta to mitochondrial toxicity in Alzheimer's disease. Science. 2004; 304: 448-52.

Markesberry WR, Montine TJ, Lovell MA. Oxidative alterations in neurodegenerative diseases. In: Mattson MP, editor, Pathogenesis of neurodegenerative diseases. Totowa, New Jersey: Humana Press, 2001; p: 21-51.

Marttila RJ, Lorentz H, Rinne UK. Oxygen toxicity protecting enzymes in Parkinson's disease. Increase of superoxide dismutase-like activity in the substantia nigra and basal nucleus. J Neurol Sci 1988; 86: 321-31.

Munch G, Luth HJ, Wong A, Arendt T, Hirsch E, Ravid R, Riederer P. Crosslinking of alpha-synuclein by advanced glycation endproducts—an early pathophysiological step in Lewy body formation? J Chem Neuroanat. 2000; 20: 253-7.

Narhi L, Wood SJ, Stevenson S, Jiang Y, Wu GM, Anafi D, Kaufman SA, Martin F, Sitnev K, Denis P, Louis JC, Wypych J, Biere AL, Citron M. Both familial Parkinson's disease mutations accelerate α-synuclein aggregation J Biol Chem 1999; 274: 9843-6.

Paik SR, Shin HJ, Lee JM. Metal-catalyzed oxidation of α-synuclein in the presence of Copper(II) and hydrogen peroxide. Arch Biochem Biophys 2000; 378: 269-7.

Pamplona R, Portero-Otin M, Requena J, Gredilla R, Barja G.. Oxidative, glycoxidative and lipoxidative damage to rat heart mitochondrial proteins is lower after 4 months of caloric restriction than in age-matched controls. Mech Ageing Dev 2002; 123:1437-46.

Perry TL, Godin DV, Hansen S. Parkinson's disease: a disorder due to nigral glutathione deficiency. Neurosci Lett 1982; 33: 305-10.

Polymeropoulos MH, Lavedan C, Leroy E, Ide SE, Dehejia A, Dutra A, Pike B, Root H, Rubenstein J, Boyer R, Stenroos ES, Chandraserkharappa S, Athanassiadou A, Papapetropoulos T, Jonson WG, Lazzarini AM, Duvoisin RC, Dorio GD, Golbe LI, Nussbaum RL. Mutation in the α-synuclein gene identified in families with Parkinson's disease. Science 1997; 276: 2045-7.

Portero-Otin M, Pamplona R, Ruiz MC, Cabiscol E, Prat J, Bellmunt MJ. Diabetes induces an impairment in the proteolytic activity against oxidized proteins and a heterogeneous effect in nonenzymatic protein modifications in the cytosol of rat liver and kidney. Diabetes 1999; 48: 2215-20.

Requena JR, Chao CC, Levine RL, Stadtman ER. Glutamic and aminoadipic semialdehydes are the main carbonyl products of metal-catalized oxidation of proteins. Proc Natl Acad Sci USA 2001; 98: 69-74.

Requena JR, Fu MX, Ahmed MU, Jenkins AJ, Lyons TJ, Baynes JW, Thorpe SR. Quantification of malondialdehyde and 4-hydroxynonenal adducts to lysine residues in native and oxidized human low-density lipoprotein.Biochem J 1997; 322: 317-25.

Saggu H, Cooksey J, Dexter D, Wells FR, Lees A, Jenner P, Marsden CD. A selective increase in particulate superoxide dismutase activity in Parkinson's substantia nigra. J Neurochem 1989; 53: 692-7.

Sanchez-Ramos JR, Overvik E, Ames BN. A marker of oxyradical-mediated DNA damage (8-hydroxy-2'-deoxyguanosine) is increased in nigrostriatum of Parkinson's disease brain. Neurodegeneration 1994; 3: 197-204.

Schmidt AM, Yan SD, Yan SF, Stern DM. The biology of the receptor for advanced glycation end products and its ligands. Biochim Biophys Acta 2000: 1498: 99-111.

Sharma N, McLean P, Kawamata H, Irizarry MC, Hyman BT. Alpha-synuclein has an altered conformation and shows a tight intermolecular interaction with uqbiquitin in Lewy bodies. Acta Neuropathol 2001; 102: 329-34.

Sharon R, Goldberg MS, Bar-Josef I, Betensky RA, Shen J, Selkoe DJ. alpha-Synuclein occurs in lipid-rich high molecular weight complexes, binds fatty acids, and shows homology to the fatty acid-binding proteins. Proc Natl Acad Sci USA 2001; 98: 9110-5.

Sharon R, Bar-Joseph I, Frosch MP, Walsh DM, Hamilton JA, Selkoe DJ. The formation of highly soluble oligomers of alpha-synuclein is regulated by fatty acids and enhanced in Parkinson's disease. Neuron 2003a; 37:583-95.

Sharon R, Bar-Joseph I, Mirick GE, Serhan CN, Selkoe DJ. Altered fatty acid composition of dopaminergic neurons expressing α-synuclein and human brains with α-synucleinopathy. J Biol Chem 2003b; 278: 49874-81.

Shelley ML. 4-hydroxy-2-nonenal may be involved in the pathogenesis of Parkinson's disease. Free Radic Biol Med 1998; 25: 169-174.

Sian J, Dexter DT, Lees AJ, Daniel S, Agid Y, Javoy-Agid F, Jenner P, Mrsden CD. Alterations in glutathione levels in Parkinson's disease patients. Genomics 1994; 17: 171-84.

Silva MT, Schapira AHV. Parkinson's disease. In: Mattson MP, editor, Pathogenesis of neurodegenerative disorders. Totowa, New Jersey: Humana Press; 2001, p: 53-79.

Singleton AB, Farrer M, Johnson J, Singleton A, Hague S, Kachergus J, Hulihan M, Peuralinna T, Dutra A, Nussbaum R, Lincoln S, Crawley A, Hanson M, Maraganore D, Adler C, Cookson MR, Muenter M, Baptista M, Miller D, Blancato J, Hardy J, Gwinn-Hardy K. α-synuclein locus triplication causes Parkinson's disease. Science 2003; 302: 841-2.

Spillantini MG, Crowther RA, Jakes R, Hasegawa M, Goedert M. α-synuclein in filamentous inclusions of Lewy bodies from Parkinson's disease and dementia with Lewy bodies. Proc Natl Acad Sci USA 1998; 95: 369-6473.

Yoritaka A, Hattori N, Uchida K, Tanaka M, Stadtman ER, Mizuno Y.Immunohistochemical detection of 4-hydroxynonenal protein adducts in Parkinson disease. Proc Natl Acad Sci USA 1996; 93: 696-2701.

Zarranz JJ, Alegre J, Gómez-Esteban JC, Lezcano E, Ros R, Ampuero I, Vidal L, Hoenicka J, Rodriguez O, Atarés B, Llorens V, Gómez Tortosa E, del Ser T, Muñoz DG, de Yébenes J. The new mutation, E46K, of α-synuclein causes Parkinson and Lewy body dementia. Ann Neurol 2004; 55: 164-73.

Zhang J, Perry G, Smith MA, Robertson D, Olson SJ, Graham DG, Montine TJ. Parkinson's disease is associated with oxidative damage to cytoplasmc DNA and RNA in substantia nigra neurons. Am J Pathol 1999; 154: 1423-9.

ACKNOWLEDGEMENTS

This work was funded by grants from the Spanish Ministry of Science and Technology (BFI2003-01287), Spanish Ministry of Health, Instituto de Salud Carlos III (FIS 02-0891), the Amyotrophic Lateral Sclerosis Association, and the Generalitat of Catalunya (2001SGR00311) to RP and MPO, and FIS grants: C03-006; G03-167, FIS P02-0004 and European Brain Bank Network (BrainNet II) to IF. We thank T. Yohannan for editorial help.

Figure legends

Fig. 1: Cortex from PD patients exhibit increased protein oxidative damage. Upper panels: Detection of DNP-reactive carbonyls in total homogenates (*left)* and delipidated samples (*middle*). It is also shown the distribution of AGE and CML protein modifications (*right*). Lower panels: Quantification of modification levels, normalized by the Coomassie-blue signal (for anti-DNP) or by the anti-actin signal (for anti-AGE and anti-CML).

Fig. 2: Protein lipoxidative damage is increased in cortex from PD patients. *Upper panel*: Effect of PD in the protein content of MDA-L with reference to control samples (** $p<0,01$ Student's T test). Values (mean±SEM, n=7) were 260±31 μmol/mol lysine for control samples and 560±32 μmol/mol lysine for PD samples. *Lower panel*: Effect of PD in the peroxidizability index (PI) and docoxahexaenoic fatty acid (DHA) content (* $p<0,05$; ** $p<0,01$ Student's T test).

Fig. 3: Increased RAGE expression in the frontal cortex in PD when compared with controls (C), as revealed by the presence of two bands of about 50 and 60 kDa in the upper panel. α-tubulin (55 kDa) is used as a marker of protein loading in the lower panel.

Table I. Effect of PD on the neocortex concentrations (μmol/mol lysine) of specific markers of protein oxidative damage.

	Control	PD	P<
GSA	20832±350	20644±1466	0,88
AASA	100±12	100±14	0,99
CEL	462±14	310±20	0,001
CML	497±10	475±18	0,58

TABLE II Fatty acid analysis

ACL, average chain length; SFA, saturated fatty acids; UFA, unsaturated fatty acids; PUFA n-6/n-3, polyunsaturated fatty acids n-6 or n-3 series/families; MUFA, monounsaturated fatty acids; DBI, double bond index; PI, peroxidizability index. Values: mean±SEM. N x group: 5-7.

	Ctl	**PD**
14:0	0.59±0.06	0.47±0.02*
16:0	16.60±0.15	18.72±0.16*
16:1n-7	1.76±0.11	1.12±0.04*
18:0	23.67±0.35	21.30±0.68
18:1n-9	26.78±0.12	26.65±0.94
18:2n-6	0.66±0.05	0.65±0.02
18:3n-3	0.12±0.01	0.14±0.02
20:0	1.97±0.19	1.59±0.18
20:1	0.13±0.01	0.27±0.05*
20:2n-6	0.26±0.02	0.19±0.009*
20:3n-6	0.76±0.09	0.96±0.08*
20:4n-6	6.91±0.46	6.07±0.61
22:4n-6	5.99±0.29	4.46±0.10*
22:5n-6	0.52±0.09	0.69±0.03
22:5n-3	0.10±0.006	0.13±0.01
22:6n-3	11.43±0.46	14.08±0.20*
24:0	0.20±0.03	0.45±0.02*
24:1n-9	1.45±0.15	1.97±0.15
ACL	18.63±0.02	18.68±0.2
SFA	43.05±0.11	42.55±0.77
UFA	56.94±0.11	57.44±0.77*
MUFA	30.14±0.24	30.02±1.06
PUFA	26.79±0.33	27.41±0.65
PUFAn-6	15.12±0.45	13.05±0.56*
PUFAn-3	11.66±0.46	14.36±0.21*
DBI	158.08±1.78	165.87±2.42
PI	150.38±2.82	163.62±3.30*

Fig. 1

Values shown are mean±SEM (n=6 for each group)

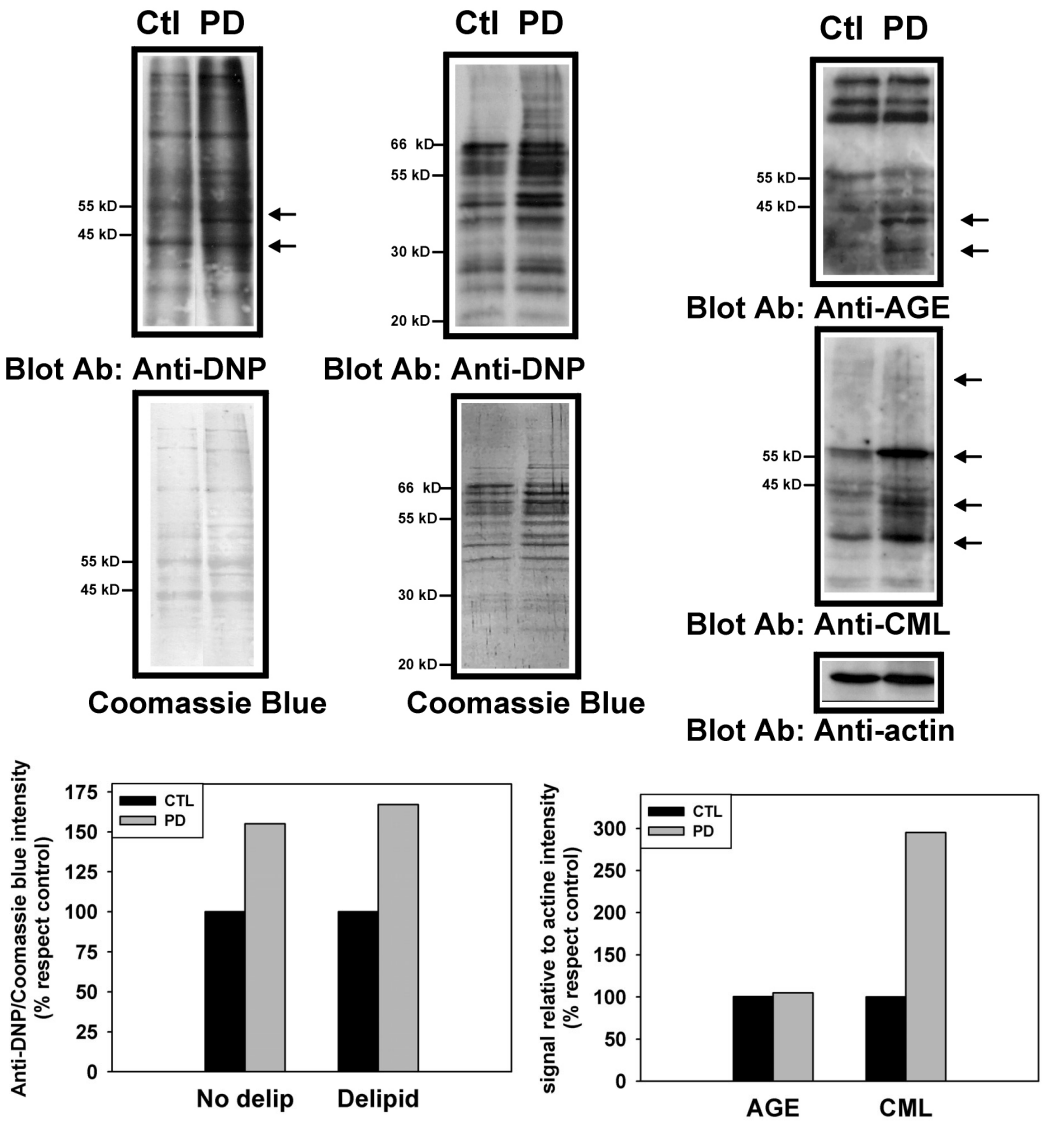

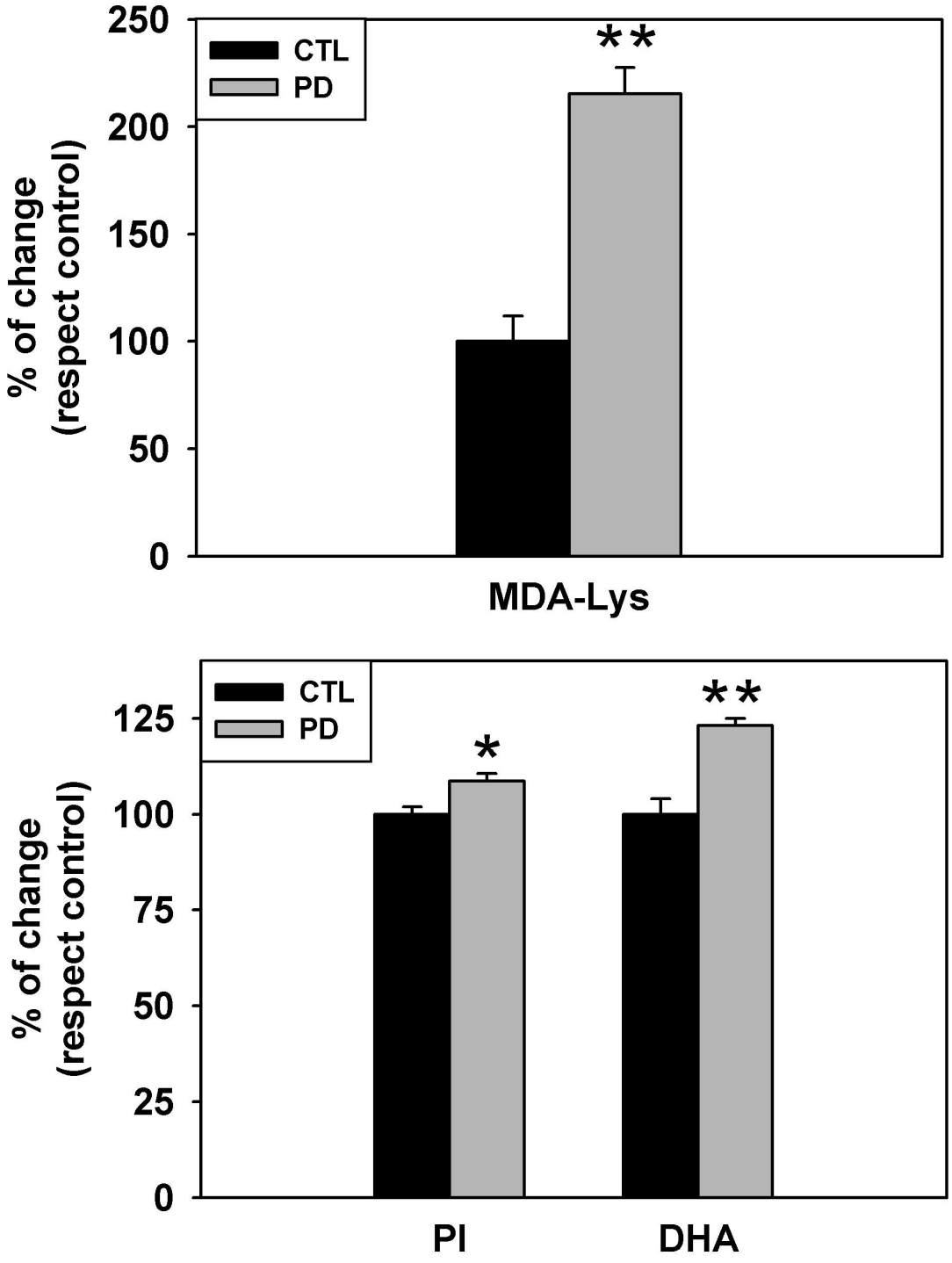
250
200
150
100
50
0
% of change
(respect control)
CTL
PD
**
MDA-Lys
125
100
75
50
25
0
% of change
(respect control)
CTL
PD
*
**
PI
DHA

Fig. 2

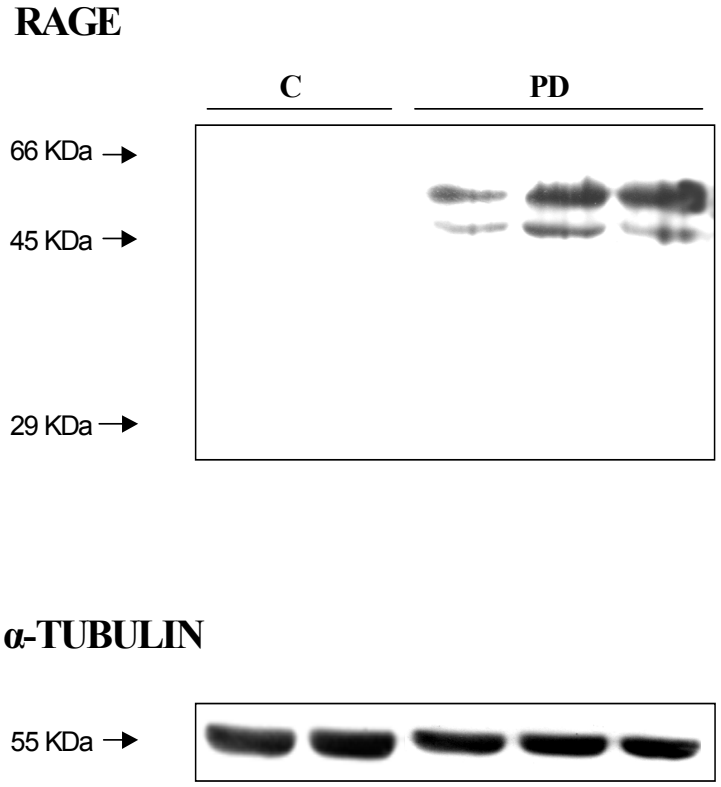

Fig. 3

III. II. Pamplona R, Dalfó E, Ayala MV, Bellmunt MJ, Ferrer I, Portero-Otín M, (2004) *Markers of protein oxidative damage, AGEs and RAGEs in brain cortex from Alzheimer's disease patients. (Enviat a Journal of Biological Chemistry).*

La patogènesi de la malaltia d'Alzheimer implica la modificació oxidativa de les proteïnes. Existeixen diverses vies oxidatives a partir de les quals s'obtindrien els grups carbonil, com són la modificació de diversos residus susceptibles, la glicooxidació i la lipoooxidació. De moment només hi ha descrits mètodes indirectes per a la mesura d'aquests compostos resultants de l'oxidació, que alhora poden mancar d'especificitat. Així en el treball que presentem a continuació hem analitzat els aspectes següents: la presència i la concentració d'aquest compostos mitjançant cromatografia de gasos/masses, la resposta biològica a través de l'expressió del RAGE i finalment la composició d'àcids grassos en cervells de pacients de la malaltia d'Alzheimer comparat amb cervells control. La malaltia d'Alzheimer està associada doncs a un augment de tots els marcadors estudiats, així com a un augment en l'expressió del RAGE. Aquests pacients presenten també canvis en el contingut d'àcids grassos específics, particularment l'àcid docosahexanoic, que augmenta la peroxidabilitat lipídica. Així doncs amb el següent estudi aconseguim quantificar per espectrometria de masses les evidències oxidatives descrites per la malaltia d'Alzheimer, les quals al seu torn ens ofereixen evidències de la peroxidació lipídica que pateixen les proteïnes en l'esmentada malaltia. Per tant, a part d'estudiar la producció de radicals lliures descrits fins ara per a la malaltia d'Alzheimer, els canvis produïts en la composició d'àcids grassos no pot passar desapercebuda quan s'estudia aquesta demència.

MARKERS OF PROTEIN OXIDATIVE DAMAGE, AGES AND RAGES IN BRAIN CORTEX FROM ALZHEIMER'S DISEASE PATIENTS

Reinald Pamplona[a,d], Esther Dalfó[b,d], Maria Victoria Ayala[a], Maria Josep Bellmunt[a], Isidre Ferrer[b,c] and Manuel Portero-Otín[a*]

[a]Metabolic Pathophysiology Research Group, Departament de Ciències Mèdiques Bàsiques, Facultat de Medicina, Universitat de Lleida. Avda Rovira Roure,44 E-25198 Lleida, SPAIN

[b]Institut de Neuropatologia, Servei Anatomia Patològica, Hospital de Bellvitge, [c]Departament de Biologia Cel.lular i Anatomia Patológica, Facultad de Medicina, Universitat de Barcelona , c/ Feixa Llarga sn, 08907, Hospitalet de Llobregat, Spain Hospitalet de Llobregat, Spain

[d]R.P. and E.D. contributed equally to this work

[*]Address for correspondence:
Manuel Portero-Otin, MD,PhD. Metabolic Pathophysiology Research Group,
Departament de Ciències Mèdiques Bàsiques,
Facultat de Medicina, Universitat de Lleida
Avda Rovira Roure,44
E-25198 Lleida, SPAIN
Tel +34973702408; Fax:+34973702426
e-mail: manuel.portero@cmb.udl.es

Abstract

The pathogenesis of Alzheimer's disease (AD) may imply protein oxidative modifications. Diverse oxidative pathways, such as direct modification of susceptible residues, glycoxidation and lipoxidation, could give rise to protein carbonyl, often assessed indirectly. However, the analyses of structurally characterized probes for these reactions could overcome this lack of specificity. Consequently, in this work we analyzed i) the presence and concentrations of these compounds by means of gas-chromatography/mass spectrometry, ii) the biological response through RAGE expression, and iii) the fatty acid composition, in brain samples from AD patients and age-matched controls. AD was associated with significant increases in the concentrations of all evaluated markers and increased RAGE expression with high molecular heterogeneity. Samples from AD patients also showed changes in the content of specific fatty acids, particularly docosahexaenoic, which increased lipid peroxidizability. These results offer quantitative mass-spectrometric evidences of increased oxidation in AD. Moreover, the differences between the examined markers support an important role for lipid peroxidation-derived protein modifications in AD pathogenesis. Thus, besides potentially increased free-radical production, changes in fatty acid composition also merit attention in AD pathogenesis.

Keywords: advanced glycation, RAGE, protein carbonyl, lipid peroxidation, glutamic and aminoadipic semialdehydes, N^{ε}- carboxymethyl-lysine, N^{ε} - carboxyethyl-lysine and N^{ε}-malondialdehyde-lysine

1. Introduction

The free radical hypothesis of ageing proposes that for a given tissue, the modifications derived from oxidative stress accumulate their effects over time. This accumulation, when uncompensated, decreases homeostatic capacities of tissue, contributing to the ageing of the whole organism. The oxidative stress-induced molecular alterations affect all sorts of biological molecules, including specifically sensitive amino acid residues in proteins, such as arginine, proline and lysine [3]. Brain aging is associated with changes increasing the risk of Alzheimer's disease (AD). A corollary of this fact is that AD shows an acceleration of those phenomena underlying ageing. Accordingly, increased amount of protein bound dinitrophenylhidrazine-reactive carbonyls, generated by protein oxidation are a common finding in brain samples from AD patients [2,66,67]. These works rely on the reaction of 2,4-dinitrophenylhydrazine (DNP) with carbonyl groups. However, this assay has been criticised due to the possibility of artefacts [14]. The direct measure of the concentration of structurally characterized products could overcome this fact and be used as a complement for assessing the effects of oxidative stress in vivo. Glutamic semialdehyde (GSA) derives from the metal-catalysed oxidation (MCO) of polyproline and polyarginine while aminoadipic semialdehyde (AASA) results from polylysine oxidation [58]. These products are among the main carbonyl products of MCO of proteins [58], thus specific products of oxidation of amino-acids in protein (AAOPs, [72]). However, their presence and the factors affecting their concentrations in human brains are unknown up to date.

The chemical pathways linking increased free radical efflux and protein structural modification also involve third-party molecules, which may give rise to increased DNP-reactive carbonyls in proteins [7]. Particularly, carbohydrates, when reacting with free radicals generate highly reactive dicarbonyl compounds, such as glyoxal and methylglyoxal [71]. In the cellular context, these may be also derived from glycolysis, thriose phosphate metabolism, acetone metabolism [71], lipid peroxidation [27] and hypochlorite mediated reactions [4]. These compounds generate stable adducts reacting with lysine, arginine and cysteine in proteins[72] N^{ε} - carboxyethyl)-lysine (CEL) and N^{ε} - carboxymethyl)-lysine (CML) are two of these adducts, first described as advanced glycation endproducts (AGE), later named glycoxidation products and now recognized as mixed AGEs-advanced lipoxidation products. Despite CML has been detected in the AD lesions by immunohistochemical analyses (revised in [35]), no chemical evidences have been reported for this product in AD samples or models. Polyunsaturated fatty acids (PUFA) are other third-party molecules. PUFA are very susceptible molecules to the oxidative action of free radicals [20]. Free radical attack of PUFA generates specific

reactive aldehydes, such as malondialdehyde or 4-hydroxynonenal, among other [24]. These aldehydes could react with proteins, generating also DNP-reactive moieties in proteins [7]. The important PUFA content in brain and its high oxygen consumption support the possible significance of lipid peroxidation-derived processes in brain ageing and AD pathogenesis. Analogously to the other modifications pointed out above, evidences for lipid peroxidation-derived protein damage in AD comprise immunohistochemistry[12]. However, there are no chemical evidences for lipid peroxidative damage of proteins in AD.

Concerning the pathogenic role of these products, many recent studies of mechanisms underlying cellular dysfuction in Alzheimer's disease have focused on amyloid β-peptide (Aβ). Persistent chronic inflammation appears to have a significant role in AD pathogenesis and evidence suggest that sustained microglial response to Aβ could play a role in this process [1,23,45,54]. In AD brains, the most highly activated microglia is observed in close association with Aβ plaques [29,34]. In addition, many inflammatory mediators detected in AD brains are of microglial origin [1]. In vitro, interaction of Aβ with microglia has been shown to cause the induction of a range of inflammatory products, including proinflammatory cytokines, neurotoxic factors, reactive oxygen species, and complement pathways proteins [29,31,73,74]. Multiple Aβ-binding protein or receptors have been identified on a number of different cell types, including microglia. They cover cell surface heparan proteoglycans and signal transduction receptors [9,19,29,40,75,77,79].

The receptor for advanced-glycation endproducts (RAGE) is one of these cell surface Aβ-binding proteins [11]. RAGE is a member of the immunoglobulin superfamily of cell surface molecules whose expression is up-regulated at sites of diverse pathologies from atherosclerosis to Alzheimer's disease [62]. The generation of reactive oxygen species, an early event after ligation of the receptor, may be fundamental for many RAGE-induced changes in cellular properties. In the case of neurons, RAGE induced cellular activation ultimately results in induction of programmed cell death [63].

In this work, we attempted to identify and to quantify the amount of oxidation-derived modified amino acids in proteins from frontal cerebral cortex of human brains with AD. Furthermore, we evaluated the distribution of these protein modifications by western-blot, and studied part of the biological response to these products by examining RAGE-expression by the same methodology. Finally, given the importance of PUFA in lipid peroxidation, we also studied the fatty acid profile from these samples.

2. Methods

2.1 Human brain specimens

Brain samples were obtained from the Institute of Neuropathology Brain Bank following the guidelines of the local ethics committee. The brains of 8 patients with AD and 5 age-matched controls were obtained from 3 to 13 h after death and were immediately prepared for morphological and biochemical studies. Patients with AD were four men and four women (mean age 76.2 years) with late onset non familial dementia. Control cases were five men and three women (mean age 72.6 years) with no neurological disease. The agonal state was short with no evidence of acidosis or prolonged hypoxia. At autopsy, half of each brain was fixed in formalin, while the other half was cut in coronal sections 1 cm thick, frozen on dry ice and stored at -80ºC until use. For diagnostic morphological studies, the brains were fixed by immersion in 10% buffered formalin for 2 or 3 weeks. The neuropathological study was carried out on de-waxed 4-µm-thick paraffin sections of the frontal (area 8), primary motor, primary sensory, parietal, temporal superior, temporal inferior, anterior cingulated, anterior insular, and primary and associative visual cortices; entorhinal cortex and hippocampus; caudate, putamen and pallidum; medial and posterior thalamus; subthalamus; Meynert nucleus; amygdala; midbrain (two levels), pons and medulla oblongata; and cerebellar cortex and dentate nucleus. The sections were stained with haematoxylin and eosin, luxol fast blue-Klüver Barrera, and, for immunohistochemistry to glial fibrillary acidic protein, CD68 and *Licopericum esculentum* lectin for microglia, βA4 amyloid, *tau*, αB-crystallin, α-synuclein and ubiquitin. Cases with AD were categorized as stages VI of neurofibrillary degeneration and stage C of amyloid deposition according to Braak and Braak classification [10]. No additional vascular or degenerative anomalies were present in these cases. Age-matched controls did not show neuropathological anomalies, particularly considering absence of amyloid deposits often considered as normal old-age changes. Frozen samples of the frontal cortex (area 8) were used for biochemical studies. Samples of control and diseased brains were processed in parallel.

2.2 Distribution of damage (Western blotting)

Derivatization of proteins for carbonyl detection.

Samples were homogenized in a buffer containing KCl 180mM, MOPS 5mM, EDTA 2mM, DTPAC 1 mM and BHT 1µM, pH 7,3 (Potter-Eljeveim device,at 4ºC). After a brief centrifugation (500 x g, 5 min) to pellet cellular debris, protein concentrations were measured in the supernatants using the Bio-rad Protein Assay (Bio-rad Laboratories, München, Germany).

Prior to electrophoresis, samples were derivatized with 2,4-dinitrophenylhydrazine (2,4-DNPH) as previously described [56]. Briefly, to 15 µl homogenates adjusted to 3,75 µg/µl protein SDS was added to a final concentration of 6%, and, after boiling for 3 min, 20 µl of 10 mM 2,4-DNPH in 10% trifluoroacetic acid were added. After 10 min at room temperature, 20 µl of a solution containing 2M Tris base, 30% glycerol and 15% β-mercaptoethanol were added for neutralisation and sample preparation for loading onto SDS-gels. For delipidated samples, prior to derivatization, chloroform (2:1 v/v) was added to an aliquot of the homogenates. Samples were then vortexed for 1 min and centrifuged at 13000 x G for 10 min. The proteins in the resulting supernatant were measured using the Bio-rad method and equalized.

Immunodetection of protein-bound 2,4-dinitrophenylhydrazones, AGEs and CML.

For immunodetection, after SDS-PAGE, proteins were transferred using a Mini Trans-Blot Transfer Cell (Bio-Rad Laboratories, München, Germany) to PVDF membranes (Immobilon-P Millipore, Bedford, MA). Immunodetection was performed using as primary antibodies: a rabbit anti-DNP antiserum (1:4000,Dako V401, Carpenteria, CA); 6D12, a monoclonal anti-CML antibody (1:2000,Transgenic Inc, Kumamoto, Japan); and a polyclonal anti-AGE antiserum, raised against glyoxilic acid-treated keyhole limpet hemocyanin (1:2000). Peroxidase-coupled secondary antibodies were used from the Tropix chemiluminiscence kit (Bedford, MA). Luminiscence was recorded and quantified in a Lumi-Imager equipment (Boehringer, Mannheim, Germany), using the Lumianalyst software.

Immunodetection of RAGE.

A slightly modified protocol was used. Briefly, samples (0.2g) from diseased and control cases were homogenized in a glass homogenizer in 10 volumes of ice-cold lysis buffer (20 mM Hepes pH 7.5, 250 mM sucrose, 10 mM KCl, 1.5 mM $MgCl_2$, 1mM EDTA, 1mM EGTA, 1mM DTT ,10 µg/ ml aprotinin, 1mM phenylmethylsulfonyl fluoride) and centrifuged at 5,000 rpm for 10 min at 4°C. Pellet fractions were discarded and protein concentrations of the supernatants were determined by the BCA method with bovine serum albumin as a standard.

Samples containing 50 µg of protein were loaded onto 10% acrylamide gels. Proteins were separated by SDS-PAGE and electrophoretically transferred to nitrocellulose filters. After transfer, the filters were blocked by incubation with 5% nonfat dry milk in TBS-T buffer (100mM tris-buffered saline-tween; 140 mM NaCl, 0.1% Tween 20, pH 7.4) 1 hour at room temperature. Then the filters were incubated overnight with TBS-T containing

3% Bovine Serum Albumin (BSA) (Sigma, Barcelona) and anti-RAGE antibody at 1:100 dilution. Next, the filters were washed three times in TBS-T and incubated with TBS-T containing 5% skimmed milk and horseradish peroxidase-linked goat immunoglobulins (Dako, Barcelona) diluted 1:1000 for 45 minutes at room temperature. Filters were washed several times in TBS-T, and immunoreactivity was detected using an enhanced chemiluminescence Western blot detection system (Amersham), followed by exposure to ECL HYPER film (Amersham, Barcelona).

Goat polyclonal anti-Receptor for Advanded Glycation End products (RAGE) was from Santa Cruz (Quimigranel, Barcelona, Spain) and it was used at a dilution of 1:100, and mouse monoclonal anti-α-tubulin at a dilution of 1:5000 was from Sigma (Barcelona). Secondary antibodies and reagents were from DAKO (Barcelona, Spain).

2.3 Measurement of glutamic and aminoadipic semialdehydes, CML, CEL and MDAL

Glutamic and aminoadipic semialdehydes, CML, CEL and MDAL concentrations in total proteins from cerebral cortex homogenates were measured by gas chromatography/mass spectrometry (GC/MS) as previously described [52]. Samples containing 0.75-1 mg of protein were delipidated using chloroform:methanol (2:1 v/v), and proteins were precipitated by adding 10% trichloroacetic acid (final concentration) and subsequent centrifugation. Protein samples were reduced overnight with 500 mM $NaBH_4$ (final concentration) in 0.2M borate buffer, pH 9.2, containing 1 drop of hexanol as an anti-foam reagent. Proteins were then reprecipitated by adding 1ml of 20% trichloroacetic acid and subsequent centrifugation. The following isotopically labelled internal standards were then added: [$^2H_8$]Lysine (d8-Lys; CDN Isotopes); [$^2H_4$]CML (d4-CML), [$^2H_4$]CEL (d4-CEL), and [$^2H_8$]MDAL (d8-MDAL), prepared as described [28,44]; [$^2H_5$]glutamic semialdehyde (d5-glutamic semialdehyde) and [$^2H_4$]aminoadipic semialdehyde (d4-aminoadipic semialdehyde), prepared as described in [58]. The samples were hydrolysed at 155^{o}C for 30 min in 1ml of 6N HCl, and then dried *in vacuo*. The N,O-trifluoroacetyl methyl ester derivatives of the protein hydrolysate were prepared as previously described [38]. GC/MS analyses were carried out on a Hewlett-Packard model 6890 gas chromatograph equipped with a 30m HP-5MS capillary column (30m x 0.25mm x 0.25 µm) coupled to a Hewlett-Packard model 5973A mass selective detector (Hewlett-Packard Española, S.A., Barcelona, Spain). The injection port was maintained at 275^{o}C; the temperature program was 5 min at 110^{o}C, then 2^{o}C/min to 150^{o}C, then 5^{o}C/min to 240^{o}C, then 25^{o}C/min to 300^{o}C, and finally hold at 300^{o}C for 5 min. Quantification was performed by external standardisation using standard curves constructed from mixtures of deuterated and non-deuterated standards. Analyses were carried out by selected ion monitoring gas chromatography/mass

spectrometry. Analytes were detected by selected ion-monitoring GC/MS (SIM-GC/MS). The ions used were: lysine and d8-lysine, *m/z* 180 and 187, respectively; glutamic semialdehyde and d5-glutamic semialdehyde, *m/z* 280 and 285, respectively; aminoadipic semialdehyde and d4-aminoadipic semialdehyde, *m/z* 294 and 298, respectively; CML and d4-CML , *m/z* 392 and 396, respectively; CEL and d4-CEL, *m/z* 379 and 383, respectively; and MDAL and d8-MDAL, *m/z* 474 and 482, respectively. The amounts of products were expressed as the ratio μmol glutamic semialdehyde, aminoadipic semialdehyde, CML, CEL or MDAL/mol lysine.

2.4 Fatty Acid Analysis

Fatty acid analysis was performed as previously described [52]. Total lipids from human brain homogenates were extracted with chloroform:methanol (2:1, v/v) in the presence of 0.01% butylated hydroxytoluene. The chloroform phase was evaporated under nitrogen, and the fatty acids were transesterified by incubation in 2.5 ml of 5% methanolic HCl for 90 min at 75^{o}C. The resulting fatty acid methyl esters were extracted by adding 2.5 ml of n-pentane and 1 ml of saturated NaCl solution. The n-pentane phase was separated, evaporated under nitrogen, redissolved in 75 μl of carbon disulphide and 1 μl was used for GC/MS analysis. Separation was performed in a SP2330 capillary column (30m x 0.25mm x 0.20μm) in a Hewlett Packard 6890 Series II gas chromatograph (Hewlett-Packard Española, S.A., Barcelona, Spain). A Hewlett Packard 5973A mass spectrometer was used as detector in the electron-impact mode. The injection port was maintained at 220^{o}C, and the detector at 250^{o}C; the temperature program was 2 min at 100^{o}C, then 10^{o}C/min to 200^{o}C, then 5^{o}C/min to 240^{o}C, and finally hold at 240^{o}C for 10 min. Identification of fatty acid methyl esters was made by comparison with authentic standards and on the basis of mass spectra. Results are expressed as mol%.

From fatty acid composition, the following FA indexes were calculated: Saturated Fatty Acids (SFA)= Σ % of saturated fatty acids; Unsaturated Fatty Acids (UFA)= Σ % unsaturated fatty acids; Monounsaturated Fatty Acids (MUFA)= Σ % of monoenoic fatty acids ; Polyunsaturated n-3 Fatty Acids (PUFAn-3)= Σ % of polyunsaturated fatty acids n-3 serie; Polyunsaturated n-6 Fatty Acids (PUFAn-6)= Σ % of polyunsaturated fatty acids n-6 serie; Average Chain Length (ACL)= [(Σ %Total$_{14}$ x 14) + …+ (Σ %Total$_{n}$ x n)]/100 (n= carbon atom number);Unsaturation Index (UI)= [(Σ mol% Monoenoic x 1) + (Σ mol% Dienoic x 2) + (Σ mol% Trienoic x 3) + (Σ mol% Tetraenoic x 4) + (Σ mol% Pentaenoic x 5) + (Σ mol% Hexaenoic x 6)]; Peroxidizability Index (PI) = [(Σ mol% Monoenoic x 0.025) + (Σ mol% Dienoic x 1) + (Σ mol% Trienoic x 2) + (Σ mol% Tetraenoic x 4) + (Σ mol% Pentaenoic x 6) + (Σ mol% Hexaenoic x 8)][20].

2.5 Statistical analyses

All statistics calculations were performed using the SPSS software (SPSS, Chicago). Differences between groups were analyzed by the Student's t tests. The 0.05 level was selected as the point of minimal statistical significance in every comparison.

3. Results

Although the western-blot analyses of total homogenates did not show major differences in the distribution of oxidative damage, after delipidation several bands around 40 to 65 kDa showed increased oxidative damage in AD samples (Figure 1a). Staining with a polyclonal anti-AGE did not reveal any evident difference. AD samples exhibited increased glycoxidative (6D12 antibody) damage, and the targets of these modifications showed diverse molecular weights, from 30 to 50 kDa (Figure 1b). Immunoblotting for RAGE demonstrated three major bands at approximately 30 kd, 50 kd, and 60 kDa in AD cases, while as control specimens only showed one lower molecular weight band occasionally (Figure 1c).

In order to offer a more accurate quantitative measurement of oxidation in brain proteins, we used isotope-dilution GC/MS. Proteins from human brain samples contained oxidation products resulting from MCO, glycoxidation and lipoxidation. An analysis of their distribution reveals than the more abundant products were those derived from MCO, AASA and GSA (almost 95% of measured markers) (Figure 2). GSA stood as the more MCO derived frequent modification, with levels being 40 fold higher than of those of AASA. The mean concentrations of both GSA and AASA were significantly higher ($p<0,001$ and $p<0,0001$, respectively) in brain samples from AD patients than in control, age-matched individuals (Figure 3). The mean concentrations of CEL and CML were also significantly higher ($p<0,04$ and $p<0,03$, respectively) in brain proteins from AD patients than in control individuals (Figure 3). The concentration of MDA-Lys, a lipoxidation product, was also significantly increased in samples from AD patients ($p<0,0001$; Figure 4).

The analyses of fatty acid revealed significant differences in brain samples, both in individual fatty acids and in global indexes (Table 1). The 24:0 and 22:5, quantitatively minor fatty acids, exhibited three-fold increases in their % content in AD samples. The highly peroxidizable docosahexaenoic acid (DHA) also showed a significant increase in its content ($p<0,001$;Figure 4) in these samples. In contrast, AD samples showed almost half of the % contents of 18:3 and 16:1, compared to the control samples. With reference to the derived indexes, AD samples showed significant decreases for monounsaturated fatty acids, with subsequent increases in the content of PUFA of the n-3 family. This resulted in a significantly increased double bond index (Table 1) and a higher peroxidizability index (Figure 4).

4. Discussion

The results of this work reinforce and expand previous analyses showing increased oxidative damage of proteins in brains from AD patients and experimental models. Further, this increased oxidative modification is associated with changes in fatty acid profile, which may exacerbate protein damage. The western blot analyses shown here agree with the generally accepted concept of specific damage [15,16]. Thus, a series of works using proteomic methodologies have identified several enzymes, such as creatine kinase BB, glutamine synthase, and ubiquitin carboxy-terminal hydrolase L-1, □-enolase, and other proteins, as heat-shock cognate 71 and DRP2 to be oxidativelly modified in AD. In our study, at least eight different bands showed increased DNP reactivity in AD homogenates. Among these, the region comprising 55 to 60 kDa may include heat-shock cognate 71 and DRP2. The lower molecular weight region (30 to 55 kDa) may also contain creatine kinase BB and glutamine synthase. This profile contrasted with the western blot obtained with anti-AGE and anti-CML antibodies, which showed apparently different targets. In contrast with the knowledge of DNP reactive protein targets in AD, the identity of AGE or glycoxidativelly modified proteins is unknown. Immunohistochemical evidences demonstrate that CML epitopes accumulate with age in the pyramidal neurons of hypocampus [36]. Other AGE are present in histological features associated with aging [37,39]. With reference to AD, it is known that AGE is a frequent modification in patients with presenilyn mutations [49], and that those products are found in senile plaques and neurofibrillary tangles[35,67,69].Therefore, AGE should modify the protein components of these pathological hallmarks. Hypothetically, one could assign propose that tau and βA (around 70 kDa) as well as presenilin (around 30 kDa) are targets of increased CML staining. In this line, AGE modification may increase aggregability of Aβ and tau. Both DNP and 6D12 blots exhibited increased staining in common regions of molecular weight. Therefore, it may be suggested that some of the targets may be the same for oxidative and glycoxidative processes. Alternatively, the possibility that some of the DNP reactive products derive from glycoxidation or lipoxidation cannot be dismissed [7]. Coexistence of AGE immunoreactivity with heme-oxygenase on neurofibrillary tangles would support this later hypothesis[76]. In addition, this assay, depending on reaction conditions, can be plagued with artefacts[14]. Measurement of characterized products by GC/MS solve these pitfalls [38,58,59].

Our data support the presence of this and other nonenzymatic markers in samples from aged individuals and AD patients by mass-spectrometric evidences. In the present work brain proteins have been analyzed, and we found the specific carbonyl AASA and GSA in these samples. The content of these AAOPs in AD samples was significantly increased.

This fact could be related to a mitochondrial dysfunction that would promote the leakage of reactive oxygen species, subsequently increasing protein oxidative damage [41]. Furthermore, the results agree with those previously suggesting that increased oxidative damage occurs in AD [2,42], although in these reports it affects specifically some key brain regions, such as temporal inferior cortex [8] or parietal lobe cortex [42]. The magnitude of the increase (9 to 13 in [42]; 5 to 7,5 in [8]) is lower than that reported here for AASA, but not for GSA. Interestingly, patients with familial forms of AD exhibit much higher increases [8] even in peripheral cells [17].

It has been reported that samples from AD patients do not have an increased amount of CML and pentosidine, another glycoxidation product [64]. Regional differences shown for protein oxidative damage may account for this discrepancy [33,42]. However, our mass-spectrometric data demonstrate an increase in glycoxidative damage in AD. These findings agree with the fact that the major energy source of brain is glycolysis as glycolytic intermediates are able to generate CML and CEL [71]. Vulnerable neurons may have increased dicarbonyl products and/or decreased turnover of modified proteins [49]. This fits with the fact that brain samples from AD patients exhibit increased carbonyl reductase, alcohol dehydrogenase [5] and pentose phosphate pathway activities [51]. In addition, recent data stress the potential importance of glyoxalase I, an enzyme against reactive dicarbonyls, as a risk factor in AD pathogenesis [18]. These could constitute a potential response to increased carbonyl stress. This contrasts with other counter-measures against oxidation, such as methionine sulfoxide reductase, whose activity decreases in several brain regions damaged in AD [28].Concerning AD pathogenesis, it has been proposed that CML increased immunostaining is tipicaly distributed among astrocytes and glia in an AD-specific fashion[69,70]. In this context, coexistence of the RAGE with AGE in astrocytes may be a more pathogenically relevant finding than AGE alone. In this work, RAGE expression was increased in brain cortex from AD patients. This finding would agree with a pathogenic role for this multiligand receptor in AD. In some control individuals anti-RAGE immunoreactivity was not evident or it was limited to a band around 30 kDa, a very low molecular weight that may be related to the $\square^{8}$-RAGE, a novel secreted splice variant of the RAGE, recently identified in brain astrocytes and in peripheral blood mononuclear cells [53]. The lack of constitutive expression in control samples agrees with interindividual differences of expression of this protein [53]. In clear contrast with brains from control patients, brain cortex from AD patients exhibited a marked increase in immunoreactivity as well as in the molecular heterogeneity of the immunoreactive forms. Thus, at least 4 to 5 anti-RAGE immunoreactive bands were detected. These may belong to full-length RAGE (55 kDa), N-terminal RAGE (35 kDa), already identified in human brain tissue [61]. Different RAGE variants have been

described, such as the C-truncated, encoding a soluble, secreted from of RAGE (50 kDa), as well as its form lacking glycosilation (46 kDa) in pericytes and in endothelial cells [78]. The pathophysiological relevance of these findings is unknown but it is proposed that RAGE overexpression may reflect different responses to increased AGE or Aβ concentrations. Thus, as C-truncated RAGE forms are cytoprotective for endothelial cells [78] its overexpression would constitute a defensive response. In contrast, expression of full-length RAGE could contribute to the acceleration of neuronal damage throughout activation of inflammatory responses [76,77] and/or the accumulation of Aβ in brain parenquima [22]. Nevertheless, recent data suggest a novel pathogenic pathway, were IgG against RAGE, increased three-fold in serum from AD patients, could participate in a chronic activation of peripheral immune cells [48]. Further investigations are needed to solve these questions.

Lipid peroxidation-derived protein damage was also evidenced by GC/MS. MDA-Lys appears to be the more sensible marker, as it increases almost two-fold in samples from AD patients. This agrees with previous reports, stating pronounced protein modification by 4-hydroxynonenal [46,47] and acrolein [13] in AD. Nevertheless, levels of HNE correlate with the severity of the disease [21]. However, these reports were mainly based on immunohistochemical analyses. Our results offer mass-spectrometric evidences for this type of oxidative damage in proteins in AD. In a close relationship with this fact, we found that AD samples exhibit differences in fatty acid content. Thus, increased lipid peroxidizability index and DHA content sustain increased lipid-peroxidation. Both lipid peroxidation and protein modification show a tight relation [21]. It is known that Aβ induces hippocampal neuronal death by a mechanism that requires lipid peroxidation [43,44,55]. It could be proposed that Aβ could induce lipid peroxidation and this fact, besides changing levels of ceramides, cholesterol and cholesterol esters could modify key proteins collaborating to neuronal death. Results of our work agree with previous data showing moderate changes in fatty acid profiles. It has been found for cardiolipin that PUFA content decreases moderately in AD[30]. In contrast with our data, other authors detected increased levels of adrenic acid (22:4 n-6) in grey matter from AD patients [65]. The reasons for this discrepancy may arise from regional differences in sampling or from predominance of white matter lipids in our samples, as the content of this fatty acid is decreased in the white matter of AD patients [65]. More importantly, increased levels of DHA reported by these authors agree with our data. Marked modifications in the PUFA content of phosphatidylethanolamine (the phospholipids fraction with higher PUFA content) have been reported in the grey matter of AD samples [68]. While as we detected an increased content in 16:0 this previous report indicated increased contents of 14:0, 16:0 and 18:0. Noteworthy, and in agreement with our data, this report shows

significant decreases in the content of adrenic acid, but not for 22:6 whose values were decreased [68]. Disturbances in the metabolism and transport of essential fatty acids may explain these changes [25,57], but they could also originate from a defensive response. The neuroprotective role of DHA in several experimental models would sustain this later hypothesis [6,26]. However, this protective role may have an important negative impact, as this is a highly peroxidizable fatty acid. Thus, besides the reported roles of cholesterol metabolism [21] in Aβ production, our data point for an important role of PUFA redistribution as a contributor of AD pathogenesis through protein oxidative damage.

Collectively, the results presented here support, by independent methodologies, a role for both protein oxidative damage and changes in fatty acid composition in AD pathogenesis. Although, with the used approach, we are not able to distinguish between intracellular and extracellular proteins, intracellular oxidation of target proteins could increase calcium concentrations [32]. This would lead to cytoeskeletal disturbances that ultimate would contribute to the generation of neurfibrillary tangles with the participation of lipid peroxidation. In addition, mitochondrial-derived superoxide, whose concentrations may increase with age [50] could be reflected in rising intercellular H_2O_2 levels [32], contributing to the modification of extracellular proteins. Furthermore, free radicals generated by RAGE-activated microglia [60,69,76,77] could also react with cellular and extracellular targets, accelerating the deleterious effects of oxidative stress.

5. Acknowledgements

This work was funded by grants from the Spanish Ministry of Science and Technology (BFI2003-01287), Spanish Ministry of Health, Instituto de Salud Carlos III (FIS 02-0891), the Amyotrophic Lateral Sclerosis Association, and the Generalitat of Catalunya (2001SGR00311) to R.P and M.P.O; and FIS grants 020004 and 03-006, CICYT SAF-2001-4681E , and EU project Brain Net Europe II to I.F.

6. References

1. Akiyama HS, Barger S, Barnum S, Bradt B, Bauer J, Cole GM, Cooper NR, Eikelenboom P, Emmerling M, Fiebich BL, Finch CE, Frautschy S, Griffin WS, Hampel H, Hull M, Landreth G, Lue L, Mrak R, Mackenzie IR, McGreer PL, O'Banion MK, Pachter J, Pasinetti G, Plata-Salaman C, Rogers J, Rydel R, Shen Y, Streit W, Strohmeyer R, Tooyoma I, Van Muiswinke FL, Veerhuis R, Walker D, Webster S, Wegryniak B, Wenk G, Wysscoray T Inflammation and Alzheimer's disease. Neurobiol Aging 2000; 21:383-421.
2. Aksenov MY, Aksenova MV, Butterfield DA, Geddes JW, Markesbery WR. Protein oxidation in the brain in Alzheimer's disease. Neuroscience 2001; 103(2):373-83.
3. Amici A, Levine RL, Tsai L, Stadtman ER. Conversion of amino acid residues in proteins and amino acid homopolymers to carbonyl derivatives by metal-catalyzed oxidation reactions. J Biol Chem 1988;365:3341-6.
4. Anderson MM, Requena JR, Crowley JR, Thorpe SR, Heinecke JW. The myeloperoxidase system of human phagocytes generates Nepsilon-(carboxymethyl)lysine on proteins: a mechanism for producing advanced glycation end products at sites of inflammation. J Clin Invest. 1999;104:103-13.
5. Balcz B, Kirchner L, Cairns N, Fountoulakis M, Lubec G. Increased brain protein levels of carbonyl reductase and alcohol dehydrogenase in Down syndrome and Alzheimer's disease. J Neural Trans Suppl 2001;61:193-201.
6. Barcelo-Coblijn G, Hogyes E, Kitajka K, Puskas LG, Zvara A, Hackler L, Nyakas C, Penke Z, Farkas T. Modification by docosahexaenoic acid of age-induced alterations in gene expresión and molecular composition of rat brain phospholipids. Proc Natl Acad Sci USA 2003; 100:11321-6.
7. Berlett BS, Stadtman ER. Protein oxidation in aging, disease, and oxidative stress. J Biol Chem. 1997;272:20313-6.
8. Bogdanovic N, Zilmer M, Zilmer K, Rehema A, Karelson E. The Swedish APP670/671 Alzheimer's disase mutation: The first evidence for strikingly increased oxidative injury in the temporal inferior cortex. Dement Geriatr Cogn Dis 2001;12:364-71.
9. Boland K, Behrens M., Choi D, Manias K, Perlmutter DH The serpin-enzyme complex receptor recognizes soluble, nontoxic amyloid-beta peptide but not aggregated, cytotoxic amyloid-beta peptide. J Biol Chem 1996: 271:18032-44.
10. Braak H, Braak E. Temporal sequence of Alzheimer's disease-related pathology. In: Cerebral Cortex, vol 14: Neurodegenerative and age-related changes in structure and function of the cerebral cortex. Peters A. and Morrison JH (Eds),

Kluwer Academic/Plenum Press: New York, Boston, Dordrecht, London, Moscow, 1999 pp: 475-12

11. Brett J, Schmidts AM, Yan SD, Zou YS, Weidman E, Pinski D, Nowygrod R, Neeper M., Przysiecki C, Shaw A. Survey of the distribution of a newly characterized receptor for advanced glycation end products in tissues. Am J Pathol 1993; 143:1699-12.
12. Butterfield DA, Castegna A, Lauderback CM, Drake J. Evidence that amyloid beta-peptide-induced lipid peroxidation and its sequelae in Alzheimer's disease brain contribute to neuronal death. Neurobiol Aging 2002; 203:655-64.
13. Calingasan NY, Uchida K, Gibson GE. Protein-bound acrolein: a novel marker of oxidative stress in Alzheimer's diseas. J Neurochem 1999;72:751-6.
14. Cao G, Cutler RG. Protein oxidation and aging. I. Difficulties in measuring reactive protein carbonyls in tissues using 2,4-dinitrophenylhydrazine. Arch Biochem Biophys 1995; 320:106-14.
15. Castegna A, Aksenov M, Aksonva M, Thongbookerd V, Klein JB, Pierce WM, Booze R, Markesbery WR, Buttefield DA. Proteomic identification of oxidatively modified proteins in Alzheimer's disease brain. Part II: dihydropyrimidinase-related protein 2, a-enolase, and heat shock cognate 71. J Neurochem, 2002; 82:1524-32
16. Castegna A, Aksenov M, Aksonva M, Thongbookerd V, Klein JB, Pierce WM, Booze R, MArkesbery WR, Buttefield DA. Proteomic identification of oxidatively modified proteins in Alzheimer's disease brain. Part I: creatine kinase BB, glutamine synthase, and ubiquitin carboxy-terminal hydrolase L-1. Free Rad Biol Med 2002; 33:562-71
17. Cechi C, Fiorillo C, Sorbi S, Latorraca S, Nacmias B, Bagnoli S, Nassi P, Liguri G. Oxidative stress and reduced antioxidant defenses in peripheral cells from familial Alzheimer's patients. Free Radic Biol Med 2002;33:1372-9.
18. Chen F, Wollmer MA, Hoerndli F, Munch G, Kuhla B, Rogaev EI, Tsolaki M,Papassotiropoulos A, Gotz J. Role for glyoxalase I in Alzheimer's disease. Proc Natl Acad Sci U S A. 2004 [Epub ahead of print]
19. Combs CK, Johnson DE, Cannady SB, Lehman TM, Landreth GE. Identification of microglial signal transduction pathways mediating a neurotoxic response to amyloidogenic fragments of beta-amyloid and prion proteins. J Neurosci 1999; 19:928-39.
20. Cosgrove JP, Church DF, Pryor WA. The kinetics of the autoxidation of polyunsaturated fatty acids. Lipids. 1987;22:299-304.

21. Cutler RG, Kelly J, Storie K, Pedersen WA, Tammara A, Hatanpaa K, Troncoso JC, Mattson MP. Involvement of oxidative stress-induced abnormalities in ceramide and cholesterol metabolism in brain aging and Alzheimer's disease.Proc Natl Acad Sci USA. 2004;101:2070-5
22. Deane R, Du Yan S, Submamaryan RK, LaRue B, Jovanovic S, Hogg E, Welch D, Manness L, Lin C, Yu J, Zhu H, Ghiso J, Frangione B, Stern A, Schmidt AM, Armstrong DL, Arnold B, Liliensiek B, Nawroth P, Hofman F, Kindy M, Stern D, Zlokovic B. RAGE mediates amyloid-beta peptide transport across the blood-brain barrier and accumulation in brain. Nat Med. 2003;9:907-13.
23. Eikelenboom P, Rozemuller, JM., Van Muiswinkel FL. Inflammation and Alzheimer's disease: Relationships between pathogenic mechanisms and clinical expression. Exp Neurol 1998; 154:89-98.
24. Esterbauer H, Schaur RJ, Zollner H. Chemistry and biochemistry of 4-hydroxynonenal, malonaldehyde and related aldehydes. Free Radic Biol Med 1991;11:81-128.
25. Farooqui AA, Horrocks LA. Plasmalogens, phospholipase A(2), and docosahexaenoic acid turnover in brain tissue. J Mol Neurosci 2001; 264-72.
26. Favreliere S; Perault MC, Huget F, De Javel D, Bertrand M, Piriou A, Durand G. DHA-enriched phospholipids diets modulate age-related alterations in rat hippocampus. Neurobiol Aging. 2003; 24:233-43.
27. Fu MX, Requena JR, Jenkins AJ, Lyons TJ, Baynes JW, Thorpe SR. The advanced glycation end product, Nepsilon-(carboxymethyl)lysine, is a product of both lipid peroxidation and glycoxidation reactions. J Biol Chem. 1996;271:9982-6.
28. Gabbita SP, Aksenov MY, Lovell Ma, Markesbery WR. Decrease in peptidemethionine sulfoxide reductase in Alzheimer's disease brain. J Neurochem 199;73:1660-6.
29. Giuliani D, Haverkamp LJ, Li J, Karshin WL, Yu J, Tom D, Li X, Kirkpatrick JB Senile plaques stimulate microglia to release a neurotoxin found in Alzheimer brain. Neurochem Int 1995, 27:119-37.
30. Guan ZZ, Soderberg M, Sindelar P, Edlund C. Content and fatty acid composition of cardiolipin in the brain of patients with Alzheimer's disease. Neurochem Int 1994; 25:295-300.
31. Haga S, Ikeda K, Sato M, Ishii T. Synthetic Alzheimer amyloid beta/A4 peptides enhance production of complement C3 component by cultured microglial cells. Brain Res 1993; 601:88-94

32. Harman D. Alzheimer's disease: role of aging in pathogenesis. Ann NY Acad Sci 2002;959:384-95.
33. Hensley K, Hall N, Subramaniam R, cole P, Harris M, Aksenov M, Aksenova M, Gabbita SP, Wu JF, Carney JM, Lovell M, Markesbury WR and Butterfield DA. Brain regional correspondence between Alzheimer's disease histopathology and biomarkers of protein oxidation . J Neurochem 1995; 65:2146-56.
34. Itagaki S, McGreer PL, Akiyama H, Zhu S, Selkoe D. Relationship of microglia and astrocytes to amyloid deposits of Alzheimer disease. J Neuroimmunol 1989; 24:173-182.
35. Kikuchi S, Shinpo K, Takeuchi M, Yamagishi S, Makita Z, Sasaki N , Tashiro K. Glycation- a sweet tempter for neuronal death. Brain Res Rev 2003; 41:306-23.
36. Kimura T, Takamatsu J, Ikeda K, Kondo A, Miyakawa T, Horiuchi S. Accumulation of advanced glycation end products of the Maillard reaction with age in human hippocampal neurons. Neurosci Lett 1996; 208:53-6.
37. Kimura T, Takamatsu J, Miyata T, Miyakawa T, Horiuchi S. Localization of identified advanced glycation end-products structures, N□ (carboxymethyl)lysine and pentosidine in age-realted inclusions in human brains. Pathol Int 1998; 48:575-9.
38. Knecht KJ, Dunn JA, McFarland KF, McCance DR, Lyons TJ, Thorpe SR, Baynes JW. Effect of diabetes and aging on carboxymethyllysine levels in human urine. Diabetes 1991;40:190-6.
39. Li JJ, Surini M, Catsicas S, Kawashima E, Bouras C. Age-dependent accumulation of advanced glycosylation end products in human neurons. Neurobiol Aging 1995; 16:69-76.
40. Lorton D, Schaler J, Lala A, De Nardin E. Chemotactic-like receptors and Aβpeptide-induced responses in Alzheimer's disease. Neurobiol Aging 2000; 21:463-473.
41. Lustbader JW, Cirilli M, Lin C, Xu HW, Takuma K, Wang N, Caspersen C, Chen X, Pollak S, Chaney M, Trinchese F, Liu S, Gunn-Moore F, Lue LF, Walker G, Kuppusamy P, Zewier ZL, Arancio O, Stern D, Yan SS, Wu H. ABAD directly links Abeta to mitochondrial toxicity in Alzheimer's disease. Science. 2004 16;304:448-52.
42. Lyras L, Cairns NJ, Jenner A, Jenner P, Halliwell B. An assessment of oxidative damage to proteins, lipids, and DNA in brains from patients with Alzheimer's disease. J Neurochem 1997; 68:2061-9.

43. Mark RJ, Pang Z, Geddes JW, Uchida K, Mattson MP. Amyloid beta-peptide impairs glucose transport in hippocampal and cortical neurons: involvement of membrane lipid peroxidation.J Neurosci 1997;17(3):1046-54
44. Mattson MP. Modification of ion homeostasis by lipid peroxidation: roles in neuronal degeneration and adaptive plasticity. Trends Neurosci. 1998;21:53-7
45. McGreer EG, McGreer PL. The importance of inflammatory mechanisms in Alzheimer's disease. Exp Gerontol 1998; 33:371-378.
46. Montine KS, Kim PS, Markesbery WR, Montine TJ. 4-hydroxy-2-nonenalpyrrole adducts in human neurodegenerative disease. J Neuropathol Exp Neurol 1997;56:866-71
47. Montine TJ, Markesbery WR, Zackert W, Sanchez ST, Roberts LJ, Morrow JD. The magnitude of brain lipid peroxidation correlates with the extentn of degeneration but not with density of neuritic plaques or neurofibrillary tangles or with APOE genotype in Alzheimer's disease patients. Am J Pathol 1999;155:863-8
48. Mruthinti S, Buccafusco JJ, Hill WD, Waller JL, Jackson TW, Zamrini EY, Schade RF. Autoimmunity in Alzheimer's disease: increased levels of circulating IgGs binding Ab and RAGE peptides. Neurobiol Aging 2004, in press.
49. Münch G, Shepherd CE, McCann H, Brooks WS, Kwok JB, Arendt T, Hallupp M, Schofield Pr, Martins RN, Halliday GM. Intraneuronal advanced glycation endproducts in presenilin-1 Alzheimer's disease. Neuroreport 2002;13:601-4.
50. Ozawa T .Mitochondrial DNA mutations and age. Ann NY Acad Sci 1998;854:128-54
51. Palmer AM. The activity of the pentose phosphate pathway is increased in response to oxidative stress in Alzheimer's disease. J Neural Transm 1999; 106:317-28.
52. Pamplona R, Portero-Otin M, Requena J, Gredilla R, Barja G. Oxidative, glycoxidative and lipoxidative damage to rat heart mitochondrial proteins is lower after 4 months of caloric restriction than in age-matched controls. Mech Ageing Dev 2002;123:1437-46.
53. Park IH, Yeon SI, Youn JH, Choi JE, Sasaki N, Choi IH, Shin JS. Expression of a novel secreted splice variant of the receptor for advanced glycation end products (RAGE) in human brain astrocytes and peripheral blood mononuclear cells. Mol Immunol 2004;40:1203-11.
54. Pasinetti GM. Inflammatory mechanisms in neurodegeneration and Alzheimer's disease: The role of the complement system. Neurobiol Aging 1996; 17:707-716.

55. Pedersen WA, Chan SL, Mattson MP. A mechanism for the neuroprotective effect of apolipoprotein E:isoform-specific modification by the lipid peroxidation product 4-hydroxynonenal.J Neurochem. 2000;74:1426-33
56. Portero-Otin M, Pamplona R, Ruiz MC, Cabiscol E, Prat J, Bellmunt MJ. Diabetes induces an impairment in the proteolytic activity against oxidized proteins and a heterogeneous effect in nonenzymatic protein modifications in the cytosol of rat liver and kidney. Diabetes 1999;48:2215-20.
57. Rapoport SI, Chang MCJ, Spector AA. Delivery and turnover of plasma-derived essential PUFAs in mammalian brain. J Lip Res 2001;42:678-85.
58. Requena JR, Chao CC, Levine RL, Stadtman ER. Glutamic and aminoadipic semialdehydes are the main carbonyl products of metal-catalized oxidation of proteins. Proc Natl Acad Sci USA 2001;98:69-74
59. Requena JR, Fu MX, Ahmed MU, Jenkins AJ, Lyons TJ, Baynes JW, Thorpe SR. Quantification of malondialdehyde and 4-hydroxynonenal adducts to lysine residues in native and oxidized human low-density lipoprotein.Biochem J. 1997;322:317-25
60. Rogers J, Webster S, Lue LF, Brachova L, Civin WH, Emmerling M, Shivers B,Walker D, McGeer P. Inflammation and Alzheimer's disease pathogenesis. Neurobiol Aging. 1996;17(5):681-6
61. Sasaki N, Toki S, Chowei H, Saito T, Nakano N, Hayashi Y, Takeuchi M, Makita Z. Immunohistochemical distribution of the receptor for advanced glycation end product in neurons and astrocytes in Alzheimer’s disease. Brain Res 2001; 888:256-62.
62. Schmidt AM, Yan SD, Wautier JL, Stern DM. Activation of receptor for advanced glycation end products: a mechanism for chronic vascular dysfunction in diabetic vasculopathy and atherosclerosis. Circ Res 1999; 84: 489-497.
63. Schmidt AM, Yan SD, Yan SF, Stern DM. The biology of the receptor for advanced glycation end products and its ligands. Biochim Biophys Acta 2000; 1498:99-111.
64. Seidl R, Schuller E, Cairns N, Lubec G. Evidence against increased glycoxidation in patients with Alzheimer’s disease. Neurosci Lett 1997; 232:49-2.
65. Skinner ER, Watt C, Besson JA, Best PV. Differences in the fatty acid composition of the grey and white matter of different regions of the brains of patients with Alzheimer’s disease and control subjects. Brain 1993; 116:717-25.
66. Smith CD, Carney JM, Starke-Reed PE, Oliver CN, Stadtman ER, Floyd RA, Markesbery WR. Excess brain protein oxidation and enzyme dysfunction in normal aging and in Alzheimer disease. Proc Natl Acad Sci USA 1991; 88:10540-3

67. Smith MA, Richey PL, Taneda S, Kutty RK, Sayre LM, Monnier VM, Perry G. Advanced Maillard end products, free radicals, and protein oxidation in Alzheimer's disease. Ann NY Acad Sci 1994;738:447-54.
68. Soderberg M, Edlund C, Krisstensson K, Dallner G. Fatty acid composition of brain phospholipids in aging and in Alzheimer's disease. Lipids 1991;26:421-5.
69. Taked A, Yasuda T, Miyata T, goto Y, Wakai M, Watanabe M, Yasuda Y, Horie K, Inagaki T, Doyu M, Maeda K, Sobue G. Advanced glycation end products co-localized with astrocytes and microglial cells in Alzheimer's disease brain. Acta Neuropathol. (Berl) 1998;95; 555-8.
70. Takeda A, Wakai M, Niwa H, Di r, Yamamoto M, Li M, Goto Y, Yasuda T, Nakagomi Y, Watanabe M, Inagaki T, Yasuda Y, Miyata T, Sobue G. Neuronal and glial advanced glycation end-product [N□ (carboxymethyl)lysine] in Alzheimer's disease brains. Acta Neuropathol (Berl) 2001;101:27-35
71. Thornalley PJ, Langborg A, Minhas HS. Formation of glyoxal, methylglyoxal and 3-deoxyglucosone in the glycation of proteins by glucose. Biochem J. 1999;344:109-16.
72. Thorpe SR, Baynes JW. Maillard reaction products in tissue proteins: new products and new perspectives.Amino Acids. 2003;25(3-4):275-81
73. Van Muiswinkel FL, Raupp SF, de Vos NM, Smits HA, Verhoef J, Eikelenboom P, Nottet HS. The amino-terminus of the amyloid-beta protein is critical for the cellular binding and consequent activation of the respiratory burst of human macrophages. J Neuroimmunol 1999; 96:121-130.
74. Walker DG, Kim SU, McGreer PL. Complement and cytokine gene expression in cultured microglia derived from postmortem human brains. J Neurosci Res 1995 ; 40:478-493.
75. Yaar M, Zhai S, Pilch PF, Doyle SM, Eisenhauer PB, Fine RE, Gilchrest BA. Binding of beta-amyloid to the p75 neurotrophin receptor induces apoptosis: A possible mechanism for Alzheimer's disease. J Clin Invest 1999; 100:2333-2340.
76. Yan SD, Chen X, Fu J, Chen M, Zhu H, Roher A, Slattery T, Zhao L, Nagashima M, Morser J, Migheli, Nawroth P, Stern D, Schmidt AM. RAGE and amyloid-beta peptide neurotoxicity in Alzheimer's disease. Nature 1996; 382:685-691.
77. Yan SD, Chen X, Schmidt AM, Brett J, Goldman G, Zou YS, Scott CW, Caputo C, Frappier T, Smith MA, Perry G, Yen S-H, Stern D. Glycated tau protein in Alzheimer's disease: a mechanism for induction of oxidant stress. Proc Natl Acad Sci USA 1994; 91:7787-91.
78. Yonekura H, Yamamoto Y, Sakurai S, Petrova RG, Abedin MJ, Li H, Yasui K, Takeuchi M, Makita Z, Takasawa S, Okamoto H, Watanabe T, Yamamoto H. Novel

splice variants of the receptor for advanced glycation end-products expressed in human vascular endothelial cells and pericytes, and their putative roles in diabetes-induced vascular injury. Biochem J. 2003;370:1097-109.

79. Zlokovic BV, Martel CL, Matsubara E, McComb JG, Zheng G, McCluskey, RT, Frangione B, Ghiso J. Glycoprotein 330/megalin: Probable role in receptor-mediated transport of apolipoprotein J alone and in complex with Alzheimer disease amyloid beta at the blood-brain and blood-cerebrospinal fluid barriers. Proc Natl Acad Sci. USA 1996; 93:4229-4234.

Table 1. Fatty acid composition and derived indexes in brain samples from AD patients and control individuals

	Ctl	AD
14:0	0.59±0.06	0.48±0.02*
16:0	16.60±0.15	19.81±0.66*
16:1n-7	1.76±0.11	1.19±0.01*
18:0	23.67±0.35	21.50±0.39*
18:1n-9	26.78±0.12	23.27±0.77*
18:2n-6	0.66±0.05	0.85±0.10
18:3n-3	0.12±0.01	0.07±0.003*
20:0	1.97±0.19	1.64±0.16
20:1	0.13±0.01	0.20±0.009
20:2n-6	0.26±0.02	0.21±0.01*
20:3n-6	0.76±0.09	0.58±0.02*
20:4n-6	6.91±0.46	6.91±0.42
22:4n-6	5.99±0.29	4.68±0.19*
22:5n-6	0.52±0.09	0.62±0.02
22:5n-3	0.10±0.006	0.30±0.03*
22:6n-3	11.43±0.46	14.53±0.48*
24:0	0.20±0.03	0.61±0.07*
24:1n-9	1.45±0.15	2.46±0.27*
ACL	18.63±0.02	18.74±0.02
SFA	43.05±0.11	44.06±0.51
UFA	56.94±0.11	55.93±0.51
MUFA	30.14±0.24	27.12±0.74*
PUFA	26.79±0.33	28.80±0.56
PUFAn-6	15.12±0.45	13.88±0.49
PUFAn-3	11.66±0.46	14.92±0.50*
DBI	158.08±1.78	169.55±2.49*
PI	150.38±2.82	171.38±3.68*

Values shown are mean±SEM. N for each group:7. ACL, average chain length; SFA, saturated fatty acids; UFA, unsaturated fatty acids; PUFA n-6/n-3, polyunsaturated fatty acids n-6 or n-3 series; MUFA, monounsaturated fatty acids; DBI, double bond index; PI, peroxidizability index. Asterisks indicates significant differences with control group as assessed by Student's t test ($p<0,05$).

8. Figure legends

Figure 1: AD induces differences in the distribution of protein oxidative modifications and in RAGE expression in homogenates from brain samples. Protein carbonyl groups, markers of protein oxidative damage, were derivatized with DNPH and, after their separation by SDS-PAGE, their amount was revealed by immunoblotting (A, left graph). After delipidation, differences between individual bands were more clear (A, right graph). Western-blot analyses measured also AGE (B, upper blot) and CML (B, middle "6D12" blot) protein modifications. Arrows indicate bands noticeably different in AD samples. Right numbers of the blots indicate apparent molecular weight. The lower panels show the quantitation of these blots by densitometry. AD also induces differences in RAGE expression as shown by western-blot analyses of individual samples which revealed differences in distribution and amount of anti-RAGE immunoreactive bands (C shows representative blots from brain cortex of control individuals and AD patients)

Figure 2: AD samples exhibit changes in the amount of protein oxidative modifications in homogenates from brain samples. GC/MS analyses measured the concentrations of metal-catalyzed oxidation (GSA,AASA), glycoxidation-lipoxidation (CML, CEL) and lipoxidation (MDA-Lys), shown in μmol/mol lysine.

Figure 3: Proteins from AD samples show significant increases in the amounts of GSA and AASA, markers of metal-catalyzed oxidation (upper graph), and in the concentrations of CML and CEL, arising from glycoxidation and lipoxidation (lower graph). Values shown are % changes of mean±SEM over values from control samples (GSA: 20832±350 μmol/mol lysine; AASA: 100±12 μmol/mol lysine; CML: 497±10; CEL: 462±14). * $p<0,01$ and ** $p<0,001$ respect to control group by Student's t test.

Figure 4: Proteins from AD samples show significant increases in lipid peroxidation-derived damage, as shown by measurements of MDA-Lys (upper graph), and the percentual changes in peroxidizability index (PI) and DHA content (lower panel). Values shown are % changes of mean±SEM over values from control samples (MDA-Lys: 260±31 μmol/mol lysine; DHA: 11,43±0,46% ;PI: 150.38±2.82) ** $p<0,001$ respect to control group by Student's t test.

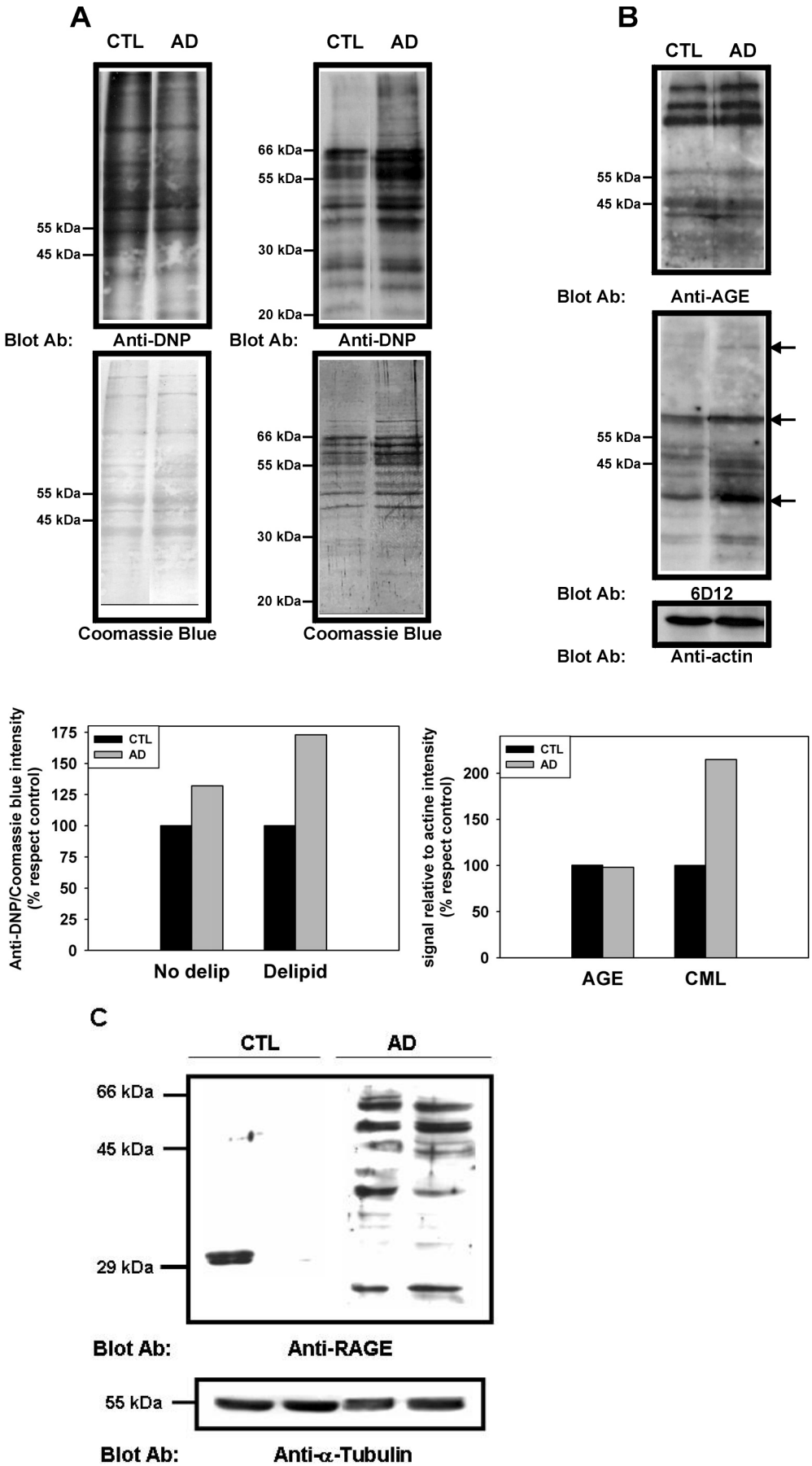
A
CTL
AD
55 kDa
45 kDa
Blot Ab:
Anti-DNP
Coomassie Blue
66 kDa
30 kDa
20 kDa
B
Anti-AGE
6D12
Anti-actin
Anti-DNP/Coomassie blue intensity (% respect control)
No delip
Delipid
signal relative to actine intensity (% respect control)
AGE
CML
C
Anti-RAGE
Anti-α-Tubulin

Figure 1

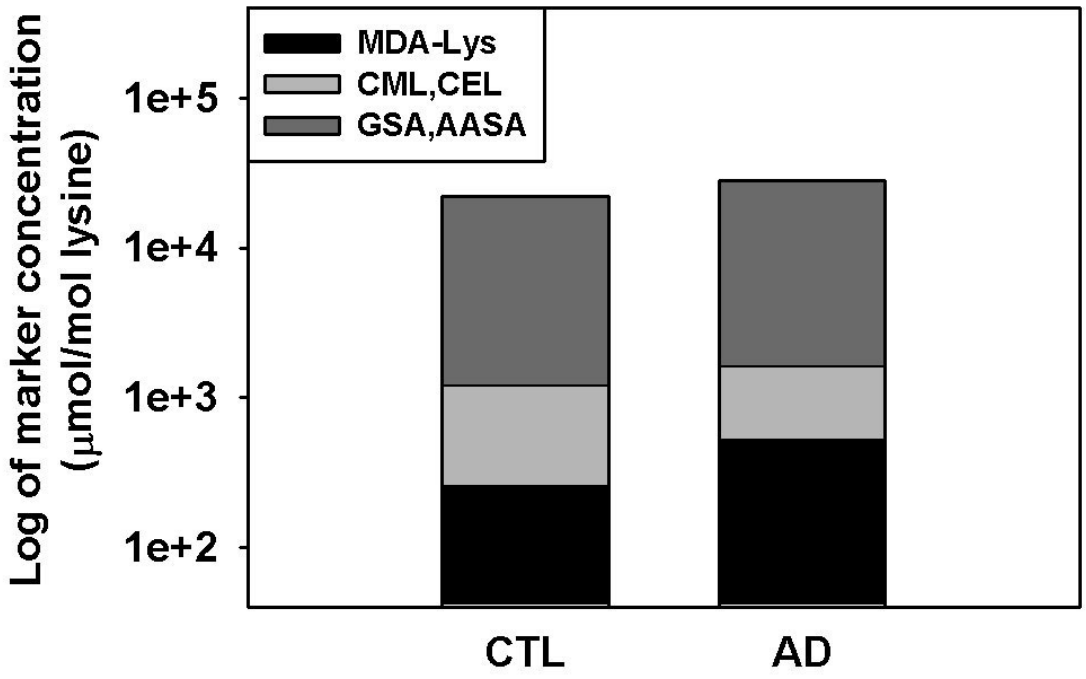
MDA-Lys
CML,CEL
GSA,AASA
Log of marker concentration (μmol/mol lysine)
1e+5
1e+4
1e+3
1e+2
CTL
AD

Figure 2

Figure3

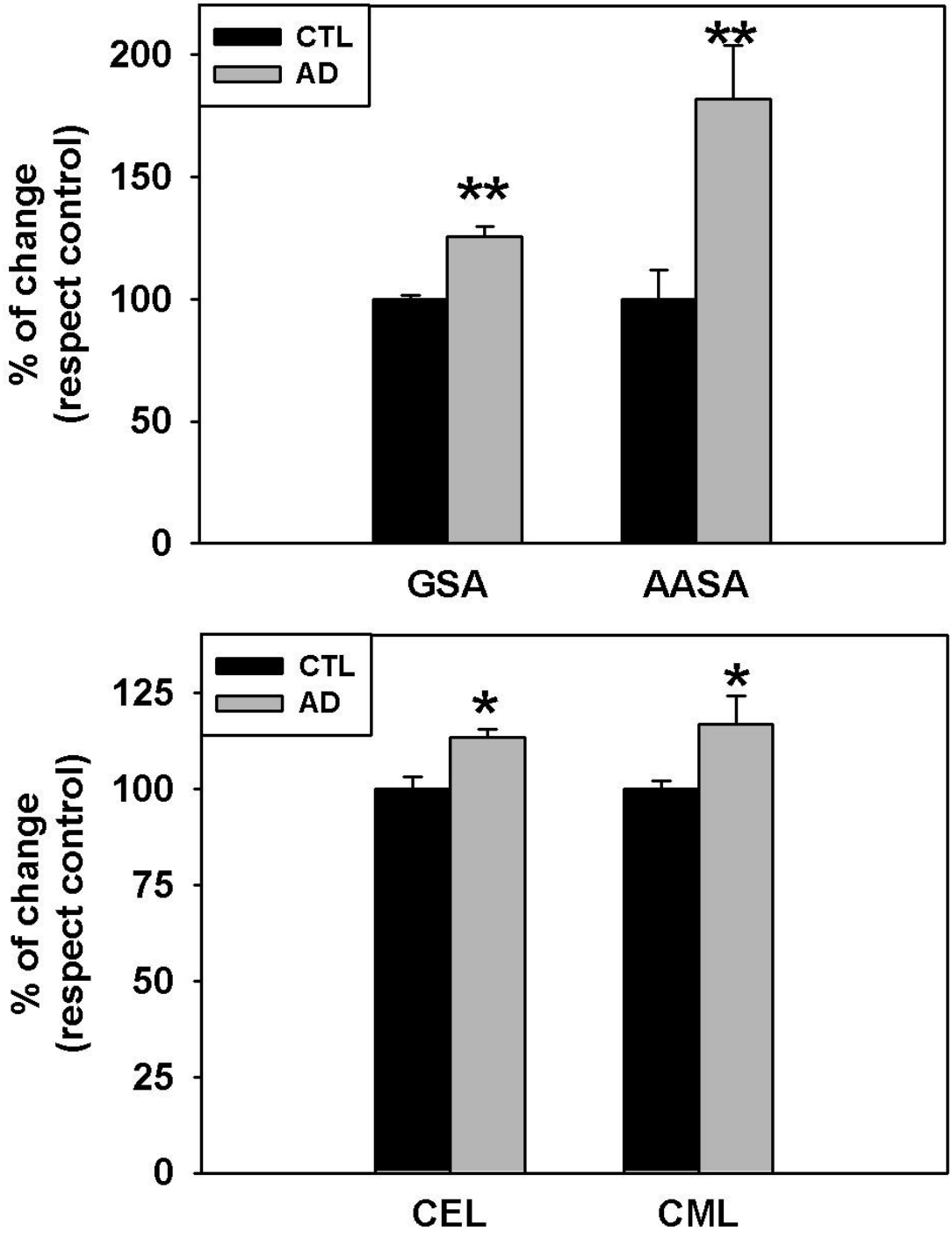
CTL
AD
% of change
(respect control)
200
150
100
50
0
**
**
GSA
AASA
CTL
AD
% of change
(respect control)
125
100
75
50
25
0
*
*
CEL
CML

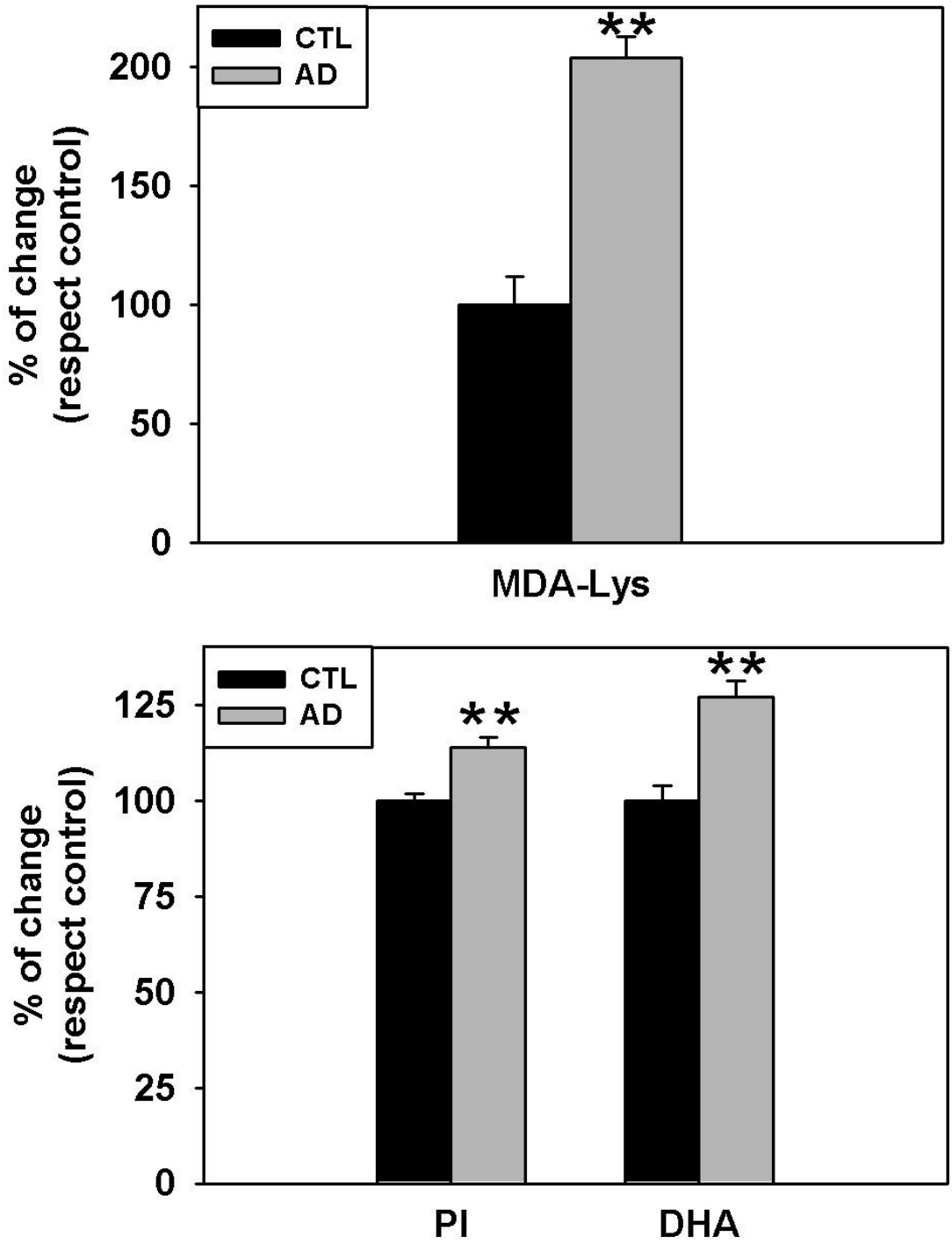
CTL
AD
**
200
150
100
50
0
% of change
(respect control)
MDA-Lys
CTL
AD
**
**
125
100
75
50
25
0
% of change
(respect control)
PI
DHA

Figure 4

Figure 1

Reinald Pamplona, Esther Dalfó, Maria Victoria Ayala, Maria Josep Bellmunt, Isidre Ferrer and Manuel Portero-Otín

Figure 2

Reinald Pamplona, Esther Dalfó, Maria Victoria Ayala, Maria Josep Bellmunt, Isidre Ferrer and Manuel Portero-Otín

Figure 3

Reinald Pamplona, Esther Dalfó, Maria Victoria Ayala, Maria Josep Bellmunt, Isidre Ferrer and Manuel Portero-Otín

Figure 4

Reinald Pamplona, Esther Dalfó, Maria Victoria Ayala, Maria Josep Bellmunt, Isidre Ferrer and Manuel Portero-Otín

IV. L'AβPP EN LES DLBs

IV. I. Barrachina M, Dalfó E, Puig B, Vidal N, Freixes M, Castaño E, Ferrer I (2004) *Amylioid-β deposition in the cerebral cortex in Dementia with Lewy bodies is acompained by a relative increase in AβPP mRNA isoforms containing the Kunitz protease inhibitor. (Acceptat a Neurochemistry International)*

La forma comú de la DLB està caracteritzada per alteracions tipus Alzheimer, dins de les quals s'hi troben els filaments del neuròpil i la formació de plaques senils. El principal component de la deposició amiloidea és el pèptid β-amiloide, derivat del processament de l' AβPP (Masters i col., 1985). Aquesta proteïna de membrana està codificada per 19 exons, dels quals, després de patir *splicing* alterantiu, en deriven diferents isoformes. Dues d'elles, l'AβPP751 i l'AβPP770, contenen l'exó 7, que codifica per un inhibidor de serin-proteases anomenta Inhibidor de proteases Kunitz (KPI). S'ha descrit que una elevada expressió prteica d'aquestes dues variants podria estar associada a la patologia d'Alzheimer (Moir i col., 1998). Donada la relació entre la forma comú de la DLB i la malaltia d'Alzheimer, hem volgut estudiar les tres formes d'ARNm principals, derivades de l'splicing alternatiu de l'AβPP (l'AβPP695, l'AβPP751 i l'AβPP770) en les dues formes de Demència amb cossos de Lewy, la pura i la comú, en la malaltia de Parkinson, com a altra forma de sinucleinopatia, a la malaltia d'Alzheimer i a l'Angiopatia cerebral amiloidea (AA), com a neurodegeneracions amiloidees, i a la paràlisi supranuclear progressiva (PSP) com a exemple de malaltia neurodegenerativa sense deposició amiloidea (Lee i col., 2001).

Amyloid-β deposition in the cerebral cortex in Dementia with Lewy Bodies is accompanied by a relative increase in AβPP mRNA isoforms containing the Kunitz protease inhibitor

Marta Barrachina, PhD[1], Esther Dalfó[1], Berta Puig, PhD[1], Noemi Vidal, MD[1], Meritxell Freixes[1], Esther Castaño, PhD[2] and Isidro Ferrer, MD, PhD*[1]

[1]Institut de Neuropatologia, IDIBELL-Hospital Universitari de Bellvitge, L'Hospitalet de Llobregat; [2] Unitat de Bellvitge, Serveis Cientifico-Tècnics, Universitat de Barcelona; Spain

*Corresponding author:
Isidro Ferrer, MD, PhD, Institut de Neuropatologia, Servei Anatomia Patològica, IDIBELL-Hospital Universitari de Bellvitge, carrer Feixa Llarga sn, 08907 L'Hospitalet de Llobregat, Spain
Tel.: +34 93 403 5808
e-mail: 8082ifa@comb.es
or
iferrer@csub.scs.es

Running title: AβPP in Dementia with Lewy bodies

Abstract

Deposition of amyloid-β, the fibrillogenic product of the cell surface protein AβPP (amyloid-β protein precursor), occurs in the cerebral cortex of patients with Dementia with Lewy bodies (DLB). Amyloid deposition, basically in the form of senile plaques, occurs not only in the common form (DLBc), which is defined by changes consistent with diffuse Lewy body disease accompanied by Alzheimer's disease (AD), but also in the pure form (DLBp), in which neurofibrillary tangles are absent. The present study analyses the expression of AβPP mRNA isoforms with (AβPP751 and AβPP770) and without (AβPP695) the Kunitz-type serine protease inhibitor (KPI) domain, in the cerebral cortex in DLBc (n=4), DLBp (n=4), Parkinson's disease (PD, n=5), AD (n=3 stages I-IIA, and n=4 stage VC of Braak and Braak), amyloid angiopathy (AA, n=2) and progressive supranuclear palsy (PSP, n=4) compared with age-matched controls (n=6). For this purpose, TaqMan RT-PCR assay was used on frozen post-mortem samples of the frontal cortex (area 8) obtained with short post-mortem delays (8.29 ± 4.57 h) and strict RNA preservation ($A_{260/280}$ of 1.78 ± 0.15). A 3.66-fold, 6.67-fold, 4.28-fold and 5.24-fold increases, in the (AβPP751+AβPP770)/AβPP695 mRNA ratio were found in DLBc, DLBp, AD stage VC and AA, respectively, when compared with controls. No modifications in the ratio were found in PD, AD stage I-IIA and PSP. These findings suggest that alternative splicing of the AβPP mRNA may play a role in βA4 amyloidogenesis in DLBp, DLBc, AD stage VC and Amyloid angiopathy.

Keywords: AβPP, DLB, PD, Amyloid angiopathy, AD, PSP

Introduction

AβPP (amyloid-β protein precursor) is a widely expressed cell surface protein, the fibrillogenic product of which, amyloid-β, is associated with the pathogenesis of Alzheimer's disease (AD). Deposition of amyloid senile (diffuse and neuritic) plaques, together with the presence of neurons with neurofibrillary tangles, are the most characteristic pathological findings in AD (Kang et al., 1987; Selkoe et al., 1988; Duyckaerts et al., 2003). Amyloid-β deposition also occurs in the blood vessel walls in AD and in cases in which cerebral amyloid angiopathy (AA) is the main pathological finding. The principal component of amyloid-β deposition is the βA4 peptide which is released by the processing of AβPP (Masters et al., 1985). AβPP is encoded by a single 19-exon gene in the chromosome 21 that produces several isoforms resulting from alternative splicing; AβPP695, AβPP751 and AβPP770 are the predominant transcripts (Yoshikai et al., 1990). AβPP751 and AβPP770 contain the exon 7, which encodes a serine protease inhibitor domain called the Kunitz protease inhibitor (KPI). AβPP695 is the predominant form in neuronal tissue, whereas AβPP751 and AβPP770 are expressed ubiquitously (Kitaguchi et al., 1988; Ponte et al., 1988; Tanzi et al., 1988: Kang and Muller-Hill, 1990). Increased protein expression of KPI+ variants in homogenates of AD brains has been suggested as a possible origin of amyloid-β deposition (Moir et al, 1998).

Parkinson's disease (PD) and Dementia with Lewy bodies (DLB) are characterized by the presence of intracytoplasmic neuronal inclusions called Lewy bodies (LBs) and α-synuclein-containing aberrant neurites in the substantia nigra pars compacta, locus ceruleus and other selected nuclei of the brain stem, as well as in several nuclei of the basal forebrain and hippocampus (Hurtig et al., 2000; Jellinger et al., 2003). In addition, DLB is characterized by the widespread distribution of LBs and α-synuclein-containing neurites in the cerebral cortex (Ince and McKeith, 2003). The presence of senile plaques and neurofibrillary tangles is frequent in DLB (Gibb et al., 1987; Lippa et al., 1994; McKeith et al., 1996; Ince et al., 1998). DLB with no AD changes is known as the pure form of DLB, whereas DLB with associated AD is recognized as the common form of DLB (Kosaka, 1990, 1993).

The present study is focused on the examination of AβPP gene expression in PD, DLB (pure and common forms: DLBp and DLBc), AD, AA and progressive supranuclear palsy (PSP), a neurodegenerative disease without amyloid-β deposition (Lee et al., 2001). For this purpose, the three major alternative-splicing AβPP mRNAs (AβPP695, AβPP751 and AβPP770) have been analysed using the TaqMan RT-PCR assay, which has emerged as a rapid and reliable method for semi-quantitative analysis of gene expression in the nervous system (Horii et al., 2002).

Material and methods

Brain samples

Frozen samples of the cerebral cortex frontal lobe (area 8) were collected from five patients with PD, four with DLBp (DLB plus amyloid plaques stage B), four with DLBc (DLB plus AD stage VC), three with AD stages I-IIA of Braak and Braak, four with AD stage VC of Braak and Braak, two with AA (plus amyloid plaques stage B), four with PSP and six aged-matched controls, following informed consent of the patients or their relatives and the approval by the local Ethics Committee of the donor program of tissue samples for research (Table I). 56% of cases were men and 43% were women. The average time and the standard deviation of the delay between death and tissue processing were 8.2 ± 4.5 hours. The neuropathological diagnosis was conducted following well-established protocols using formalin-fixed, paraffin-embedded sections of randomised brain areas which were processed with neuropathoplogical methods, including immunohistochemistry (Ferrer, 2002). Characterization of DLB was according to consensus criteria (McKeith et al., 1996), whereas AD stages were established depending on the amyloid-β deposition burden and neurofibrillary pathology (Braak and Braak, 1999). Stages of amyloid-β deposition refer to initial deposits in the basal neocortex (A), deposits extended to the association areas of the neocortex (B), and heavy deposition throughout the entire cortex (C). Stages of neurofibrillary pathology correspond to transentorhinal (I-II), limbic (III-IV) and neocortical (V and VI). Details of amyloid burden and neurofibrillary pathology in the present series are found in Table I.

mRNA isolation

mRNA isolation was carried out in two steps. Total RNA was isolated using TRizol Reagent (Life Technologies) followed by RNA isolation excluding 5 S rRNA, 5.8 rRNA and tRNAs using the RNeasy Protect Mini Kit (Qiagen). Frozen human brain tissues were directly homogenised in 1 ml of TRizol reagent per 100 mg tissue and total RNA was extracted following the manufacturer's suggested protocol. Purified total RNA was resuspended in 100 µl of RNase-free water, and RNA purification was obtained following the protocol provided with the RNeasy Protect Mini Kit, with minor modifications. Dnase I treatment was avoided due to the elimination of genomic DNA in the TRizol extraction. The concentration of each sample was obtained from A_{260} measurements, and the RNA integrity was confirmed using formaldehyde-agarose gel electrophoresis.

cDNA synthesis

For each 10 µl reverse transcription reaction, 200 ng human RNA (in 3.85 µl water) was mixed with 2.5 µM oligodT primer, 1x TaqMan RT buffer, 5.5 mM $MgCl_2$, 500 µM of each

of dATP, dTTP, dCTP and dGTP, 0.08 U Rnase Inhibitor and 0.31 U MultiScribe Reverse transcriptase (Applied Biosystems). Reactions were performed for 10 min at 25°C to maximize primer-RNA template binding, followed by 30 min at 48ºC, and then terminated by incubation for 5 min at 95°C to deactivate reverse transcriptase. Parallel reactions for each RNA sample were run in the absence of MultiScribe Reverse transcriptase to assess the degree of contaminating genomic DNA.

TaqMan PCR

The TaqMan probe (Applied Biosystems) anneals to one strand of the DNA template between forward and reverse PCR primers. It contains a reporter dye which is released by Taq polymerase during the amplification step, with the fluorescence originated being proportional to the amount of product accumulated.

Primers and fluorescence probes specific for each AβPP isoform were purchased from three Assays by Design (Applied Biosystems). A 620 pb sequence of each AβPP isoform was obtained from the GeneBank numbers NM_000484, M34867, M34868, M34869, M34870, and the assigned positions for the exon6-exon9 boundary (AβPP695), exon7-exon9 boundary (AβPP751) and exon7-exon8 boundary (AβPP770) were 313, 339 and 308, respectively. TaqMan probes were designed over these exon-exon boundaries to remove genomic DNA signals. β-actin was obtained from Assay-on-Demand (Applied Biosystems) to be used as endogenous reference.

TaqMan PCR assays for each AβPP isoform and endogenous reference (β-actin) were performed in triplicate on cDNA samples in 96-well optical plates on an ABI Prism 7700 Sequence Detection system (PE Applied Biosystems). The plate was capped using optical caps (Applied Biosystems). For each 20 µl TaqMan reaction, 9 µl cDNA (diluted 1/100, which corresponds approximately to cDNA from 2 ng of RNA) was mixed with 1 µl 20X Assays by Design gene expression Assay Mix and 10 µl of 2X TaqMan Universal PCR Master Mix (Applied Biosystems). Parallel assays for each sample were carried out using primers and probe with β-actin for normalization. The reaction was carried out using the following parameters: 50ºC for 2 min, 95ºC for 10 min, and 40 cycles of 95ºC for 15 s, 60ºC for 1 min. Standard curves were prepared for each target (AβPP695, AβPP751 and AβPP770) and for the endogenous reference (β-actin) using serial dilutions of control human brain RNA. Finally, all TaqMan PCR data were captured using the Sequence Detector Software (SDS version 1.9; Applied Biosystems).

Western Blot

100 mg of frozen human frontal cortex tissues were directly homogenised in 1 ml of lysis buffer (20 mM Hepes, 10 mM KCl, 1.5 mM $MgCl_2$, 1 mM EDTA, 1 mM EGTA, 1 mM DDT, 2

mM PMSF, 1 μg/ml aprotinin, leupeptin and pepstatin) and then sonicated. Lysates were centrifugated at 5,000 rpm for 10 minutes at 4ºC and protein concentration was determined with BCA (Pierce) method. 50 μg of total protein were boiled at 95°C for 3 min and loaded in each lane of SDS-polyacrylamide gels with Tris-glycine running buffer. Proteins were electrophoresed using a mini-protean system (Bio-Rad) and transferred to nitrocellulose membranes (Bio-Rad) with a Trans-Blot SD Semi-Dry Transfer Cell (Bio-Rad) for 45 min at 40 mA. Nitrocellulose membranes were blocked with Tween 20 TBS (TBST) containing 5% skimmed milk for 30 minutes. Subsequently, the membranes were incubated at 4°C overnight with antibodies to the different compounds analysed in TBST containing 3% BSA. After GFAP antibody incubation (DAKO) at a dilution of 1:1000, membranes were washed three times with TBST for 5 minutes at room temperature. Subsequently, membranes were incubated with the corresponding secondary antibody labeled with horseradish peroxidase (DAKO) at a dilution of 1:1000, for 1 h at room temperature. Then they were washed again four times with TBST having each wash a duration of 5 minutes at room temperature. Finally, washed membranes were developed with the chemiluminescence ECL Western blotting system (Amersham/Pharmacia) followed by apposition of the membranes to autoradiographic films (Hyperfilm ECL, Amersham). The monoclonal α-tubulin (clone DM 1A; Sigma) was used at a dilution of 1:5000.

Data analysis

AβPP KPI+/AβPP KPI- mRNA ratio was calculated for each control and pathological sample and the average value was determined. Fold increase for every sample, calculated using this average value, was compared with the average value of controls. Statgraphics Plus (version 5) software was used for statistical analysis.

Results

A critical measure in comparing different cDNAs amplified in the PCR reaction is the purification grade of initial mRNA due to differences in template amounts between samples in the RT reaction. In the present study, all the mRNAs presented optimal absorbance at 260 and 280 nm; the A_{260}/A_{280} ratio showed an average and standard deviation of 1.78 ± 0.15 (Table I). In fact, the cases selected here were the only considered suitable for cDNA study from a larger series of cases, on the basis of mRNA preservation.

TaqMan PCR assay was used to analyse the expression levels of AβPP695, AβPP751 and AβPP770 mRNAs. For this purpose, a RT reaction was carried out with 200 ng of each total RNA collected. The ABI Prism 7700 measures the fluorescent accumulation of PCR product by continuous monitoring cycle threshold (Ct), which is an arbitrary value assigned manually to a level somewhere above baseline but in the exponential phase of PCR where there are no rate-limiting components. The Ct value sets the point at which the sample amplification plot crosses the threshold (Figure 1A). For each experimental sample, the amount of target and endogenous reference was determined from the appropriate standard curve which was plotted showing the cycle threshold, Ct (y), versus log ng total control RNA (x) (Figure 1B). Then the amount of each target A□PP isoform was divided by the endogenous reference (β-actin) amount to obtain a normalized target value which permits determination of the relative mRNA levels of each AβPP isoform and the fold increase value in relation with control samples. β-actin mRNA levels used to normalize AβPP mRNA isoform values were not modified in pathologic samples when compared with controls and they were similar among individual pathologies (data not shown).

Decreased AβPP695 relative mRNA levels were observed in DLBp, DLBc, AD stage VC of Braak and Braak, PSP and AA when compared with controls: $p<0.05$ for DLBc, ADV and AA; and $p<0.01$ for DLBp and PSP, ANOVA with post-hoc Fisher's least significant difference (LSD) test (Table II). AβPP751 relative mRNA levels were decreased in DLBp, DLBc, PSP and AA respect to controls: $p<0.05$ for DLBp, DLBc and AA; and $p<0.01$ for PSP, ANOVA with post-hoc LSD test. AβPP770 relative mRNA levels were increased in DLBp when compared with controls: $p<0.05$ ANOVA with post-hoc LSD test. These modifications were not dependent on the gender, age, and duration of the disease.

The AβPP KPI+/AβPP KPI- mRNA ratio fold increase was calculated for each sample and was not modified in PD when compared with controls (1.23 ± 0.37 vs 1.00 ± 0.10) (Figure 2). However, a 6.67 ± 1.64 and a 3.66 ± 0.62 fold increase in the (AβPP751+AβPP770)/AβPP695 mRNA ratio were obtained in DLBp and DLBc samples, respectively, compared to control samples: $p<0.001$ and $p<0.05$, ANOVA with post-hoc

LSD test. Stages I-IIA of AD did not show an increased AβPP KPI+/AβPP KPI- mRNA ratio when compared with controls (1.43 ± 0.10 vs 1.00 ± 0.10). However, stages VC of AD presented an increase in the ratio (4.28 ± 1.46 vs 1.00 ± 0.10, $p<0.05$ ANOVA with post-hoc LSD test). Also, an increase in the mentioned ratio was obtained in AA when compared to control samples (5.04 ± 0.24 vs 1.00 ± 0.10; $p<0.05$ ANOVA with post-hoc LSD test). Yet no significant modifications in the AβPP KPI+/AβPP KPI- mRNA ratio were seen in PSP in respect to control samples (2.20± 0.25 vs 1.00 ± 0.10).

Since differences in AβPP KPI+/AβPP KPI- mRNA ratio might be attributed to changes in the number of astrocytes (see later), Western blots GFAP were carried out as a measure of gliosis. GFAP protein levels were statistically not modified in PD, DLBp, DLBc, AD, PSP and AA compared to control samples (Figure 3).

Discussion

Several post-mortem studies have analysed the expression of AβPP695, AβPP751 and AβPP770 mRNA isoforms in AD. Some studies have shown a decrease in the AβPP695 mRNA levels, or an increase in KPI+ mRNA isoforms (AβPP751 and AβPP770), or an increase in the AβPP KPI+/AβPP KPI- mRNA ratio (Johnson et al., 1988, 1989, 1990; Palmert et al., 1988; Spillantini et al., 1989; Golde et al., 1990; Tanaka et al., 1992; Moir et al., 1998). Yet no changes in the three mRNA isoforms in AD when compared with controls have been noted in other studies (Neve et al., 1988; Koo et al., 1990; Konig et al., 1991). It can been suggested that discrepancies in the AβPP mRNA expression detected in these reports are due to several factors, including variable post-mortem delays as has been described (Lukiw et al., 1990; Burke et al., 1991), artefacts of sub-optimal freezing, methods employed in the analysis of mRNAs, biological differences between the pathological groups and clinical backgrounds.

For these reasons, special care has been taken in the selection of cases analysed in the present series. First, stress should be placed on the fact that amyloid-β deposition was absent in area 8 in control cases, in patients with PD (only one control and one PD had stage A of amyloid-β deposition) and in PSP cases. All cases with DLBp showed lesions consistent with stage B of amyloid deposition, whereas all cases with DLBc were stage C of Braak and Braak. This is an important point, as amyloid-β deposits in the cerebral cortex may be found in normal aging and in advanced PD (Braak and Braak, 1990; Mastaglia et al., 2003) although AβPP751 and AβPP770 mRNAs are unaffected by age (Flood et al., 1997). Selection of control and PD cases with no apparent neocortical amyloid-β pathology minimizes sample dispersion in the control groups. Second, post-mortem delay between death and tissue processing was very low when compared with other series (8.2 ± 4.5 h). Moreover, samples used in the present study were only those with strict preservation and purification of mRNA showing an absorbance ratio A_{260}/A_{280} of 1.78 ± 0.15. Finally, in contrast to previous studies that have used Northern blot analysis, PCR, *in situ* hybridisation or RNAse protection assays, we have utilized the TaqMan RT-PCR assay that permits the measurement of an accumulating PCR product in real time by using a TaqMan fluorogenic probe. The method is very useful for the analysis of splice variants. The sensitivity of each primer/probe set was suitable for further comparison analysis because the equations obtained in the standard curve were very similar. Moreover, very similar values for the AβPP KPI+/AβPP KPI- mRNA ratio were obtained among the individuals of the control group. CT values on which the relative quantification was based were precisely defined, and a clear reverse linear correlation was demonstrated for the representative standard curves of β-actin, AβPP695, AβPP751 and AβPP770. Taken together, these methodological procedures confer a robust

credibility on the observations in a limited number of patients in the present series.

No modifications in the AβPP KPI+/AβPP KPI- mRNA ratio in respect to control samples were demonstrated in PD, in accordance with the observations of a seminal study (Tanaka et al., 1992). On the other hand, we analysed the AβPP mRNA isoforms in AD differentiating among stages of Braak and Braak and detecting an increase in the AβPP KPI+/ AβPP KPI- mRNA ratio as previously reported by others (Tanaka et al., 1992; Preece et al., 2004), only in AD samples with stage VC of Braak and Braak. Interestingly, the increase was due to the decrease of AβPP695 mRNA levels as already described (Johnson et al., 1988, 1989, 1990). Also, the AβPP KPI+/AβPP KPI- mRNA ratio was increased in AA, but in this case due to a reduction of the AβPP695 and AβPP751 mRNA levels. Moreover, a significant increase in the AβPP KPI+/AβPP KPI- mRNA ratio was demonstrated in DLB, as a consequence of a reduction in AβPP695 and AβPP751 mRNA levels in DLBp and DLBc plus an increase in AβPP770 only in DLBp. A higher increase occurred in DLBp than in DLBc, thus inversely correlating increase in the AβPP KPI+/AβPP KPI- ratio and amyloid-β burden in cases with demonstrated cortical amyloid-β deposition. Interestingly, decreased transcripts (especially non-Kunitz forms) may play an important role in neurodegeneration process by loss of function. These modifications were not related with gender, age, and duration of the disease.

In vitro, AβPP751 and AβPP770 mRNA isoforms are detected predominantly in astrocyte and microglia enriched cultures (Ohyagi et al., 1990). For this reason, it can be suggested that the present observations are merely sub-products of gliosis accompanying neurodegeneration. Yet no apparent relationship exists between amyloid deposition, gliosis and modifications in AβPP mRNA isoform expression in the different pathologies examined in these series. Moreover, no significant differences in cortical GFAP levels were observed in the present series, as revealed by Western Blot, thus indicating that the AβPP751 and AβPP770 mRNA values obtained in the TaqMan PCR were not due to differences in gliosis. Finally, the AβPP KPI+/AβPP KPI- mRNA ratio was unchanged in PSP respect to control cases, albeit total AβPP mRNA was lower in PSP when compared with all the diseases studied and with control samples.

In summary, AβPP695 and AβPP751 mRNA levels are decreased in DLB and AA, whereas AβPP695 mRNA levels only in AD stage VC. More important, AβPP mRNA isoforms that have alternative-splicing (AβPP695 lacks exons 7 and 8, AβPP751 lacks exon 8) are reduced in diseases with amyloid-β deposits. It is feasible that control elements exist in the flanking sequences of the alternatively-spliced exons (Li et al., 1999). In this line, the CUG-BP protein has been characterized as a potential regulator of alternative splicing of the AβPP gene excluding strongly the exon 8 (Poleev et al., 2000). It would be interesting

to analyze the CUG-BP protein levels in the series with reduce AβPP695 and AβPP751 mRNA levels. Finally, the present findings show that a relative increase in AβPP KPI+/ AβPP KPI- mRNA ratio in the cerebral cortex is associated with cortical amyloid-β deposition in DLB, AA and AD stage VC, and suggest that this abnormal ratio perturbs normal degradation of AβPP, thereby favouring deposition of amyloid-β. However, further studies are necessary, a: to characterize and determine the expression levels of AβPP gene alternative splicing regulator proteins in diseases with amyloid-β depostion, and b: to confirm that variations of AβPP mRNA isoforms are translated to similar variations of the corresponding proteins.

Acknowledgements

This work was supported in part by grants FIS P1020004, SAF 2001-4681E, QLRT-CT 2000-66 and Brain Net II. We are grateful to T. Yohannan for editorial assistance.

References

Braak, H., Braak, E. 1990. Cognitive impairment in Parkinson's disease: amyloid plaques, neurofibrillary tangles, and neuropil threads in the cerebral cortex. J. Neural Transm. 2, 45-57.

Braak, H., Braak, E. 1999. Temporal sequence of Alzheimer's disease related pathology. In: Peters, A., Morrison, J.H. (Eds) Cerebral cortex. Vol 14, Neurodegenerative and age-related changes in structure and function of cerebral cortex. Kluwer Academic/Plenum Publishers, New York, Boston, Dordrecht, London, Moscow, pp. 475-512.

Burke, W.J., O'Malley, K.L., Chung, H.D., Harmon, S.K., Miller, J.P., Berg, L. 1991. Effect of pre- and postmortem variables on specific mRNA levels in human brain. Brain Res. Mol. Brain Res. 11, 37-41.

Duyckaerts, C., Dickson, D.W. 2003. Neuropathology of Alzheimer's disease. In: Dickson, D. (Ed.) Neurodegeneration: The molecular pathology of dementia and movement disorders. ISN Neuropathol Press, Basel, pp. 47-68.

Ferrer, I. 2002. The neuropathological spectrum of Lewy body disorders. In: Tolosa, E., Schulz, J.B., McKeith, I.G., Ferrer, I. (Eds.) Neurodegenerative disorders associated with α-synuclein pathology. Ars Medica, Barcelona, pp. 83-98.

Flood, F.M., Cowburn, R.F., Johnston, J.A. 1997. Presenilin-1, amyloid precursor protein and amyloid precursor-like protein 2 mRNA levels in human superior frontal cortex during aging. Neurosci. Lett. 235, 17-20.

Gibb, W.R., Esiri, M.M., Lees, A.J. 1987. Clinical and pathological features of diffuse cortical Lewy body disease (Lewy body dementia). Brain. 110, 1131-1153.

Golde, T.E., Estus, S., Usiak, M., Younkin, L.H., Younkin, S.G. 1990. Expression of beta amyloid protein precursor mRNAs: recognition of a novel alternatively spliced form and quantitation in Alzheimer's disease using PCR. Neuron. 4, 253-267.

Horii, A., Smith, P.F., Darlington, C.L. 2002. Application of real-time quantitative polymerase chain reaction to quantification of glutamate receptor gene expression in the vestibular brainstem and cerebellum. Brain Res. Brain Res. Protoc. 9, 77-83.

Hurtig, H.I., Trojanowski, J.Q., Galvin, J., Ewbank, D., Schmidt, M.L., Lee, V.M., Clark, C.M., Glosser, G., Stern, M.B., Gollomp, S.M., Arnold, S.E. 2000. Alpha-synuclein cortical Lewy bodies correlate with dementia in Parkinson's disease. Neurology. 54, 1916-1921.

Ince, P.G., Perry, E.K., Morris, C.M. 1998. Dementia with Lewy bodies. A distinct non-Alzheimer dementia syndrome? Brain Pathol. 8, 299-324.

Ince, P.G., McKeith, I. 2003. Dementia with Lewy bodies. In: Dickson, D. (Ed.) Neurodegeneration: The molecular pathology of dementia and movement disorders. ISN Neuropathol Press, Basel, pp. 188-199.

Jellinger, K.A., Mizuno, Y. 2003. Parkinson’s disease. In: Dickson, D. (Ed.) Neurodegeneration: The molecular pathology of dementia and movement disorders. ISN Neuropathol Press, Basel, pp. 159-187.

Johnson, S.A., Pasinetti, G.M., May, P.C., Ponte, P.A., Cordell, B., Finch, C.E. 1988. Selective reduction of mRNA for the beta-amyloid precursor protein that lacks a Kunitz-type protease inhibitor motif in cortex from Alzheimer brains. Exp. Neurol. 102, 264-268.

Johnson, S.A., Rogers, J., Finch, C.E. 1989. APP-695 transcript prevalence is selectively reduced during Alzheimer's disease in cortex and hippocampus but not in cerebellum. Neurobiol Aging. 10, 755-760.

Johnson, S.A., McNeill, T., Cordell, B., Finch, C.E. 1990. Relation of neuronal APP-751/APP-695 mRNA ratio and neuritic plaque density in Alzheimer's disease. Science. 248, 854-857.

Kang, J., Lemaire, H.G., Unterbeck, A., Salbaum, J.M., Masters, C.L., Grzeschik, K.H., Multhaup, G., Beyreuther, K., Muller-Hill, B. 1987. The precursor of Alzheimer's disease amyloid A4 protein resembles a cell-surface receptor. Nature. 325, 733-736.
Kang, J., Muller-Hill, B. 1990. Differential splicing of Alzheimer's disease amyloid A4 precursor RNA in rat tissues: PreA4(695) mRNA is predominantly produced in rat and human brain. Biochem. Biophys. Res. Commun. 166, 1192-1200.

Kitaguchi, N., Takahashi, Y., Tokushima, Y., Shiojiri, S., Ito, H. 1988. Novel precursor of Alzheimer's disease amyloid protein shows protease inhibitory activity. Nature. 331, 530-532.

Konig, G., Salbaum, J.M., Wiestler, O., Lang, W., Schmitt, H.P., Masters, C.L., Beyreuther, K. 1991. Alternative splicing of the beta A4 amyloid gene of Alzheimer's disease in cortex of control and Alzheimer's disease patients. Brain Res. Mol. Brain Res. 9, 259-262.

Koo, E.H., Sisodia, S.S., Cork, L.C., Unterbeck, A., Bayney, R.M., Price, D.L. 1990. Differential expression of amyloid precursor protein mRNAs in cases of Alzheimer's disease and in aged nonhuman primates. Neuron. 4, 97-104.

Kosaka, K. 1990. Diffuse Lewy body disease in Japan. J. Neurol. 237, 197-204.

Kosaka, K. 1993. Dementia and neuropathology in Lewy body disease. Adv. Neurol. 60, 456-463.

Lee, V.M., Goedert, M., Trojanowski, J.Q. 2001. Neurodegenerative tauopathies. Annu. Rev. Neurosci. 24, 1121-1159.

Li, L., Ohman, T., Deeb, S.S., Fukuchi, K.I. 1999. Analysis of mouse intron 7 DNA sequence of the APP gene: comparison with the human homologue. DNA Seq. 10, 219-228.

Lippa, C.F., Smith, T.W., Swearer, J.M. 1994. Alzheimer's disease and Lewy body disease: a comparative clinicopathological study. Ann. Neurol. 35, 81-88.

Lukiw ,W.J., Wong, L., McLachlan, D.R. 1990. Cytoskeletal messenger RNA stability in human neocortex: studies in normal aging and in Alzheimer's disease. Int. J. Neurosci. 55, 81-88.

Mastaglia, F.L., Johnsen, R.D., Byrnes, M.L., Kakulas, B.A. 2003. Prevalence of amyloid-beta deposition in the cerebral cortex in Parkinson's disease. Mov. Disord. 18, 81-86.

Masters, C.L., Simms, G., Weinman, N.A., Multhaup, G., McDonald, B.L., Beyreuther, K. 1985. Amyloid plaque core protein in Alzheimer disease and Down syndrome. Proc. Natl. Acad. Sci. USA. 82, 4245-4249.

McKeith, I.G., Galasko, D., Kosaka, K., Perry, E.K., Dickson, D.W., Hansen, L.A., Salmon, D.P., Lowe, J., Mirra, S.S., Byrne, E.J., Lennox, G., Quinn, N.P., Edwardson, J.A., Ince,

P.G., Bergeron, C., Burns, A., Miller, B.L., Lovestone, S., Collerton, D., Jansen, E.N., Ballard, C., de Vos, R.A., Wilcock, G.K., Jellinger, K.A., Perry, R.H. 1996. Consensus guidelines for the clinical and pathologic diagnosis of dementia with Lewy bodies (DLB): Report of the consortium on DLB international workshop. Neurology. 47, 1113-1124.

Moir, R.D., Lynch, T., Bush, A.I., Whyte, S., Henry, A., Portbury, S., Multhaup, G., Small, D.H., Tanzi, R.E., Beyreuther, K., Masters, C.L. 1998. Relative increase in Alzheimer's disease of soluble forms of cerebral Abeta amyloid protein precursor containing the Kunitz protease inhibitory domain. J. Biol. Chem. 273, 5013-5019.

Neve, R.L., Finch, E.A., Dawes, L.R. 1988. Expression of the Alzheimer amyloid precursor gene transcripts in the human brain. Neuron. 1, 669-677.

Ohyagi, Y., Takahashi, K., Kamegai, M., Tabira, T. 1990. Developmental and differential expression of beta amyloid protein precursor mRNAs in mouse brain. Biochem. Biophys. Res. Commun. 167, 54-60.

Palmert, M.R., Golde, T.E., Cohen, M.L., Kovacs, D.M., Tanzi, R.E., Gusella, J.F., Usiak, M.F., Younkin, L.H., Younkin, S.G. 1988. Amyloid protein precursor messenger RNAs: differential expression in Alzheimer's disease. Science. 241, 1080-1084.

Poleev, A., Hartmann, A., Stamm, S. 2000. A trans-acting factor, isolated by the three-hybrid system, that influences alternative splicing of the amyloid precursor protein minigene. Eur. J. Biochem. 267, 4002-4010.

Ponte, P., Gonzalez-DeWhitt, P., Schilling, J., Miller, J., Hsu, D., Greenberg, B., Davis, K., Wallace, W., Lieberburg, I., Fuller, F. 1988. A new A4 amyloid mRNA contains a domain homologous to serine proteinase inhibitors. Nature. 331, 525-527.

Preece, P., Virley, D.J., Costandi, M., Coombes, R., Moss, S.J., Mudge, A.W., Jazin, E., Cairns, N.J. 2004. Amyloid precursor protein mRNA levels in Alzheimer's disease brain. Brain Res. Mol. Brain Res. 122, 1-9.

Selkoe, D.J., Podlisny, M.B., Joachim, C.L., Vickers, E.A., Lee, G., Fritz, L.C., Oltersdorf, T. 1988. Beta-amyloid precursor protein of Alzheimer disease occurs as 110- to 135-kilodalton membrane-associated proteins in neural and non-neural tissues. Proc. Natl. Acad. Sci. U S A. 85, 7341-7345.

Spillantini, M.G., Hunt, S.P., Ulrich, J., Goedert, M. 1989. Expression and cellular localization of amyloid beta-protein precursor transcripts in normal human brain and in Alzheimer's disease. Brain Res. Mol. Brain Res. 6, 143-150.

Tanaka, S., Liu, L., Kimura, J., Shiojiri, S., Takahashi, Y., Kitaguchi, N., Nakamura, S., Ueda, K. 1992. Age-related changes in the proportion of amyloid precursor protein mRNAs in Alzheimer's disease and other neurological disorders. Brain Res. Mol. Brain Res. 15, 303-310.

Tanzi, R.E., McClatchey, A.I., Lamperti, E.D., Villa-Komaroff, L., Gusella, J.F., Neve, R.L. 1988. Protease inhibitor domain encoded by an amyloid protein precursor mRNA associated with Alzheimer's disease. Nature. 331, 528-530.

Yoshikai, S., Sasaki, H., Doh-ura, K., Furuya, H., Sakaki, Y. 1990. Genomic organization of the human amyloid beta-protein precursor gene. Gene. 87, 257-263.

Table I. Summary of the main clinical and neuropathological findings in the present series. Parkinson's disease (PD), Dementia with Lewy Bodies pure form (DLBp) and common form (DLBc), Alzheimer's disease stages I-II (ADI) and V of Braak and Braak (ADV), Progressive Supranuclear Palsy (PSP), Amyloid angiopathy and controls. Information related to RNA purification grade for each sample is provided by the ratio of RNA absorbance at 260 nm and 280 nm ($A_{260/280}$). M: male, F: female. NFT: neurofibrillary tangles.

Patient	Disease	Gender	Age (y)	Duration of the disease (y)	Post-mortem (h)	Braak stages		$A_{260/280}$
						βA4 amyloid	NFT	
1	Control	M	35	-	8	0	0	1.89
2	Control	M	70	-	13	0	0	2.16
3	Control	M	79	-	7	0	I-II	1.83
4	Control	F	49	-	7	0	0	1.8
5	Control	F	65	-	4	0	I	2.13
6	Control	F	82	-	11	A	III	1.99
7	PD	M	57	14	11	0	0	2.1
8	PD	M	70	12	19	0	0	1.73
9	PD	M	81	17	5	A	I-II	1.78
10	PD	F	70	7	4	0	0	1.79
11	PD	F	84	10	4	0	0	2
12	DLBp	M	85	8	7	B	I	1.81
13	DLBp	M	68	13	12	B	0	1.74
14	DLBp	M	71	17	6	B	0	1.83
15	DLBp	F	77	12	5	B	0	1.72
16	DLBc	M	78	11	6	C	V	1.71
17	DLBc	M	78	18	7	C	V	1.72
18	DLBc	F	71	22	5	C	V	1.71
19	DLBc	F	91	15	5	C	V	1.71
20	ADI	M	59	-	7	A	I-II	1.75
21	ADI	M	66	-	18	A	I-II	1.69
22	ADI	F	88	-	5	A	I-II	1.64
23	ADV	M	69	8	6	C	V	1.70
24	ADV	F	78	12	19	C	V	1.75
25	ADV	F	86	8	10	C	V	1.68
26	ADV	F	82	13	10	C	V	1.76
27	PSP	M	72	6	4	0	0	1.60
28	PSP	F	70	13	7	0	0	1.77
29	PSP	M	65	6	9.3	0	0	1.63
30	PSP	F	86	?	16	0	0	1.60
31	Amyloid angiopathy	M	69	7	6	B	0	1.64
32	Amyloid angiopathy	M	71	12	3	B	0	1.7
	Average ± SD		72.56 ± 11.71		8.29 ± 4.57			1.78 ± 0.15

Table II: Relative mRNA expression levels (mean ± SEM) of AβPP695, AβPP751 and AβPP770 isoforms normalized with β-actin in controls (C), Parkinson's disease (PD), Dementia with Lewy Bodies pure form (DLBp) and common form (DLBc), Alzheimer's disease stages I-IIA (ADI) and stage VC of Braak and Braak (ADV), progressive supranuclear palsy (PSP) and amyloid angiopathy (AA). * $p<0.05$ and ** $p<0.01$ compared to control samples (ANOVA with post-hoc LSD test).

Disease	AβPP695	AβPP751	AβPP770
C	2.27 ± 0.84	2.50 ± 0.97	1.36 ± 0.46
PD	2.31 ± 0.73	2.23 ± 0.63	1.47 ± 0.23
DLBp	0.38 ± 0.07**	0.98 ± 0.19*	3.08 ± 0.97*
DLBc	0.42 ± 0.11*	1.01 ± 0.21*	1.53 ± 0.22
ADI	0.81 ± 0.27	1.15 ± 0.21	0.86 ± 0.37
ADV	0.48 ± 0.20*	1.41 ± 0.36	1.60 ± 0.62
PSP	0.18 ± 0.08**	0.31 ± 0.09**	0.48 ± 0.32
AA	0.30 ± 0.05*	0.84 ± 0.06*	1.89 ± 0.27

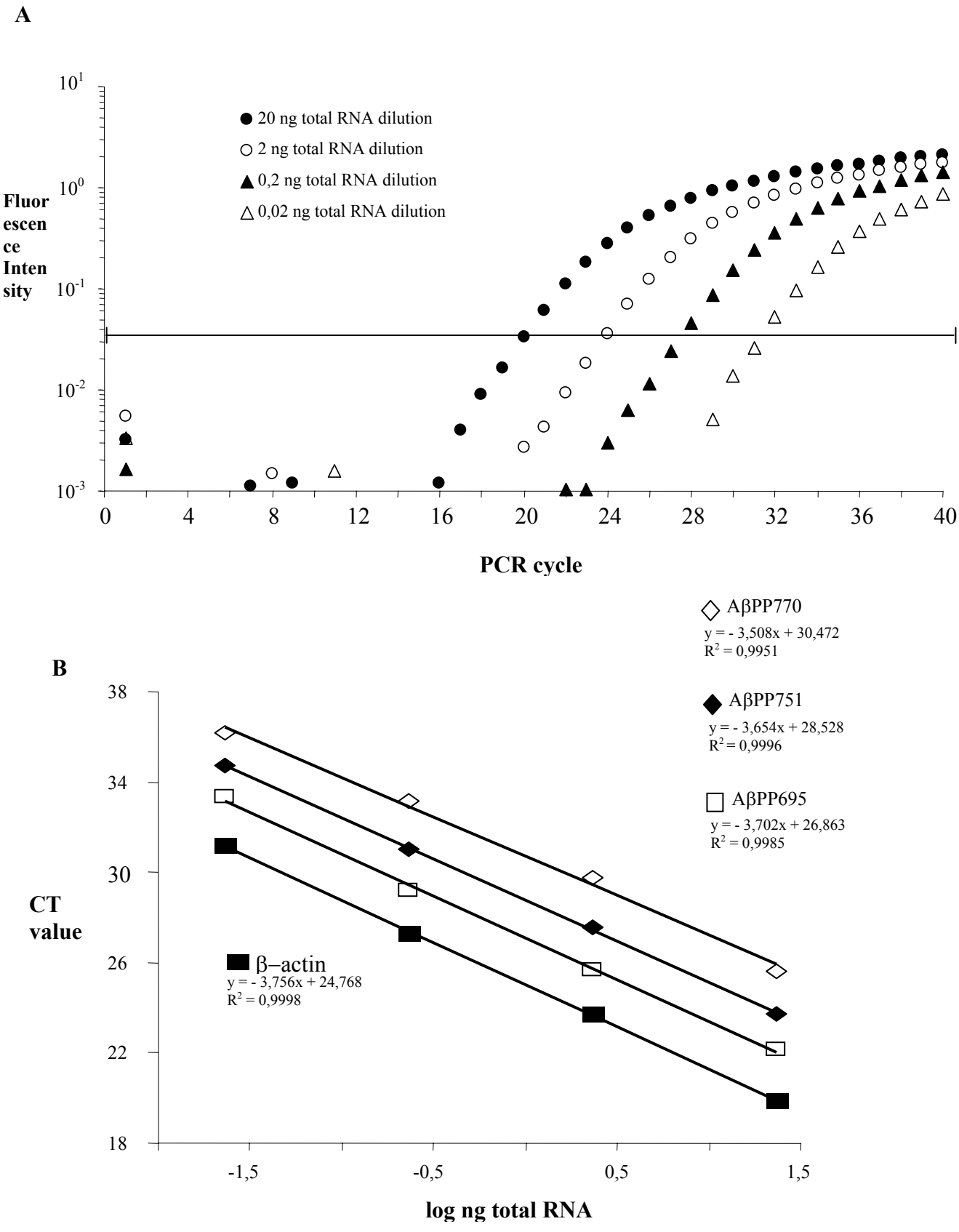
A
Fluorescence Intensity
10^1
10^0
10^-1
10^-2
10^-3
20 ng total RNA dilution
2 ng total RNA dilution
0,2 ng total RNA dilution
0,02 ng total RNA dilution
0
4
8
12
16
20
24
28
32
36
40
PCR cycle
B
CT value
38
34
30
26
22
18
AβPP770
y = - 3,508x + 30,472
R2 = 0,9951
AβPP751
y = - 3,654x + 28,528
R2 = 0,9996
AβPP695
y = - 3,702x + 26,863
R2 = 0,9985
β–actin
y = - 3,756x + 24,768
R2 = 0,9998
-1,5
-0,5
0,5
1,5
log ng total RNA

Figure 1

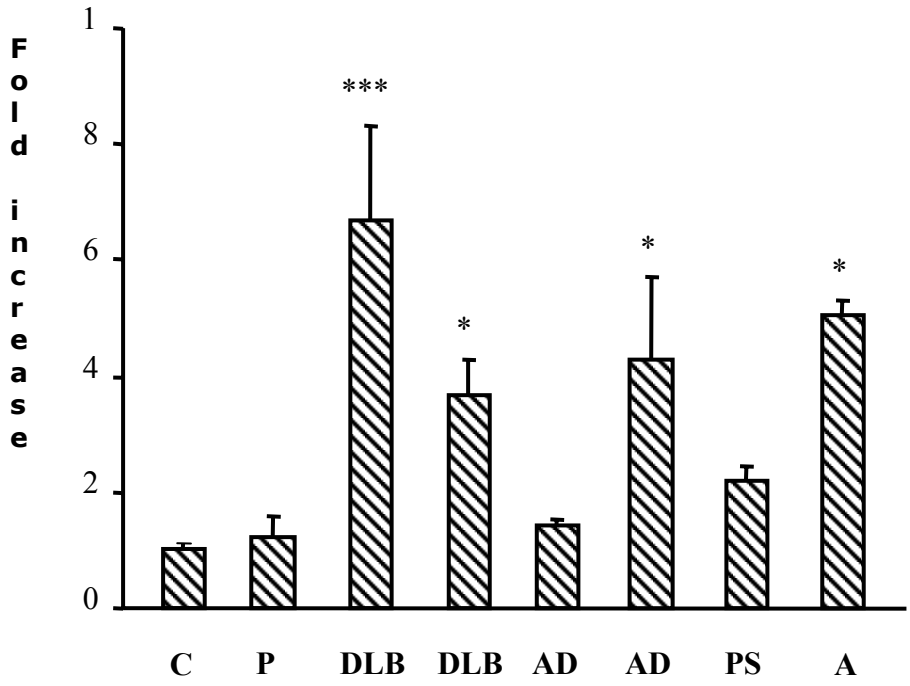

Figure 2

A

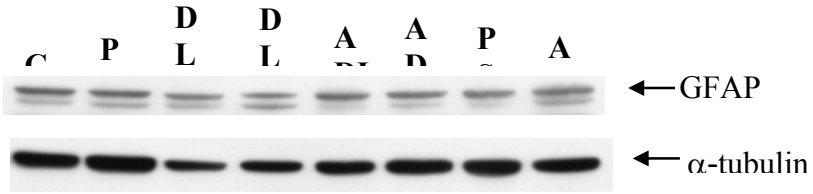
P
D L
D L
A D
P
A
GFAP
α-tubulin

B

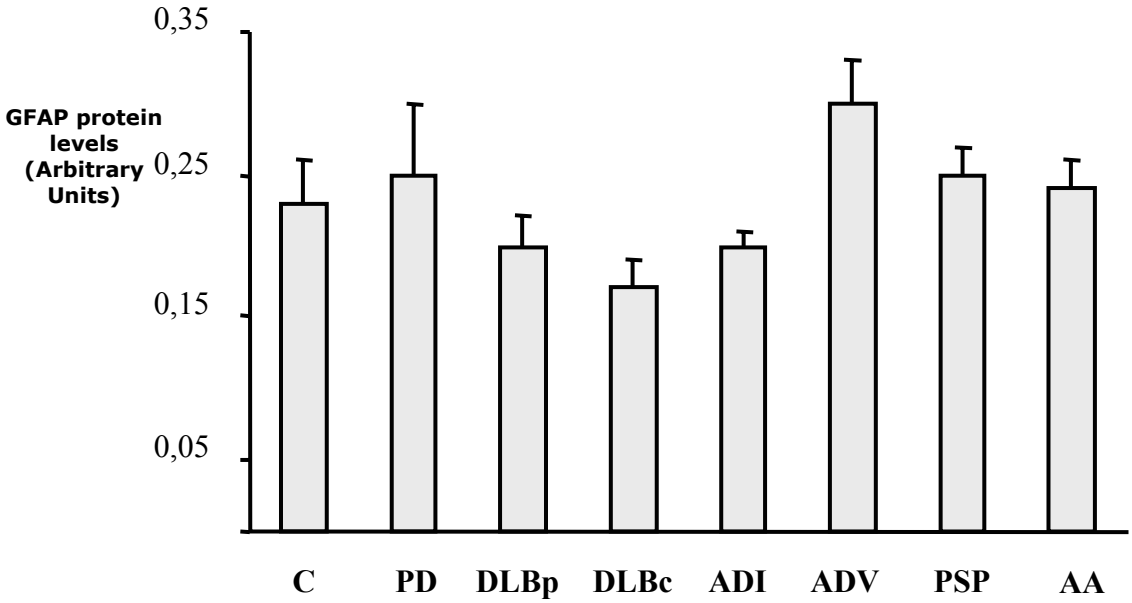
GFAP protein levels (Arbitrary Units)
0,35
0,25
0,15
0,05
C
PD
DLBp
DLBc
ADI
ADV
PSP
AA

Figure 3

Figure 1: (A) Amplification plot of endogenous reference (β-actin) using serial dilutions of control human brain RNA. The horizontal line represents the threshold line adjusted manually in the exponential phase. The fluorescence intensity increased as the PCR cycles increased. The number of PCR cycles at which the fluorescence intensity exceeded the threshold line was defined as the CT values on which the relative quantification was based. (B) Representative standard curves for β-actin, AβPP695, AβPP751 and AβPP770, constructed from several concentrations of control human brain RNA. CT values (y-axis) vs log of several RNA concentrations of control samples (x-axis) showed reverse linear correlation.

Figure 2: (AβPP751+AβPP770)/AβPP695 mRNA ratio fold increase (mean ± SEM) in controls (C), Parkinson's disease (PD), Dementia with Lewy Bodies pure form (DLBp) and common form (DLBc), Alzheimer's disease stages I-IIA (ADI) and stage VC of Braak and Braak (ADV), Progressive Supranuclear Palsy (PSP) and Amyloid Angiopathy (AA). * $p<0.05$ (DLBc, ADV and AA) compared with control values, *** $p<0.001$ (DLBp compared with controls; ANOVA with post-hoc LSD test).

Figure 3: (A) GFAP protein levels were detected by Western Blot in total homogenates from frontal cortex of controls (C), Parkinson's disease (PD), Dementia with Lewy Bodies pure form (DLBp) and common form (DLBc), Alzheimer's disease stages I-IIA (ADI) and stage VC of Braak and Braak (ADV), Progressive Supranuclear Palsy (PSP) and Amyloid Angiopathy (AA). The figure is representative of all the samples indicated in the Table I. (B) Densitometry of GFAP was done normalizating by α-tubulin protein levels in each sample. TotalLab software was used. No statiscally difference was determined among all the samples analysed (ANOVA with post-hoc LSD test).